Characterization of Oncostatin M Receptor (OSMR) Complexes in Glioblastoma

Laura Raco

Department of Medicine
Division of Experimental Medicine
McGill University Montreal, Canada
October 2022
Lady Davis Institute for Medical Research Jewish General Hospital
Montréal, Quebec, Canada

Supervisor: Dr. Arezu Jahani-Asl,
Department of Medicine
Division of Experimental Medicine
McGill University Montreal, Canada
October 2022

Co-Supervisor: Dr. Vahab Soleimani
Lady Davis Institute for Medical Research Jewish General Hospital
Montréal, Quebec, Canada

A thesis submitted to McGill University in partial fulfilment of the requirements of the degree of Master of Science

© Laura Raco 2022

Abstract

Brain tumour stem cells (BTSC) are thought to be the driving cause of glioblastoma tumour recurrence and aggressiveness, yet identification of effective treatments targeting these cell populations has been largely unsuccessful due to the complex nature and signalling networks at play in these cells. Oncostatin M Receptor (OSMR) has been identified to be a key mediator in BTSCs maintenance and glioma progression. This receptor was found to be an Epidermal Growth Factor Receptor variant III (EGFRvIII) co-receptor in the activation of a feedback loop with STAT3 and a mediator of oxidative phosphorylation in BTSCs. Furthermore, OSM/OSMR signalling was identified as a key signalling pathway in the transition to mesenchymal-like glioma states and was found to play a role in regulating the immune microenvironment. This data points to OSMR having multiple roles not just in glioblastoma progression but specifically in BTSCs that render glioma tumours resistant to therapy. In this thesis, I report a novel OSMR binding partner, Chloride Intracellular Channel 1 (CLIC1), identified originally through a Mammalian Membrane Two Hybrid High Throughput Screen (MaMTH-HTS). In order to validate that CLIC1 and OSMR are binding partners, I used a proximity ligation assay (PLA) in BTSC147 to show the interaction of these two molecules in situ. Next, to study how CLIC1 impacts BTSC proliferation and maintenance, I employed CLIC1 siRNA introduced to BTSC147 via electroporation as a pilot experiment. The pilot data was then validated in transgenic CLIC1 clones which I generated using CRISPR-CAS9 technology in a patient-derived BTSC lines. Importantly, not only were OSMR and CLIC1 validated to be novel binding partners, but CRISPR-CAS9 CLIC1 clones were shown to have significantly impaired self-renewal capabilities through extreme limiting dilution assay (ELDA). In addition, CLIC1 knockout cells had significantly lower proliferative capacity compared to WT patient-derived BTSCs. These data suggest that in fact OSMR is impacting glioblastoma progression through additional mechanisms such as alternate binding partners that may also present novel targetable proteins for therapy.

Résumé

Les cellules souches de tumeurs cérébrales (BTSCs) sont responsables de la récidive et de l'agressivité du glioblastome. Cependant, aucun traitement efficace ciblant ces cellules n'a pu être identifié, en raison du caractère complexe de ces cellules et la présence de multiples voies de signalisation cellulaires présentent dans ces cellules. Le récepteur de l'oncostatine M (OSMR) a été identifié comme étant un médiateur clé dans la maintenance des BTSCs et la progression du gliome. Ce récepteur a été identifié comme étant un co-récepteur du récepteur du facteur de croissance épidermique variant III (EGFRvIII) et responsable de l'activation de STAT3. OSMR a également été identifié comme un médiateur de la phosphorylation oxydative dans les BTSCs. De plus, la signalisation OSM/OSMR a été identifiée comme une voie de signalisation clé dans la transition vers des états de gliome de type mésenchymateux et s'est avérée jouer un rôle dans la régulation du microenvironnement immunitaire en faveur de la tumorigenèse. Ces données indiquent qu'OSMR a plusieurs rôles, non seulement dans la progression du glioblastome, mais plus spécifiquement dans la population de BTSC, qui rend les tumeurs du gliome résistantes au traitement. Dans cette thèse, je rapporte un nouveau partenaire d'OSMR, Chloride Intracellular Channel 1 (CLIC1), identifié par un Mammalian Membrane Two Hybrid High Throughput Screen (MaMTH-HTS). Afin de valider que CLIC1 et OSMR sont des partenaires, j'ai effectué des des tests de ligature de proximité (PLA) dans les BTSC147, qui identifie une interaction possible. Ensuite, pour étudier l'impact de l'inactivation de CLIC1 sur la prolifération et la maintenance des BTSCs, en tant qu'expérience pilote, j'ai utilisé des siARN ciblant CLIC1, introduit dans BTSC147 par électroporation. Les données pilotes ont ensuite été validées dans des clones CLIC1 transgéniques générés à l'aide de la technologie CRISPR-CAS9 dans une lignée de BTSC dérivée de patients. De plus, non seulement OSMR et CLIC1 ont été validés pour être de nouveaux partenaires d'intéraction, par test de dilution extrême (ELDA), les clones CRISPR-CAS9 CLIC1 ont montré une capacité d'auto-renouvellement significativement altérée. Aussi, ils ont montré une capacité proliférative significativement inférieure à celle des BTSCs contrôle dérivé de patients. Ces données suggèrent qu'OSMR a un impact sur la progression du glioblastome par des mécanismes supplémentaires tels que des intéractions avec des partenaires alternatifs qui peuvent également présenter de nouvelles protéines ciblables pour la thérapie.

Acknowledgements

I would first like to thank Dr. Jahani-Asl for providing me the opportunity to join her lab and take part in research efforts for cancer and for her support both technically/theoretically and financially through her CIHR grants. Also, I would like to thank Dr. Jahani-Asl for guidance and insightful comments in writing this thesis. Finally, I would like to thank Dr. Soleimani for serving as my co-supervisor and welcoming me into his lab during the Jahani-Asl lab transition period.

I would like to extend a big thank you to Dr. Ahmad Sharanek and Dr. Audrey Burban (post-doctoral fellows) for taking the time to teach me all that they know. I would especially like to thank them, as well as my lab mates and friends, for their support throughout my master's journey. Their patience, kindness, and friendship has been a constant reminder of the importance of community.

I would like to thank all the members of my thesis committee, including my academic advisor, Dr. Autexier, Dr. Mercier, and Dr. Borchers, for their guidance and feedback.

Finally, I would like to thank Vivian, Rocco, and Louis for their constant encouragement, love and support throughout this journey. I would not have made it without them.

Contributions

The experiments in this thesis were performed with consultation from Dr. Jahani-Asl. I generated the CRISPR-CAS9 CLIC1 construct with the guidance of Dr. Sharanek. Fluorescence Activated Cell Sorting (FACS) of CRISPR-CAS9 CLIC1 cells was performed by Christian Young, manager of the Flow Cytometry Facility at the Lady Davis Institute. The Mammalian Membrane Two Hybrid – High Throughput Screen was performed in collaboration with Dr. Igor Stagljar's laboratory at the University of Toronto.

Table of Contents

List of Figures

List of Tables

List of Abbreviations

(RTq) PCR:	(Reverse Transcriptase Quantitative) Polymerase Chain Reaction
ACTB:	Actin Beta
ADORA2A:	Adenosine A2a Receptor
Akt:	Protein Kinase B
APC:	Antigen Presenting Cells
Aβ:	β-amyloid protein
BCNU:	Carmustine
BCRP:	Breast Cancer Resistance Protein
BFP:	Blue Fluorescent Protein
BMDC:	Bone Marrow Derived Dendritic Cells
BMP:	Bone Morphogenic Protein
BrdU:	Bromodeoxyuridine
BSA:	Bovine Serum Albumin
BTSC:	Brain Tumour Stem Cells
c-myc/myc:	MYC Proto-Oncogene, BHLH Transcription Factor
Ca^{2+}:	Calcium
CAS9:	CRISPR-Associated Protein 9
CD79a:	Cluster Differentiation CD79A
CDKN2A:	Cyclin Dependent Kinase Inhibitor 2A
CLC:	Chloride Channel
Cl^-:	Chloride
CLIC:	Chloride Intracellular Channel
CLIC1:	Chloride Intercellular Channel 1
CLT1:	Fluorescein-Conjugated Cyclic Decapeptide
CRISPR:	Clustered Regularly Interspaced Short Palindromic Repeats
CSC:	Cancer Stem Cells
CTL:	Control
Cub:	C-terminus ubiquitin
Cys24:	Cysteine residue 24

DAPI:	4',6-Diamidino-2-Phenylindole
DAVID:	Database for Annotation, Visualization and Integrated Discovery
DMEM:	Gibco Dulbecco's Modified Eagle Medium
DMSO:	Dimethyl Sulfoxide
DNA:	Deoxyribonucleic acid
DUBs:	Deubiquitinating Enzymes
E.Coli:	Escherichia coli
EAG2:	Ether-A-Go-Go Potassium Channel 2
EGFR:	Epidermal Growth Factor Receptor
EGFRvIII:	Epidermal Growth Factor Receptor variant III
ELDA:	Extreme Limiting Dilution Assay
EMT:	Epithelial-to-Mesenchymal Transition
ER:	Endoplasmic Reticulum
ERM proteins:	Ezrin/Radixin/Moesin
ETC:	Electron Transport Chain
EV:	Extracellular Vesicles
FACS:	Fluorescence Activated Cell Sorting
FBS:	Fetal Bovine Serum
FGF:	Fibroblast Growth Factor
FSC (A/H/W):	Forward Scatter (Area/Height/Width)
FWD:	Forward
G0 phase:	Resting phase (cell cycle)
G1 phase:	Gap 1 phase (cell cycle)
G2 phase:	Gap 2 phase (cell cycle)
GAL4TF:	GAL4 Transcription Factor
GB:	Glioblastoma
GFP:	Green Fluorescent Protein
Gp130:	Glycoprotein 130kDA
gRNA:	Guide Ribonucleic Acid
GSEA:	Gene Set Enrichment Analysis
GSC:	Glioma Stem Cell

GST:	Glutathione S-transferase
GUSB:	Glucuronidase Beta precursor
HRP:	Horseradish Peroxidase
IAA-94:	Indanyloxyacetic acid 94
IDH (1):	Isocitrate Dehydrogenase (1)
IgG:	Immunoglobulin G
IL:	Interleukin
IP:	Immunoprecipitation
IR:	Ionising Radiation
ITGa10:	Integrin Subunit Alpha 10
ITGb1:	Integrin Subunit Beta 1
Jak1/Jak2/Jak3:	Janus Kinase 1 and 2 and 3
JNK:	c-Jun N-terminal Kinases
K^+:	Potassium
KD:	Knockdown
kDa:	Kilodalton (molecular weight)
KO:	Knockout
LIF:	Leukaemia Inhibitory Factor
LIFR:	Leukaemia Inhibitory Factor Receptor
LPCAT1:	Lysophosphatidylcholine Acyltransferase 1
M phase:	Mitosis (cell cycle)
MaMTH-HTS:	Mammalian Membrane Two Hybrid – High Throughput Screen
MAPK:	Mitogen-Activated Protein Kinase
MDR:	Multi-Drug Resistance
MDR1:	Multi-Drug Resistance Protein 1
MLC:	Myosin Light Chain
MMP-2/9:	Matrix Metallopeptidase 2 and 9
mRNA:	Messenger RNA
MRP1:	MDR-associated Protein 1
MTT:	3-(4, 5-dimethylthiazol-2-yl)-2,5-diphenyltetrazolium bromide (assay)
Na^+:	Sodium

NDUFS1/NDUFS2: NADH ubiquinone oxidoreductase 1 and 2

NF-κB: Nuclear Factor kappa B

NK: Natural Killer Cells

NLRP3: NOD-, LRR- and pyrin domain-containing protein 3

NPC: Neural Progenitor Cells

NSC: Neural Stem Cells

Nub: N-terminus ubiquitin

ORF: Open Reading Frame

OSM: Oncostatin M

OSMR: Oncostatin M Receptor

OXPHOS: Oxidative Phosphorylation

PAM: Presequence Translocase-Associated Motor

PBS: Phosphate Buffered Saline

PDAC: Pancreatic Ductal Adenocarcinoma

PDL: Poly-D-Lysine

PI: Propidium Iodide

PI3K: Phosphoinositide 3-Kinases

PIP5K1A: Phosphatidylinositol-4-Phosphate 5-Kinase type 1 alpha

PIP5K1C: Phosphatidylinositol-4-Phosphate 5-Kinase type 1 gamma

PLA: Proximity Ligation Assay

PPI: Protein-Protein Interaction

PSEN1: Presenilin 1

PTEN: Phosphatase and Tensin Homolog

PTK: Protein-Tyrosine Kinases

Rac2: Rac Family Small GTPase 2

Ras: Mitogen-activated protein kinase

RCA: Rolling Circle Amplification

REV: Reverse

RFP: Red Fluorescent Protein

RhoA: Ras Homolog Family Member A

RIPA: Radio Immunoprecipitation Assay Buffer

RNA:	Ribonucleic acid
ROS:	Reactive Oxygen Species
RVD:	Regulatory Volume Decrease
S phase:	DNA synthesis phase (cell cycle)
SCF:	Stem Cell Frequency
SD:	Standard Deviation
SDS:	Sodium Dodecyl Sulfate
SHH:	Sonic Hedgehog
siRNA:	Short Interfering RNA
SOX2:	SRY-box Transcription Factor 2
SSC (A/H/W):	Side Scatter (Area/Height/Width)
STAT3/1:	Signal Transducer and Activator of Transcription 3 and 1
SVOP:	Synaptic Vesicle 2 Related Protein
TBST:	Tris-buffered saline with 0.1% Tween- 20 detergent
TCGA:	The Cancer Genome Atlas
TDGF1:	Teratocarcinoma-Derived Growth Factor 1
TILs:	Tumor Infiltrating Lymphocytes
TF:	Transcription Factor
TMZ:	Temozolomide
TNF-a:	Tumour Necrosis Factor alpha
TP53/p53:	Tumor Protein p53
TRIzol:	Total Ribonucleic acid Isolation
TRPM7:	Transient Receptor Potential Cation Channel Subfamily M Member 7
WB:	Western Blot (immunoblotting)
WNT:	Wingless/Integrated
WT:	Wild Type

A. Introduction

A.1 Glioblastoma heterogeneity

Glioblastoma (GB) is characterised as a highly advanced and aggressive brain cancer in which the survival remains around 14 to 16 months after diagnosis, despite research efforts attempting to find effective treatments (Gilard et al., 2021; Shergalis et al., 2018). The incidence of glioblastoma onset has been characterised as either a primary or secondary glioblastoma (Tan et al., 2020). Primary or isocitrate dehydrogenase (IDH)-wild type GB refers to *de novo* tumour formations and is thought to account for around 90% of all GB cases (Ohgaki & Kleihues, 2013; Tan et al., 2020). Secondary IDH-mutant GB, on the other hand, is thought to arise from pre-existing brain cancers, such as low grade or diffuse astrocytoma (Ohgaki & Kleihues, 2013). Both primary and secondary GBs carry a multitude of mutations and genetic alterations that lead to their aggressive nature. Major genetic alterations include epidermal growth factor receptor (EGFR) amplification/overexpression, cyclin dependent kinase inhibitor 2A (CDKN2A) deletion and phosphatase and tensin homolog (PTEN) mutation in primary, and tumour protein p53 (TP53) mutation in secondary tumours (Ohgaki et al., 2004). In addition, different transcriptional/molecular subtypes, each possessing distinct transcriptional and phenotypic characteristics, have been identified. These states include proneural, classical and mesenchymal states, although some research has suggested there is an additional subtype known as the neural subtype. Each subtype possesses intrinsic genetic and molecular elements that aid in defining the subtype, but it is important to note that these states exist on a continuum rather than being separate entities (Olar & Aldape, 2014; Sidaway, 2017; Zhang et al., 2020). The mesenchymal subtype has been suggested to be the most aggressive and chemo-resistant brain tumours. Their aggressive nature can be attributed in part to the activity of master regulator transcription factors including signal transducer and activator of transcription 3 (STAT3), as well as the expression of mesenchymal proteins, such as N-cadherin and vimentin. These elements endow the cells with the ability to enter an epithelial-to-mesenchymal (EMT) like state and metastasize (Kim et al., 2021). Furthermore, the mesenchymal GB subtype has an altered immunologic and pro-inflammatory microenvironment including, increased macrophage/microglia with pro inflammatory signatures (M1 macrophages), tissue repair/proliferation signatures (M2 macrophages), increased tumour

infiltrating lymphocytes (TILs), and decreased natural killer (NK) cells compared to proneural or classical GB subtypes (Gabrusiewicz et al., 2016; Orecchioni et al., 2019; Wang et al., 2017).

Despite the various molecular and genetic differences across GB, the current standard treatment plan for newly diagnosed patients includes maximal surgical resection followed by chemotherapy using Temozolomide (TMZ) and Ionising Radiation (IR), although currently there are no standard of care options for recurrent GB diagnosis (Fernandes et al., 2017; Stupp et al., 2005). This, in part, is due to the complex nature of the tumour and the surrounding environment upon initial diagnosis, and the presence of a select population of slower growing or quiescent cells deemed as brain tumour stem cells (BTSCs) or cancer stem cells (CSCs) (**Figure 1**) (Singh et al., 2003; Singh et al., 2004).

Figure retrieved from Reya et al., 2001 in Nature

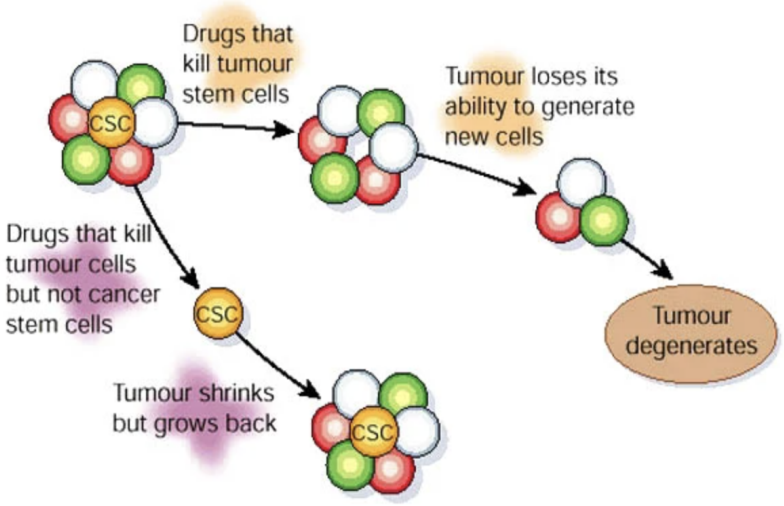

Figure 1. The stem cell hypothesis depicts the inherent need to target cancer tem cells (CSCs) as the most effective way to combat tumour recurrence after targeted therapy, as they are the ones that are responsible for relapse (Hale et al., 2013; Reya et al., 2001).

How BTSCs arise in the brain is still under investigation, although there seems to be two general modes of presentation that are widely accepted. This includes the hierarchical and the stochastic models of BTSC formation (Adams & Strasser, 2008; Shackleton et al., 2009). The notion that tumours arise from a select hierarchical population of self-renewing cells is known as the stem cell hypothesis (Tan et al., 2006). This theory posits that individual CSCs can give rise to a heterogeneous population of cells composed not only of CSCs but also differentiated lineages

(**Figure 1**) (Galli et al., 2004; Tan et al., 2006). This theory is opposed by the stochastic model of tumour formation which suggests that cancerous cells arise by spontaneous and rare mutational events giving rise to a heterogeneous population of cells harbouring various driver mutations (Nowell, 1976). Although both theories may be at play in GB progression, much research has suggested that in order to effectively terminate GB recurrence, BTSCs can be targeted as a first line of treatment along with current treatment options (**Figure 1**) (Kalkan, 2015; Yang et al., 2020).

A.1.1 Brain tumour stem cells (BTSCs)

In order to target BTSCs as a therapeutic option, understanding the underlying mechanisms of maintenance and propagation of these cell populations is essential. Numerous signalling pathways have been identified that all lead to the expression of stemness genes (e.g. SRY-box Transcription Factor 2 - SOX2) (Gangemi et al., 2009) thus, maintaining this stem-like pool of cells. These signalling pathways include but are not limited to: Wingless/Integrated (WNT)/β-Catenin, Notch, Bone Morphogenic Protein (BMP), Nuclear Factor Kappa B (NF-κB), Epidermal Growth Factor (EGF) and Sonic Hedgehog (SHH) signalling pathways (Liebelt et al., 2016; Matsui, 2016). Each of these pathways, however, possesses its own intrinsic complexity when it comes to signalling in BTSCs in comparison to its non-oncogenic counterparts, the neural stem cells (NSCs). For instance, in BTSCs, the epidermal growth factor receptor (EGFR) is frequently amplified leading to its increased signalling potential (Brennan et al., 2013). However, in addition to the amplification of the wild-type EGFR, activating mutations of EGFR leads to other splice variants including the epidermal growth factor receptor variant III (EGFRvIII). This variant is generated by a significant deletion of a portion of the extracellular ligand binding domain (Abou-Fayçal et al., 2017; Gan et al., 2009). Unlike EGFR, the truncated EGFRvIII maintains a constitutively active status in the absence of its natural ligand leading to the continued phosphorylation and subsequent activation of the transcription factor STAT3 (Gan et al., 2009). Thus, to effectively target signalling pathways in BTSCs it is essential to understand the nuances that pertain to each pathway.

The identification of EGFRvIII led to a greater understanding of the complexity of increased activation of this pathway, but it did not answer the question of how this mutated EGFR

receptor remains active or can be effectively targeted for therapy in clinic (Gan et al., 2009; Sorscher, 2004; Zadeh et al., 2013). In 2016, a novel discovery identified that the Oncostatin M receptor (OSMR) is acting as a required co-receptor for EGFRvIII, promoting the activity of the EGFRvIII-STAT3 signalling pathway in BTSCs, and thus promoting GB tumorigenesis (Jahani-Asl et al., 2016). The full spectrum of OSMR function remains to be investigated.

A.2 Oncostatin M (OSM) and Oncostatin M Receptor (OSMR) signalling

Oncostatin M (OSM), is a 28kDa circulating cytokine of the interleukin (IL)-6 cytokine family. This family also includes other cytokines including, IL-6, IL-11, IL-31, IL-27 and Leukaemia Inhibitory Factor (LIF) among others (Malik et al., 1989; Rose & Bruce, 1991). These cytokines are classified as members of a family based on their signalling mode that all involve a receptor complex that includes one or multiple glycoprotein 130kDA (gp130) subunits (Rose-John et al., 2015). Functionally, IL-6 family cytokines are involved in multiple biological processes including immune cell stimulation/regulation and metabolic functioning (Tanaka et al., 2014).

Like most cytokines, OSM is secreted as a circulating product from immune cells (dendritic cells, macrophages, T cells and neutrophils) as well as non-immune cells such as hematopoietic cells. Interestingly, the expression of OSM is generally low in tissues of healthy individuals compared to individuals with cancer (Chen et al., 2021; Tawara et al., 2019). One of the OSM receptors, OSMR, is a 979 amino acid receptor of the type-1 cytokine receptor family (Mosley et al., 1996). This receptor mediates signal transduction of its natural ligand, OSM, through the formation of a high affinity type-II receptor complex with gp130 (OSMR/OSM/gp130). This high affinity receptor is generated once the low affinity OSM/gp130 complex encounters OSMR to generate signal transduction (**Figure 2**). Although OSM signals through a type-II receptor complex, it can also signal through a type-I receptor complex generated by the dimerization of the Leukaemia Inhibitory Factor Receptor (LIFR) and gp130/OSM (LIFR/OSM/gp130) in human cells (**Figure 2**). Interestingly, the Leukaemia Inhibitory Factor (LIF) may also signal through the type-I receptor but not through the OSMR/gp130 (type-II) complex suggesting the type-II receptor complex may possess unique signalling properties (Heinrich et al., 2003; Mosley et al., 1996; Thoma et al., 1994). Of note, the murine form of OSM was once thought to only signal through

the type-II receptor complex (OSMR/OSM/gp130) but additional research has suggested that there may be a potential for cross species activation of both receptor complexes (Hermanns, 2015; Walker et al., 2010). Signalling events through the type-II receptor compex by OSM are driven by interaction with Protein-Tyrosine Kinases (PTK) such as Janus Kinase 1/2 (Jak1/Jak2) and adaptor proteins which mediate activation of the JAK-STAT pathway leading to signal transduction through STAT3 in both human and murine receptor models. This signal transduction is mediated by STAT3 phosphorylation via the PTK/Janus Kinases in the cytoplasm, leading to STAT3 dimerization. The dimeric structure is then able to travel to the nucleus where it acts as a transcription factor for the expression of downstream effector genes (Yu et al., 2014). Additionally, receptor signalling in both human and murine receptor models can activate STAT5, although the mechanism used by the human receptors is through a double tyrosine motif, which is not present in the murine receptor complexes (Hermanns, 2015). In addition to STAT3, other signalling pathways include the Phosphoinositide 3-Kinases/Protein Kinase (PI3K/AKT) pathway, c-Jun N-terminal kinases/Mitogen-Activated Protein Kinase (JNK/MAPK) pathway and Ras/MAPK pathways. These pathways are both necessary and important for cellular processes and have been identified as key pathways in disease, including cancer (Böing et al., 2006; Dey et al., 2013; Hermanns et al., 2000; Kan et al., 2011; Levy et al., 1996).

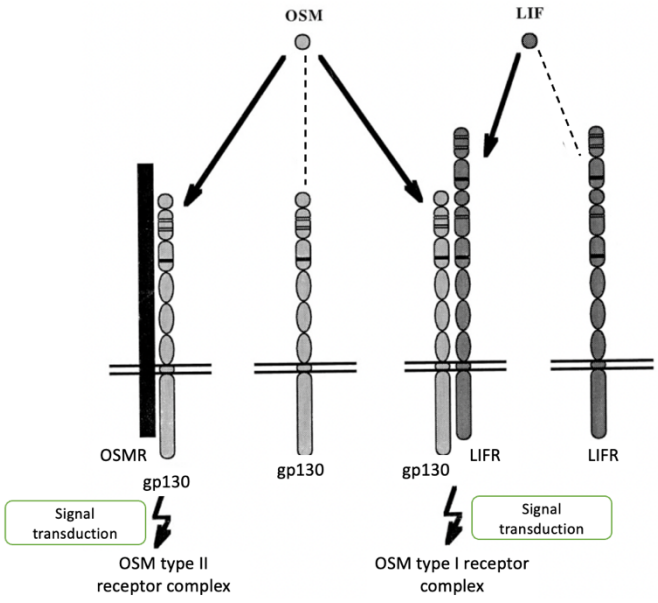

Figure adapted from Mosley et al., 1996 in The Journal of Biological Chemistry

Figure 2. OSM signalling through type-I and type-II receptor complexes in humans. Bolded arrows represent high affinity binding of ligand and receptor leading to signal transduction. The dotted line represents low affinity binding and does not lead to signal transduction (Mosley et al., 1996).

A.2.1 OSM/OSMR signalling in cancer

The role of OSM/OSMR signalling has been a subject to debate within the cancer research community as there has been both evidence that this signalling pathway acts in an oncogenic as well as in a tumour suppressive capacity (Junk et al., 2017; Masjedi et al., 2021). For instance, in Pancreatic Ductal Adenocarcinoma (PDAC), OSM/OSMR signalling in the tumour microenvironment was found to regulate fibroblast programs in a paracrine manner. OSM released by macrophages in the tumour microenvironment stimulated signal transduction through OSMR in cancer associated fibroblast (mesenchymal cells) and endothelial cells (Lee et al., 2021). It was identified that this type of signalling in the fibroblast cells leads to an increase in the production and release of pro-inflammatory cytokines in favour of tumour progression and metastasis (Lee et al., 2021). A similar feature of OSM/OSMR signalling was observed in breast cancer such that this signalling pathway was identified to not only be overexpressed in terms of ligand and receptor in cancerous tissue, but it also contributed to a supportive niche environment for tumorigenic cells. This niche environment was found to be populated by both immune (macrophages and neutrophils) and non-immune cells (cancer associated fibroblast and tumour cells) either stimulated by OSM or inducing OSM expression to impact neighbouring cells, thereby forming a positive feedback loop for tumorigenesis (Araujo et al., 2022). The pro-tumorigenic effect of OSM/OSMR signalling has further been demonstrated across a wide variety of cancer types including, but not limited to colon cancer (Kim et al., 2009), lung cancer (Chen et al., 2008; Shien et al., 2017), cervical cancer (Kucia-Tran et al., 2016; Ng et al., 2007; Winder et al., 2011) and Ewing sarcoma (David et al., 2012). Conversely, there has also been considerable evidence that OSM in the tumour microenvironment takes on a tumour suppression and growth inhibition role, sometimes even in the same cancer in which it was found to have a pro-tumorigenic effect (Friedrich et al., 2001; Halfter et al., 2006; Li et al., 2001; Lu et al., 1993; Pan et al., 2016). For instance, OSM signalling was found to produce growth inhibitory effects on chondrosarcoma cells while sensitizing these

cells to death by the activation of p53. The growth inhibitory effects were found to be mediated by Jak3 and STAT1 activation, such that a Jak3 inhibitor abolished the growth inhibitory effects and was accompanied by a significant decrease in STAT1 activation while STAT3 activation remained unchanged (David et al., 2011). Data in support of OSM as an oncogenic player and in support of its role in tumour suppression, even in the same cancer type, suggests that there may be intrinsic factors to determine its role through varying signalling pathways (Masjedi et al., 2021). Interestingly, prior research has shown that in human mammary epithelial cells the MYC Proto-Oncogene, BHLH Transcription Factor (c-myc) regulates the response of OSM to that of a pro-tumorigenic or tumour suppressive role. It was identified that the expression levels of c-myc and its activity are key regulators in signalling pathways, such that if c-myc can no longer be repressed by STAT3 activation as a tumour suppressor, proliferation will continue in the presence of OSM/OSMR and activate signalling pathways in favour of tumorigenesis (Kan et al., 2011). Although there has been evidence of how OSM/OSMR signalling may have different effects in certain cell lines, by delving deeper into the intricacies of this pathway new therapeutic targets may present themselves. This includes novel binding partners that may influence the activity of OSM/OSMR signalling to favour tumorigenesis or tumour suppression.

A.2.2 OSMR/OSM Expression in glioblastoma

Expression analysis of OSM and its corresponding receptor, OSMR, has suggested that both the ligand and the receptor are highly expressed in glioblastoma, and their elevated expression significantly correlates with poor patient prognosis (Chen et al., 2021; Guo et al., 2019; McLendon et al., 2008; Natesh et al., 2015). Furthermore, the effects seen in glioblastoma by OSM were found to be mediated specifically by the overexpression of OSMR and not the expression of LIFR, suggesting that OSMR may be contributing to downstream effects that are unique to those of other OSM receptors (Natesh et al., 2015). Additionally, OSMR was found to be highly expressed in the mesenchymal molecular subtype of GB and its expression was significantly reduced in the proneural subtype. In this manner, OSM/OSMR was found to be contributing to the invasive and aggressive nature of the mesenchymal subtype in a STAT3 dependent manner (Natesh et al., 2015).

A.2.3 OSMR/OSM role in glioblastoma tumorigenesis

Various mechanisms in which OSMR is implicated in glioblastoma have been identified. One of which includes OSMR acting as a co-receptor for EGFRvIII at the plasma membrane in human BTSCs and murine derived astrocytes (Jahani-Asl et al., 2016). This research identified that OSMR engages in a positive feedback loop by which its interaction with EGFRvIII or phosphorylated EGFR leads to an aberrant activation of STAT3. Activated STAT3 can then be translocated to the nucleus where it is able to directly bind the promoter of OSMR to upregulate its expression thereby promoting tumorigenesis. Importantly, loss of OSMR was shown to contribute to significant reductions in tumorigenesis and proliferation along with prolonged lifespan in a preclinical animal model (Jahani-Asl et al., 2016) (**Figure 3)**. However, the role of OSMR signalling in glioblastoma is not limited to its interaction with EGFRvIII or EGFR. OSMR was recently found to be a key regulator of mitochondrial respiration and metabolism through interaction with complex I of the electron transport chain (ETC) in BTSCs (Sharanek et al., 2020). In this instance, OSMR is translocated into the mitochondria through the Presequence Translocase-Associated Motor (PAM) complex and interacts with NADH ubiquinone oxidoreductase 1/2 (NDUFS1 and NDUFS2) of complex 1. This leads to an increase in the rate of oxidative phosphorylation (OXPHOS) in BTSCs, a decrease in generation of reactive oxygen species (ROS) followed by desensitization of these cells to IR treatment. This role of OSMR was found to be independent of EGFRvIII (Sharanek et al., 2020) (**Figure 3**). Yet, other studies have suggested that OSMR is a key receptor in the transition to mesenchymal states (Hara et al., 2021). Unlike other glioblastoma subtypes, such as the proneural subtype, that arise from intrinsic cell types such as neurons (Olar & Aldape, 2014), mesenchymal-like cells do not arise from intrinsic cells, thus suggesting that a transition to a mesenchymal phenotype is required to generate the mesenchymal subtype (Neftel et al., 2019). Research has suggested that OSM and to a lesser extent LIF, produced by macrophages, induces signal transduction through OSMR/gp130 predominantly, or LIFR/gp130, to induce the expression of mesenchymal-like programs through the activation of STAT3 in a glioblastoma cancer cell model (Hara et al., 2021) (**Figure 3**). Of note, OSMR was also found to have a role in the regulation of the immune and tumour microenvironment. It was identified that high expression of OSMR negatively correlated with cytotoxic lymphocytes (which typically do not express OSMR) but positively correlated with fibroblasts and dendritic cells in the

glioblastoma tumour microenvironment. These findings suggest that mesenchymal cells such as fibroblasts and dendritic cells express OSMR, along with the tumour cells, and may also contribute to malignancy (Guo et al., 2019). In addition, Gene Set Enrichment Analysis (GSEA) pointed to OSMR as a key element in inflammatory response pathways/phenotypes and leukocyte migration (Guo et al., 2019). Interestingly, OSMR was also identified to be strongly associated with extracellular matrix related pathways in the brain tumour microenvironment (Guo et al., 2019). However, the role of OSM/OSMR signalling in impacting the immune landscape and progression of GB has also been contrasted. It has previously been suggested that mesenchymal states have been heavily associated with suppressing the activity of T cells and thus leading to a more immune-cold and aggressive GB phenotype (Mariathasan et al., 2018), but recent evidence has suggested otherwise (Hara et al., 2021). This research has suggested that mesenchymal like glioblastoma states are more effectively targeted and killed by T cells compared to any other state (Hara et al., 2021). This data suggests that, not only does OSM/OSMR have a role in the state of the tumour, but that it also contributes to modulating the local tumour environment to either enhance tumorigenesis or induce a more favourable tumour killing immune environment (Guo et al., 2019; Hara et al., 2021; Matsumoto et al., 2020). This suggests that OSMR is contributing to malignancy or suppression through more than one pathway. These pathways may involve additional binding partners that influence the activity of OSMR to generate perhaps more malignant phenotypes such as the ones observed in the mesenchymal-like state. To follow up on this notion, I set out to identify OSMR binding partners in different contexts, as described in the Result section of this thesis. Specifically, the focus of this MSc thesis was to investigate the biology of one of these partners in BTSCs, the **Chloride Intracellular Channel 1 (CLIC1).**

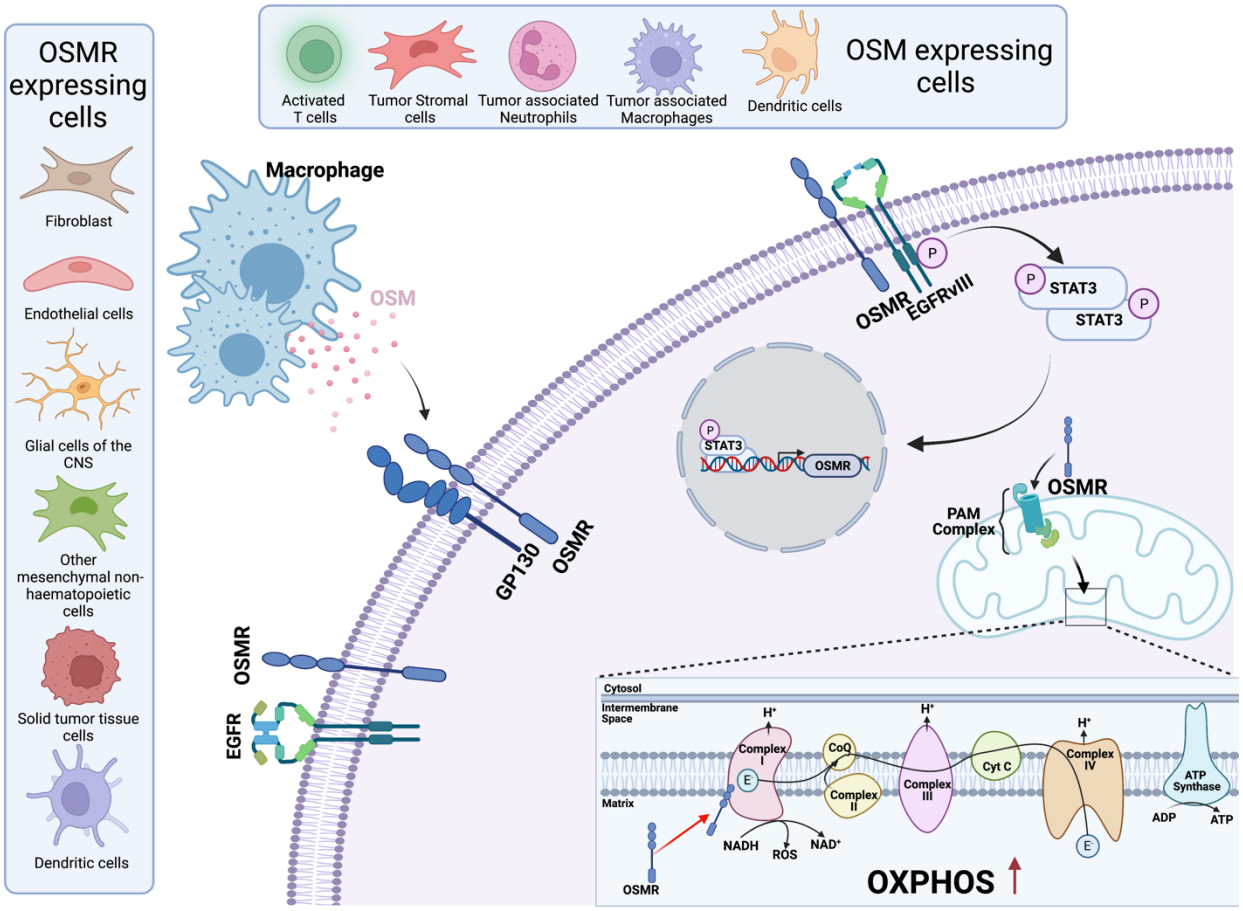

Figure adapted from Talks - Raco & Jahani-Asl 2021 in MRM Insights 2021

Figure 3. OSM and OSMR in various roles contributing to glioblastoma tumorigenesis. OSMR as an EGFRvIII co-receptor at the plasma membrane: mediates a positive feedback loop with activated STAT3. OSMR at the mitochondria: OSMR translocates into the mitochondria via the PAM complex where it regulates OXPHOS through binding to complex 1 of the ETC. OSMR signalling is correlated with malignant transformation to mesenchymal GB subtypes by the expression of OSM from macrophages (Talks) Raco & Jahani-Asl 2021. OSM-expressing cells in the cancer tumour environment that produce OSM, pertaining to glioblastoma and other cancers such as breast cancer and PDAC (Araujo et al., 2022; Lee et al., 2021; Queen et al., 2005; West et al., 2018). OSMR-expressing cells/ tumor cells that express the receptor. Some pertaining to glioblastoma and CNS specifically and other cancers such as breast cancer and PDAC (Araujo et al., 2022; Guo et al., 2019; Hermanns, 2015; Lee et al., 2021; West et al., 2018). Image created using Biorender.com

A.3 Ionic homeostasis and ion channels

Ions are electrically charged molecules with their extracellular and intracellular concentrations being maintained by the action of their corresponding channels in a process known as ionic homeostasis (Bagal et al., 2013; Dubyak, 2004; Jentsch et al., 2004). Ion currents mediate pumping of the heart, muscle contractions, cell cycle progression/proliferation (Rosendo-Pineda et al., 2020), neuronal signalling (Burke Jr & Bender, 2019), immune (Feske et al., 2015; Panyi et al., 2014) and metabolic functions including proper functioning of ETC, ROS production and maintenance of the mitochondrial membrane potential (Urbani et al., 2021) to name a few. The broad action of these molecules can be attributed to a handful of ions, including calcium (Ca^{2+}), potassium (K^{+}), chloride (Cl^{-}), and sodium (Na^{+}).

For instance, calcium is known to be one of the most ubiquitous and versatile ions in the body. It drives a multitude of critical biological pathways through its ability to act as a second messenger, as well as its ability to control the location of these signals by generating localized gradients (Giorgi et al., 2018). Two of the most recognized organelles for calcium stores and effectors of calcium gradients are the Endoplasmic Reticulum (ER) and the mitochondria (Giorgi et al., 2018; Raffaello et al., 2016). These organelles not only provide a large reservoir of calcium, but they also regulate the effect calcium will have on the cell. For instance, transient calcium fluctuations in the mitochondria, regulated by the ER, drive proper functioning of the cell; elements such as metabolism and pro-survival signals. However, prolonged Ca^{2+} elevation in the mitochondria leads to cell death through excitotoxic mechanisms in neurons; in other words, hyperactivation of neurons leading to death (Marchi et al., 2018). Another critical ion in the body is potassium. Similar to calcium, potassium is essential to a wide range of biological functions, including maintaining resting membrane potentials, action potentials, hormone secretion/activity and cell volume regulation, to name a few (Mount & Zandi-Nejad, 2012; Weiner et al., 2010). The action of this ion is so widespread throughout biological systems that it must be tightly regulated in a process known as potassium homeostasis (Gumz et al., 2015; Palmer, 2015).

In addition to Ca^{2+}, and K^{+}, chloride plays a significant role in health and disease as it is the principal anion of the human body. This anion controls and regulates many biological pathways

including, maintaining osmotic pressure to ensure proper cell-volume regulation, maintaining acid-base balance, regulating epithelial fluid secretion and playing a role in neuronal signaling (Berend et al., 2012; Verkman & Galietta, 2009). Of note, acid-base balance is one of the most important aspects of the human body as the body operates in a very narrow pH range. This pH range is critical for the proper functioning of enzymes, such as those involved in metabolism or in the immune response, proper protein folding, and efficient oxygenation of tissues and organs (Miltiadous et al., 2008).

Ion channels that regulate these charged molecules can be found at the plasma membrane of cells or intracellularly on specific organelles in which they mediate functions specifically to that organelle. They can be voltage gated, intracellular or extracellular ligand gated, mechano-sensitive or passive channels. With ion channels being so varied in their function and activity, it is evident that not only do they play a critical role in human biology, but their dysfunction can have a profound impact on human health (Hübner & Jentsch, 2002; Kullmann & Waxman, 2010). Moreover, ion channels have been implicated in a variety of malignancies, including glioblastoma, in which they function in a broad manner to mediate cancer progression (Litan & Langhans, 2015). Specifically in GB, Cl^- has been found to play a role in tumour progression through implications in proliferation (Habela & Sontheimer, 2007), migration (Watkins & Sontheimer, 2011) and apoptosis, all of which require considerable changes in cellular volume (Turner & Sontheimer, 2014).

A.3.1 Chloride Intracellular Channel (CLIC) family

The Chloride Intracellular Channel (CLIC) family, which consists of 6 members (CLIC1-6), is the most recent chloride (Cl^-) channel that has been identified (Ashley, 2003). These proteins are known to be encoded by six different genes (*clic1-6*) on various chromosomes. Structurally they are not related to classical chloride channels (CLCs), instead the CLIC motif resembles that of the Omega Glutathione S-Transferase (GST) fold superfamily (Gururaja Rao et al., 2020; Littler et al., 2010). Interestingly, these proteins can be found in both a soluble form, in which some members have been found to display possible enzymatic activity (Hernandez-Fernaud et al., 2017; Turkewitz et al., 2021), and/or in a channel form inserted in the membrane (Gururaja Rao et al.,

2020). The membrane form is made possible by one putative transmembrane domain found in the CLIC protein structure (Littler et al., 2010), which allows its insertion into the membrane. Adding to their importance, these proteins have been found to play important roles in human diseases. This includes but is not limited to organ dysfunction, specifically in the realm of the heart and the lungs (Ponnalagu et al., 2016; Wojciak-Stothard et al., 2014), neuropathology, in which CLIC proteins are functionally implicated in neuronal death (Guo et al., 2018) and in various cancers in which they are expressed in solid tumours as well as in surrounding tumour tissue (Gururaja Rao et al., 2020).

A.4 Chloride Intracellular Channel 1 (CLIC1)

Chloride Intracellular Channel 1 (CLIC1), or NCC27 is a protein of the CLIC family composed of 241 amino acids with a molecular weight of about 27 kDA (Valenzuela et al., 1997). It is expressed in various tissues and cell types; however, its expression in terms of both mRNA and protein, is rather low in the brain (Public Database Human Protein Atlas – (Sjöstedt et al., 2020). Unlike many members of the CLIC family, this specific protein is thought to have enzymatic activity in the cytoplasm when it is in its soluble monomeric form. Specifically, CLIC1 was identified to potentially possess oxidoreductase activity in a glutathione-dependent manner because of its glutaredoxin-like 'active site', although the specific activity of CLIC1 to act in this manner is not confirmed (Al Khamici et al., 2015; Board et al., 2004). The potential catalytic activity of CLIC1 in its soluble form was identified to be mediated by cysteine residue 24 (Cys24) (Al Khamici et al., 2015). This specific residue has also been highly implicated in the transition from a soluble form to that of a membrane channel (Littler et al., 2004). Research into the mechanism of transition has shown that to form a membrane channel, the CLIC1 monomer must dimerize. This is mediated by a structural re-organization of the protein and the interaction between Cys24 and Cys59, which form an intramolecular disulfide bond in response to redox states of the cell or other unidentified means (**Figure 4**). This interaction, along with a structural re-organization of key residues, exposes a large hydrophobic surface of the protein that enables channel formation and gives rise to the putative transmembrane helix in proximity to the catalytic active site. The data from these studies has suggested that the transition between states is controlled

by the redox state of the cell (Harrop et al., 2001; Littler et al., 2004) although, the exact mechanisms by which this occurs are yet to be determined.

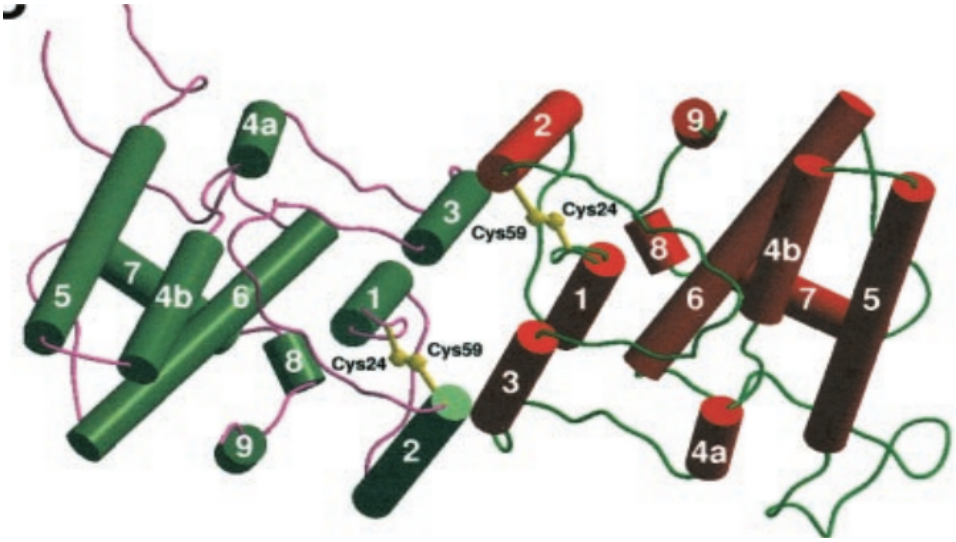

Figure retrieved from Littler et al., 2004 in The Journal of Biological Chemistry

Figure 4. Dimeric structure of CLIC1. The CLIC1 monomers are represented in green and in red respectively. The intramolecular disulfide bond between Cys24 and Cys59 is represented in yellow. The numbers represent the helices of the protein. This interaction is thought to be required for insertion in the membrane to generate a functional channel (Littler et al., 2004).

A.4.1 CLIC1 and cancer

CLIC1 is suggested to play a role in the progression of various aggressive cancer types including, gastric carcinoma (Li et al., 2018), lung cancer (Wang et al., 2011), pancreatic adenocarcinoma (Jia et al., 2016), epithelial ovarian cancer (Singha et al., 2018), medulloblastoma (Francisco et al., 2020) and glioblastoma (Djuric et al., 2019; Setti et al., 2013; L. Wang et al., 2012). Interestingly, via analysis of the mutational landscape of CLIC1 in cancer, there has been little evidence of mutations in the CLIC1 gene. For most of the tumours surveyed there seemed to be no mutations (**Figure 5**) (Barbieri et al., 2019). This may suggest that unlike some other cancer drivers, that are frequently mutated in glioblastoma, CLIC1's role in tumorigenesis is not mediated by mutational alterations, but rather other mechanisms, possibly by post-translational modification

or interaction with binding partners (Barbieri et al., 2019). Furthermore, in many studies the increased expression of CLIC1 has been associated with poor prognosis and a high degree of resistance to standard of care treatment in GB and other cancers (Peretti et al., 2015; Wu & Wang, 2017; Zhao et al., 2019).

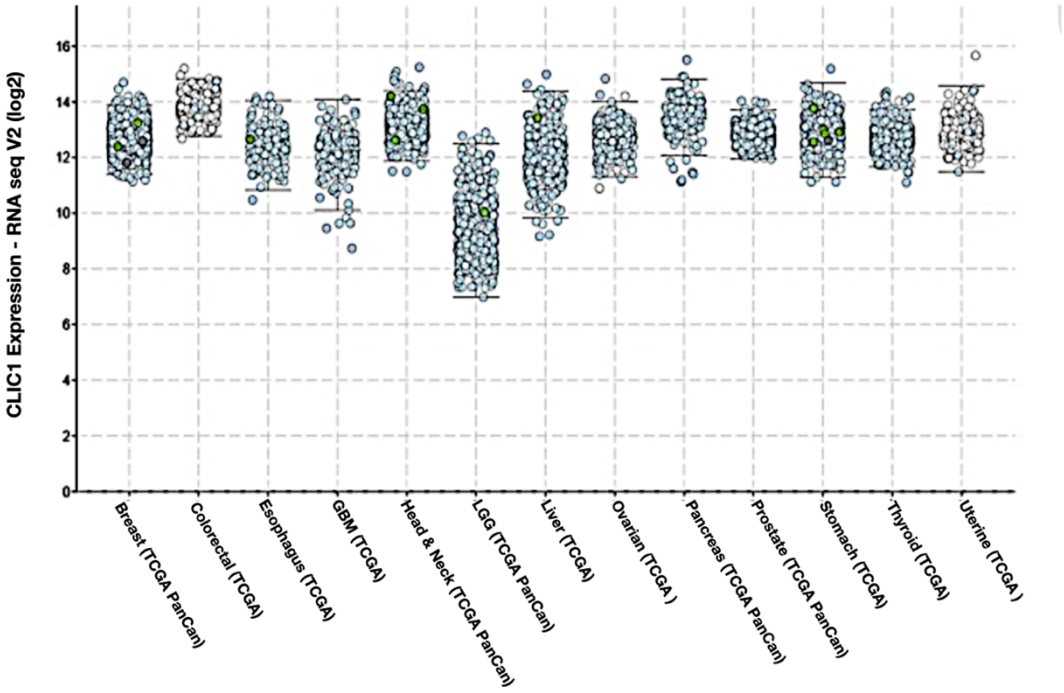

Figure retrieved from Barberi et al., 2019 in Frontiers in Oncology

Figure 5. RNA expression of CLIC1 in solid tumours. Mutational information was derived by Barberi et al., 2019 with the use of the cBioPortal/TCGA datasets. Blue dots - no mutations; Green dots - missense mutation; Purple dot - truncation mutation; White dot - mutation not identified. Residue mutations are not specified (Barbieri et al., 2019).

A.4.2 CLIC1 in glioblastoma

Research specifically focused on the role of CLIC1 in glioblastoma tumorigenesis has suggested that not only is CLIC1 highly expressed in glioblastoma compared to normal brain tissue, but its expression is significantly correlated with poor patient prognosis (Setti et al., 2013). Furthermore, when looking at cell subtypes, CLIC1 was found to be expressed in GB cells of the mesenchymal subtype and was localized to the stem cell compartments such that its expression

was colocalized with SOX2 (Setti et al., 2013). Interestingly, when looking at CLIC1 localization without permeabilization of the cellular membrane, CLIC1 was found to be highly localized to the membrane of glioma stem cells (GSCs), but this effect was not observed in neural progenitor cells (NPCs). This observation was accompanied by CLIC1 chloride conductivity experiments, using a patch clamp system, in which it was demonstrated that CLIC1-mediated chloride current was highly active in GSCs compared to NPCs (Setti et al., 2013). This suggests that the chloride current mediated by CLIC1 in its membrane form in GSC is contributing to tumorigenesis (Setti et al., 2013). In support of this hypothesis, knockdown (KD) of CLIC1, thereby reducing Cl^- current via CLIC1 in GSCs induced a significant decrease in proliferation/viability measured by Bromodeoxyuridine (BrdU) and 3-(4,5-dimethylthiazol-2-yl)-2,5-diphenyltetrazolium bromide (MTT) assay, stemness measured by methylcellulose assay, and glioblastoma development in a murine model (Setti et al., 2013). Furthermore, CLIC1 KD was shown to sensitize chemo-resistant GB lines to Carmustine (BCNU) treatment, an alkylating agent used alone or in combination for the treatment of some cancers, including brain cancer and lymphoma (Kang & Kang, 2008). Of note, CLIC1 activity in tumour cells is not the only mechanism by which CLIC1 may be contributing to tumorigenesis. It has been suggested that CLIC1 is a secreted product packaged in extracellular vesicles (EVs) and can target neighbouring cells such as other GB cells or CSCs (Setti et al., 2015). In the neighbouring cells, endocytosis of EVs containing CLIC1 is thought to be mediated by Transient Receptor Potential Cation Channel Subfamily M Member 7 (TRPM7) possibly regulating Ca^{2+} spikes, although the mechanism of release from the cell of origin is still under investigation (Setti et al., 2015; Thuringer et al., 2018). Once received by the neighbouring cell, EVs generated from U87 MG cells producing CLIC1, induced significant proliferation in U87 MG glioblastoma cells. The effect on proliferation was increased form EVs generated from FLAG-tag plasmid overexpressing CLIC1 in U87 MG cells compared to control empty EVs. This effect was, however, terminated once EVs were depleted of CLIC1 using siRNA against CLIC1 (Setti et al., 2015). This data suggests that, not only does CLIC1 impact various aspects of tumorigenesis in its cell of origin, but it is also able to modulate the activity of neighbouring cells to favour a pro-tumorigenic environment (Kang & Kang, 2008; Setti et al., 2015; Setti et al., 2013).

A potential mechanism for the action of CLIC1 in GB cells seems to be via regulation of the cell cycle and changes to chronic stress in rapidly cycling cells (Peretti et al., 2018). It was

identified that following starvation conditions, 90% of GB cancer stem cells were in the G1 phase, however, upon plating in complete media, cells quickly progressed to S phase while cells that were treated with either a specific CLIC1 channel inhibitor (Indanyloxyacetic acid 94 – IAA-94) (Al Khamici et al., 2015) or a CLIC1 antibody (Santa Cruz Biotechnology, sc 81873), against the extracellular domain, had a longer transition period to G2-M phase along with a significant delay in upregulation of Cyclin D1 (Peretti et al., 2018). Additionally, ROS production plays a significant role in the cell cycle such that its production is essential for G1-S progression (Verbon et al., 2012). In cells treated with IAA-94 or a CLIC1 antibody, there was a significant shift in ROS production such that ROS levels were reduced while cellular acidification was increased leading to a slower cycling period (Peretti et al., 2018). This suggests that CLIC1 may have a direct impact on cell cycling through the modulation of other cellular factors such as ROS and pH. Interestingly, ROS production and Ca^{2+} current have been proposed to act bidirectionally, this means that Ca^{2+} modulates ROS production and ROS acts as a messenger molecule in regulating Ca^{2+} by modulating the activity of Ca^{2+} pumps and channels (Gordeeva et al., 2003; Görlach et al., 2015). Since CLIC1 has been found to play a significant role in mediating ROS production (Peretti et al., 2018), perhaps it may also, by extension, play a role in the regulation of Ca^{2+} currents, therefore implicating CLIC1 in a broader line of cellular processes (Lee et al., 2019).

Although taking CLIC1 inhibition to the clinic still requires considerable research, there have been efforts to use either repurposed compounds, such as phenformin, proguanil, cycloguanil and moroxydine, which are all known biguanide-related drugs similar to Metformin, or new compounds to selectively target CLIC1's channel activity in GB (Barbieri et al., 2022; Barbieri et al., 2018; Gritti et al., 2014). CLIC1 was initially identified as a possible target for Metformin, a commonly used drug for diabetes that was found to possess anti-tumoral activity in many cancers. Metformin selectively inhibited CLIC1 chloride current and induced anti-proliferative effects in glioma cancer stem cells but not in umbilical cord-derived mesenchymal stem cells (Gritti et al., 2014). However, the concentration at which Metformin was found to be effective for treatment was in the mM range, which was seen as not highly translatable to clinic, thus a turn to other biguanide class related drugs. These other drugs, including phenformin, proguanil, cycloguanil and moroxydine or newly synthesised compounds, demonstrated similar effects of anti-tumoral activity as Metformin, however their effective dosage was found to be significantly lower, many

of them being extremely functional and specific at the μM range (Barbieri et al., 2022; Barbieri et al., 2018). Together, this data suggests that CLIC1 may be playing a fundamental role in GB tumorigenesis and requires further research.

A.5 Identified functions of CLIC1

A.5.1 CLIC1 in metastasis, invasion, and angiogenesis

Cellular metastasis and the angiogenic process are key elements driving cancer progression (Martin et al., 2013). When researchers looked at different cancer models including gallbladder carcinoma, oral squamous cell carcinoma, and early or late-stage hepatocellular carcinoma, CLIC1 upregulation was significantly correlated with more aggressive migration of cells (Feng et al., 2019; Peng et al., 2021; Wang et al., 2009). The metastatic potential was further elucidated when clonal lines were generated from the same gallbladder carcinoma line. Upon further analysis of the high metastatic clone, it was observed that there was a significant increase in CLIC1 expression compared to the low metastatic clone and the parental gallbladder carcinoma line that was used to generate the high and low metastatic clones (Wang et al., 2009). Experiments attempting to elucidate the mechanism by which CLIC1 contributes to metastasis and invasion have placed CLIC1 at the leading edge of the nascent cell adhesions (Peng et al., 2021). Furthermore, depletion of CLIC1 reduced and inhibited the formation of filopodia, lamellipodia, and invadopodia compared to control cells in which CLIC1 was again found to be localized to the leading edge of the formation (Gurski et al., 2015). In addition, experiments have demonstrated that CLIC1 has a role in angiogenesis through mediating branch point formations and enabling proper formation of capillary networks (Feng et al., 2019; Knowles et al., 2012). In looking at specific elements that are known to contribute to these processes in relation to CLIC1, prior research has identified that CLIC1 works with and regulates the expression of a variety of elements such as phosphatidylinositol-4-phosphate 5-kinase type-1 Alpha (PIP5K1A) and phosphatidylinositol-4-phosphate 5-kinase type-1 gamma (PIP5K1C), myosin light chain (MLC), various integrins and matrix metallopeptidase 2 (MMP-2), matrix metallopeptidase 9 (MMP-9), vimentin and E-cadherin (Feng et al., 2019; Gurski et al., 2015; Peng et al., 2021; Tung & Kitajewski, 2010).

A.5.2 CLIC1 and implications in drug resistance

A key factor determining cancer treatment outcome is the degree to which cancer cells are sensitive or resistant to therapy. Ion channels, and in particular chloride channels, have been studied such that their action has been found to mediate multi-drug resistance (MDR) (Kang & Kang, 2008; Wilczyński et al., 2021). MDR is the term given to cancer cells when they have failed to respond to multiple types of chemotherapeutic drugs that target a variety of pathways. This may suggest that the cancer is intrinsically resistant to certain types of chemotherapeutic drugs or it has gained resistance through mutations, adaptive responses or compensating mechanisms (Holohan et al., 2013). One mechanism used to render cells resistant is through drug efflux. This is accomplished by membrane transporter proteins, of which there have been three that are well described; Multi-Drug Resistance Protein 1 (MDR1), MDR-Associated Protein 1 (MRP1), and Breast Cancer Resistance Protein (BCRP) (Gottesman et al., 2002; Holohan et al., 2013). Like other chloride channels, CLIC1 was also found to be implicated in resistance to cancer therapy (Liu et al., 2017). Choriocarcinoma cell (JeG3) induced chemotherapy resistant lines were found to have upregulated CLIC1 expression compared to parental lines. Interestingly, in these cell lines CLIC1 was found to induce the expression of MRP1, suggesting that CLIC1 is a key mediator of cellular response to therapy (Wu & Wang, 2017). Another study similarly implicated CLIC1 in resistance to Vincristine through the transfer of CLIC1 in exosomes in gastric cancer. Importantly, exosomes collected from the supernatant of resistant cell lines were able to generate resistance in cell lines that were Vincristine sensitive. This data suggests that CLIC1 may be impacting drug resistance through extracellular effects on neighbouring cell populations (Zhao et al., 2019). Concurrently, CLIC1 vesicle transfer has further been implicated in glioma stem cell proliferation and mediation of the extracellular environment (Setti et al., 2015). By blocking the chloride current in these stem-like cells through the re-proposing of known pharmacological drugs, CLIC1 has shown to be a promising target for therapy (Barbieri et al., 2019; Gritti et al., 2014). These data suggest that expression of CLIC1 may be an adaptive mechanism used by cancer cells to become resistant to chemotherapy, although how CLIC1 expression itself changes in response to therapy has not been assessed.

A.5.3 CLIC1 and cell cycle

The cell cycle is a process by which one cell receives the necessary signals and undergoes a series of events to generate a fully functional daughter cell. The general steps for this process include, the resting phase (G0), the cycle gap 1 (G1) phase in which the cells grow in size, the synthesis (S) phase in which DNA is replicated, the gap 2 (G2) stage which is marked by another change in cell size, and the mitosis (M) stage in which the cell divides (Barnum & O'Connell, 2014). The cell cycle is such a critical and conserved process that the cell maintains strict paraments on the progression through the stages, regulated by checkpoints (Barnum & O'Connell, 2014; Hartwell & Weinert, 1989). One such checkpoint is at the end of the G1 phase, in which the cell commits to division (**Figure 6**). This checkpoint is marked by having adequate DNA integrity, quantity of growth factors, and nutrients along with having to meet the right size requirement for division. The size requirement of cells suggests that cells must increase their surface to volume ratio to allow adequate space for replicating DNA and increased nutrients for division to occur (Barnum & O'Connell, 2014). Cell volume homeostasis, accomplished by a variety of cellular ions, including chloride, is thus called into action (Strange, 2004).

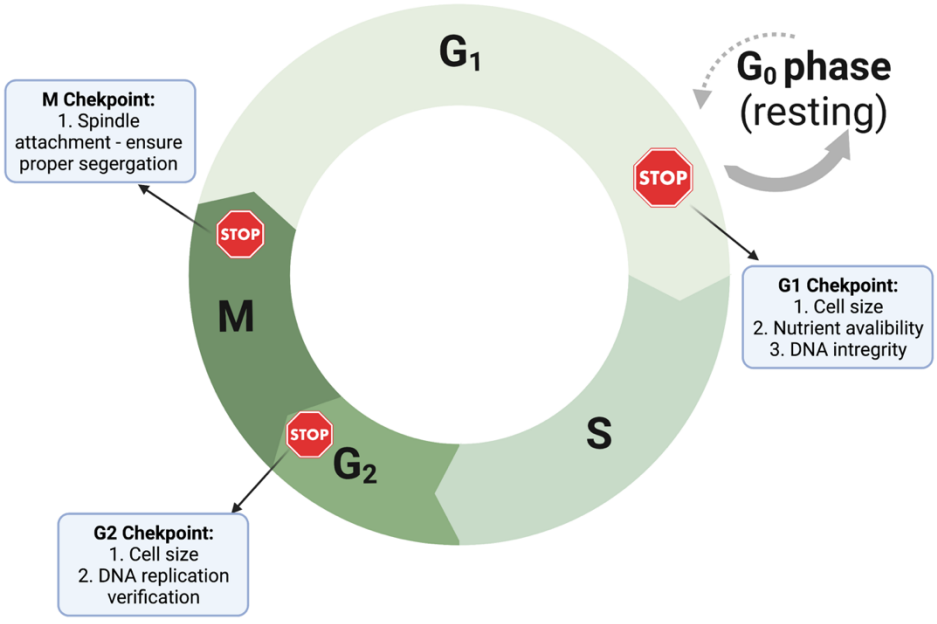

Figure 6. Cell cycle progression and key checkpoint requirements for proper progression. Resting phase (G0), gap 1 (G1), DNA synthesis (S), gap 2 (G2) and mitosis (M). The progression through the cell cycle is regulated by checkpoints (STOP); one at the end of G1, one in G2 and the last in M phase. Image generated using Biorender.com

Interestingly, CLIC1 is highly conserved across various species, including humans, mice and Arabidopsis where it is expressed in a large variety of tissues and cells. Furthermore, it is known to function in chloride ion conductance across the membrane (Littler et al., 2010). This led to the speculation that it may be involved in a key conserved biological mechanism, such as the cell cycle (Valenzuela et al., 2000). Early experiments looking specifically at this hypothesis in Chinese Hamster Ovary cancer cell lines (CHO-K1) identified that CLIC1 chloride conductance, measured using patch clamp experiments, varied along different stages of the cell cycle. Specifically, increased conductance across the membrane was identified in the G2/M transition phase. Importantly, once the conductance was inhibited using a CLIC1 inhibitor, IAA-94, cells were stuck in the G2/M transition (Valenzuela et al., 2000). However, since these first experiments, there has been conflicting evidence suggesting that CLIC1 may be impacting different stages of the cell cycle. A study looking at the cell cycle progression in GB identified that CLIC1 current was most highly active during the G1 phase and inhibition of CLIC1 current elongated the G1/S transition (Peretti et al., 2018). Yet, other studies have placed CLIC1 along with CLIC4 at the cytokinesis interphase suggesting it has a role in the final separation between cells (Kagiali et al., 2020). Furthermore, although additional research must be conducted to investigate if CLIC1 is cell cycle regulated, there is speculation that the cell cycle may impact the activity of CLIC1 through the oxidative fluctuations that occur during cell cycle progression (Menon & Goswami, 2007). CLIC1's transition to the membrane and its subsequent activation as a chloride channel is proposed to occur in response to changing oxidation states of the cell (Harrop et al., 2001; Littler et al., 2004). Interestingly, research speculation has suggested the possible involvement of oxidative fluctuation in the regulation of gene expression, thus it is not possible to rule out whether the cell cycle regulates CLIC1 itself (Menon & Goswami, 2007). Although there have been deferring conclusions about when CLIC1 is most involved in cell cycle progression or if CLIC1 itself is regulated by the cell cycle, it is clear that chloride conductance does play a role in the cell cycle by means of its ability to regulate cellular volume, a key component of the cell cycle

(Francisco et al., 2020; Miyazaki et al., 2008; Shiozaki et al., 2011). Of note, regulation of cell volume by CLIC1 outside of the cell cycle has been proposed to be enacted by CLIC1 mediating cellular regulatory volume decrease (RVD) in colorectal carcinoma (P. Wang et al., 2012). RVD is a process that enables cells to regulate their volume based on their surrounding hyper or hypotonic environments. For instance, if a cell becomes swollen because of excess osmotically active particles that induce water uptake, various ion channels and transporters will be open/active to engage the process of RDV and to ensure that the cell volume is regulated accordingly (Mongin & Orlov, 2001; Okada et al., 2001). Interestingly, RVD has been identified as a key mediator in cancer such that it plays a significant role in metastasis and migration of cancer cells (Zhou et al., 2019). This data suggests that the hypothesized cellular volume regulation generated by CLIC1 mediated Cl^- current may have a larger role to play in cancer progression, through its varied roles not only in the cell cycle where it is active in G1 and/or G2 phase, but also in metastasis and migration of cancer cells.

A.5.4 CLIC1 targets and related pathways

Analysis of protein-protein interactions and investigating the pathways in which a protein operates are two key elements in understanding the function of a gene or protein in the context of any pathological condition including cancer. Protein networks, along with transcriptional/regulatory and metabolic networks, all play a fundamental role in generating an interaction network to better understand complex biological phenomena. For instance, the functioning of proteins such as CLIC1 may change depending on the binding partners that it interacts with. In 2012, Jiang et al. described the role of CLIC1 and its interaction with the Rac family small GTPase 2 (Rac2), Ras homolog family member A (RhoA) and ERM (Ezrin/Radixin/Moesin) proteins. Interaction of these proteins with CLIC1 was shown to lead to a wide range of events including proper macrophage function by means of phagosomal acidification (Jiang et al., 2012). Yet other research has identified CLIC1 as an interacting partner with fluorescein-conjugated cyclic decapeptide (CLT1) to regulate angiogenic properties (Knowles et al., 2012) as well as with integrins such as integrin subunit beta 1 (ITGb1) and integrin subunit alpha 10 (ITGa10) where it plays a role in the regulation of the MAPK/AKT pathway (Li et al., 2018). Recently, CLIC1 has been implicated in the progression and growth of medulloblastoma

through its physical interaction with a potassium channel, the Ether-A-Go-Go Potassium Channel 2 (EAG2). This interaction is mediated by lipid rafts at the cell membrane, where these channels cooperate to regulate cell volume and thus, play a significant role in growth of medulloblastoma cells both *in vitro* and *in vivo* (Francisco et al., 2020).

CLIC1 has also been found to play a role in myc/c-myc signalling, in which CLIC1 directly interacts with c-myc to create a positive feedback loop for the transcription of CLIC1 and the activation of c-myc downstream targets (Jiang et al., 2020). The MYC oncogene family is a tightly regulated family at the level of transcription, translation, protein expression and degradation for which the myc protein acts as a transcriptional regulator for multiple downstream targets and pathways. Myc proteins have been identified to be overexpressed or highly active in multiple cancers, for which it plays a role in almost all oncogenic properties including cell cycle, metabolism, DNA repair pathways, and signal transduction to name a few (Chen et al., 2018; Dang, 2012). Activation of c-myc is generated through extracellular receptor activity leading to signal transduction. One specific receptor highly documented for c-myc activation is interleukin 6 (IL-6) cytokine family receptors (Chen et al., 2018). Interestingly, both CLIC1 and OSMR, an IL-6 family receptor, are highly expressed in glioblastoma (Jahani-Asl et al., 2016; Setti et al., 2013) and have been identified as possible binding partners in our studies with Mammalian Membrane Two Hybrid – High Throughput Screen, as outlined in this thesis.

A.6 Mammalian Membrane Two Hybrid – High Throughput Screen

The Mammalian Membrane Two Hybrid (MaMTH) screening technology utilizes exogenous expression of a tagged 'Bait' protein and a 'Prey' library of proteins to identify both stable and transient protein-protein interactions that are taking place at the membrane (Petschnigg et al., 2014). Briefly, for the use in this thesis work, the OSMR (Bait) plasmid was generated with a C-terminus fused MaMTH-HTS Bait tag (C/ub) linked to an artificial transcription factor (GAL4TF) and expressing a blue fluorescent protein maker (BFP) by a P2A linker (C/ub-GAL4TF-P2A-tagBFP). This plasmid or OSMR expressing plasmid alongside EGFRvIII expressing plasmid were stability transfected into HEK293T cells that contained the MaMTH-HTS 'Prey' library. The library consisted of ~8000 open reading frames from the Human

ORFeome V8.1 collection (Yang et al., 2011). The 'Prey' proteins from this collection were fused to MaMTH-HTS Prey tag (N/ub) at their N-terminus and P2A-mCherry at their C-terminus. The reporter HEK293T cell lines also contained chromosomally integrated green fluorescent protein (GFP) under the control of the GAL4TF promoter. In the instance that a protein-protein interaction (PPI) were to take place between the 'Bait' and any of the 'Prey' proteins, the C/ub and N/ub of the respective proteins would meet and spontaneously form a psedo-ubequitin complex. This complex would then be targeted by a deubiquitinating enzyme that would cleave the artificial transcription factor (TF) and allow it to travel to the nucleus where it would bind DNA at the GAL4TF promoter to induce GFP expression (Lim et al., 2022; Petschnigg et al., 2014; Saraon et al., 2017) (**Figure 7**). Using fluorescence activated cell sorting (FACS), the presence of an interaction was assessed based on the expression of GFP while the presence of each individual plasmid was monitored by the expression of the blue fluorescent protein (BFP) or mCherry, respectively. However, the identity of the interacting protein was determined by sequencing of ORF's using IlluminaHiSeq2500 technology. One of the main advantages of using this system to identify protein-protein interactions is the use of mammalian cells, which allows the biochemical structure of proteins to remain intact in a more natural environment. The MaMTH screening technology was developed following the use of Membrane Yeast Two Hybrid (MYTH) system in order to overcome the issue surrounding the expression of recombinant proteins in a foreign host such as yeast cells used in the MYTH technology (Iyer et al., 2005; Saraon et al., 2017). This allowed the MaMTH system to be highly sensitive to subtitle changes and elements/factors that only occur in the natural environment of the cell, such as those that occur in higher order mammalian cells (Saraon et al., 2017). Additionally, with the advent of high throughput screening, the MaMTH system can be used to identify many interactions with relatively small amounts of material (Lim et al., 2022). Although the use of mammalian cells has drastically improved the sensitivity of this assay some limitations remain, one of which is the high probability of identifying false positive interactions, or the possibly of ending up with missed interactions due to false negatives (Schneider et al., 2016). This may occur as a result of the cell type that is used when conducting this screen. For instance, in the context of this thesis work, the MaMTH-HTS was performed in HEK293T cells and, although this is a tumorigenic cell line, it may not recapitulate all the environmental and biochemical elements of brain tumour stem cells (BTSCs). Thus,

following this kind of screen it is imperative to validate results through additional methods that allow the interaction to be identified in its cell of interest.

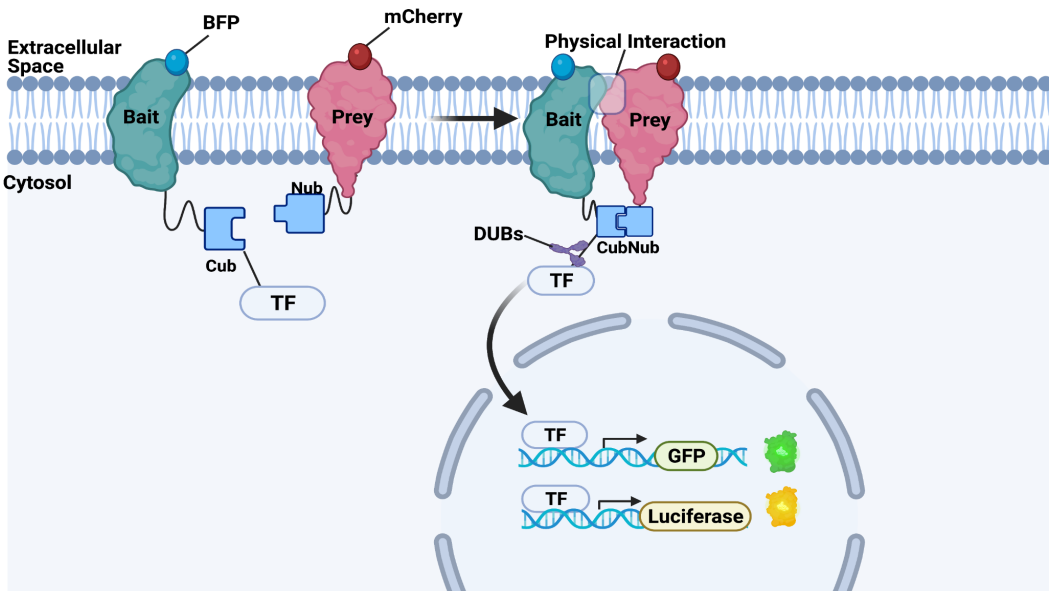

Figure adapted using BioRender.com from Petschnigg et al., 2014 in Nature Methods

Figure 7. The 'Bait' protein (green) is a modified protein of choice containing a BFP marker, C-terminus ubiquitin (Cub) and a chimeric transcription factor (TF). The 'Prey' protein (pink) is a modified protein containing a mCherry marker, and a N-terminus ubiquitin (Nub). In the event that a protein-protein interaction occurs between the 'Bait' and 'Prey' proteins, the Cub and Nub will form a pseudo-ubiquitin complex which will recruit deubiquitinating enzymes (DUBs) that will cleave the chimeric transcription factor. The transcription factor will induce the expression of either GFP or Luciferase once bound to its promoter sequence. The 'Bait' protein must be a membrane protein whereas the 'Prey' protein may be a membrane protein (as shown) or may be membrane associated (Petschnigg et al., 2014).

A.7 Hypothesis and Objectives

Research has suggested that OSMR is greatly involved in glioblastoma progression through mediating and actively taking part in multiple pathways, including as A) a co-receptor for EGFRvIII inducing a positive feedback loop with STAT3, B) a key factor mediating transition to

a mesenchymal-like state, C) a key regulator of mitochondrial respiration in BTSC and, D) a regulator of the immune microenvironment. Considering these data, I hypothesize that OSMR is impacting different aspects of glioblastoma progression through partnering with different proteins in a context-dependent manner. We have identified potential OSMR binding partners through a MaMTH-HTS screen. The subject of this thesis is to investigate one of these partners, namely the Chloride Intracellular Channel 1 (CLIC1), which appears to contribute to different hallmarks of cancer including glioblastoma. In this thesis project I pursued the following aims:

1. Analyse and validate relevant binding partner(s) based on Mammalian Membrane Two Hybrid – High Throughput Screen (MaMTH-HTS) hits
2. Establish that CLIC1 interacts with OSMR
3. Assess the role of CLIC1 in patient-derived brain tumour stem cells

B. Methods and materials

B.1 Cell lines and brain tumour stem cell (BTSC) culture

Human BTSC lines 73 and 147 were a generous gift from Dr. Samuel Weiss at the University of Calgary. These cell lines were characterized for major known glioblastoma mutations including, Epidermal Growth Factor Receptor Variant III (EGFRvIII), Tumour Protein P53 (p53), Phosphatase and Tensin Homolog (PTEN), and Isocitrate Dehydrogenase 1 (IDH1) (Jahani-Asl et al., 2016). The cell lines used in this study include BTSC73 and BTSC147 that harbour the EGFRvIII mutation. Prior to use in experiments, BTSC lines were thawed from a cryopreserved state (10% dimethyl sulfoxide – DMSO) and placed in BTSC media containing serum free NeuroCult NS-A medium (StemCell Technologies, Inc., #05750), supplemented with 100 U/mL penicillin, 100 µg/mL streptomycin (Sigma Aldrich, P4333), heparin (2 µg/mL, StemCell Technologies, Inc., #07980), human EGF (20 ng/mL, Miltenyi Biotec, #130-093-825), and human FGF (10 ng/mL, Miltenyi Biotec, #130-093-838) (**Table 1**). Cultures were kept in T-75 or T-25 culture flasks for cells in suspension (Sarstedt #833911502, 833910502) and grown as spheres in suspension. All cell lines were subject to analysis for presence of mycoplasma using the PCR method described in 2011 by Uphoff & Drexler (Uphoff & Drexler, 2011). Passaging of BTSC spheres was done every 3-7 days or once spheres reach 200-250 µm in size. This was accomplished by collecting media containing BTSC spheres followed by centrifugation at 1000xg for 10 min. Cells were dissociated into a single cell suspension by incubating with 0.2mL Accumax dissociation solution (Innovative Cell Technologies, #AM105) for 10 minutes at 37°C, followed by the addition of 0.8mL BTSC media. Cells were counted using Trypan Blue Stain 0.4% (Gibco, #15250-061) and were re-plated on low attachment flasks for suspension containing BTSC media. Cell plating densities were determined based on the size of the plating vessel (T-75 or T-25 flask) and the duration of the desired incubation (3-7 days) (**Table 2**).

Table 1: Preparation of BTSC media

Reagent	**Final Concentration**	**Volume**
Streptomycin (50 mg/mL)- penicillin 50,000 U/mL	0.5mg/mL:500U/mL	500 µL
Heparin (2 mg/mL; 1000 IU/mL)	2ug/mL:1IU/mL	50 µL
Human EGF (40 mg/mL)	20ug/mL	25 µL
Human FGF (20 mg/mL)	10ug/mL	25 µL
NeuroCult NS-A medium	N/A	49.4 mL
Total	N/A	50 mL

Table 2: BTSC plating densities for maintenance

Platting Vessel	**Number of cells for 2–3 days of incubation**	**Number of cells for 6–7 days of incubation**	**Volume BTSC Media**
T-75 flask	3.0×10^6	7.5×10^5	7 mL
T-25 flask	1.0×10^6	2.5×10^5	3 mL

B.2 Generation of transient CLIC1 knockdown by short interfering RNA (siRNA)

Short interfering RNA (siRNA) was used to generate a transient knockdown (KD) of CLIC1 in patient-derived BTSC147. BTSCs were processed into a single cell suspension. ON TARGET-plus SMART pool human CLIC1 siRNA (Dharmacon, #L-009530-00-0005) at a concentration of 100nM, and ON TARGET-plus non-targeting pool (Dharmacon, #D-001810-10-05), at a concentration of 100nM, was delivered to patient-derived BTSC147 (10^6) cells using electroporation by the AMAXA nucleofector 2b device, set at 1300 volts (Lonza, #AAB1001). Electroporated cells were plated in a T-75 culture flask for cells in suspension containing BTSC media and incubated at 37°C and 5% CO_2. Plating for experiments took place 24 hours after electroporation, while collection of cells for gene expression analysis by RT-qPCR and protein expression by immunoblotting was done 72 hours after electroporation.

B.3 Generation of transgenic BTSC lines

CRISPR-CAS9 technology was used to generate a stable knockout or knockdown of the CLIC1 gene located on chromosome 6 in patient-derived BTSC147 and BTSC73. To design the gRNA, Off-Spotter software (https://cm.jefferson.edu/Off-Spotter/) was used. Two guide RNA strands (Forward and Reverse complement) were generated to target exons 5-9 of the CLIC1 gene. To generate the construct, the Golden Gate Assembly Cloning strategy (Engler et al., 2009) was used in which gRNA1 and gRNA2 were cloned into pL-CRISPR.EFS.GFP (Addgene plasmid #57818), and pL-CRISPR.EFS.tRFP (Addgene plasmid, #57819), plasmids respectively according to **Table 3**. The thermocycler was then used to generate the plasmid based on the following parameters: Cycle 1 to 20 at 37°C for 5 min followed by 5 min at 20°C and Cycle 21 for 20 min at 80°C. Plasmids were amplified in competent Escherichia coli (E.coli; Invitrogen One shot OmniMAX 2-T1, #C8540-03) then extracted from bacteria and sent for sequencing (Genome Quebec) to verify the sequence of the gRNA in each plasmid construct. Once the plasmid sequencing was completed by Genome Quebec, the gRNA sequences were cross referenced with the plasmid sequence to verify if the gRNA sequences had been inserted into their respective plasmid. Electroporation at 1300 volts by the AMAXA nucleofector 2b device (Lonza, #AAB1001) was used to deliver 3µg of each plasmid construct (gRNA1-GFP and gRNA2-RFP) to ~2 million cells of patient-derived BTSC147 or BTSC73. Following electroporation, cells were collected from the electroporation cuvette and transferred to a T-75 low attachment flask with 7 mL of BTSC media and incubated at 37°C in a 5% CO_2 incubator. 48 hours after electroporation with each plasmid, spheres were dissociated into a single cell suspension using Accumax dissociation solution (Innovative Cell Technologies, #AM105) and subject to fluorescent activated cell sorting (FACS) analysis using the BD FACSAriaTM Fusion (BD Biosciences) to sort for double positive GFP/RFP cells. Sorted cells were plated at a density of 1 cell/well into two 96 well plates containing 100µl of BTSC media. Wells were monitored every two days to assess sphere formation. Clonal samples were collected from multiple positive clones and were subject to genomic DNA isolation. Isolated DNA was analysed by PCR using internal primers and external primers to the gRNA guided CAS9 cut site, designed using Primer3Plus software (https://www.primer3plus.com/) to determine mono-allelic, bi-allelic or non-deletion clones. Mono-allelic deletion clones were determined by PCR in which the presence of one internal and

one external band, suggested a possible knockdown, while a bi-allelic deletion was determined by a single external band. This suggested a possible knockout, on a 2% Agarose gel. Knockout or knockdown of CLIC1 was validated using RT-qPCR to determine gene expression and immunoblotting to determine protein expression. Since there were no clones identified that presented no cuts in the CLIC1 gene following incubation with the CRISPR-CAS9 construct, the chosen control for my experiments using the CRISPR-CAS9-CLIC1 cells was that of the parental BTSC73 or BTSC147 line. Although this method was used, future experiments could employ the use of a control gRNA non-targeting sequence. The following gRNA and primer sequences were used in this method:

gRNA1-*CLIC1*-Fwd: caccGTCAACGGTGGTAACATTGA

gRNA1-*CLIC1*-RC: aaacTCAATGTTACCACCGTTGAC

gRNA2-*CLIC1*-Fwd: caccGTACCGATGCACTCCCCGGA

gRNA2-*CLIC1*-RC: aaacTCCGGGGAGTGCATCGGTAC

CLIC1 Internal-Fwd: TAGCTGAGGTTCCTCCCAGG

CLIC1 Internal-Rev: TATTCCTCCCAGGACCCAGG

CLIC1 External-Fwd: AGGGACTGGCCTAGGGATG

CLIC1 External-Rev: AAAATGGAGGGGGTTGAGGG

Table 3: Golden Gate Cloning PCR mix for each gRNA

Reagent	**Final Concentration**	**Volume**
Addgene Plasmid (#57818, #57819)	100ng/ul	1 µL
Annealed gRNA oligonucleotide	1µM	1 µL
Restriction enzyme buffer R3.1 (New England Biolabs, #B6003S)	10x	5 µL
BbsI/BSMBI-v2 restriction enzyme (10,000U/mL, New England Biolabs, #R0739S)	5,000U/mL	2 µL
Adenosine 5'-triphosphate – ATP (100mM, BioBasics, #AB0311)	10mM	5 µL
Bovine Serum Albumin – BSA (BioShop, # ALB001.250)	5mg/mL	1 µL
T4 DNA ligase (400,000U/mL, New England Biolabs, #M0202S)	2,000,000U/mL	1.875 µL
Autoclaved water	N/A	33.11 µL
Total	N/A	50 µL

B.4 Gene expression analysis by RT-qPCR

RNA was extracted from cells using the TRIzol method. In this method, pelleted cells were incubated with 1mL TRIzol digestive reagent (Invitrogen, #15596026) at room temperature (22-25°C) for 5 minutes. Next, 0.2mL chloroform (Sigma Aldrich, #288306) was added to the samples and shaken vigorously for 20 seconds followed by a 2-3 minute incubation at room temperature (22-25°C). Samples were then centrifuged for 15 minutes at 12 000xg, 4°C after which 0.5mL of the upper aqueous phase was added to a clean tube containing 0.5mL isopropanol. Samples were again incubated at room temperature (22-25°C) for 15 min followed by centrifugation at 12 000xg for 10 min, 4°C. Resultant supernatant was removed from each sample and the RNA pellet was washed first with 75% ethanol and then with 100% ethanol. Each wash step was followed by centrifugation at 7500xg for 5 min (4°C). Supernatant was removed and RNA samples were left to dry for 10 minutes at room temperature (22-25°C) in a sterile biological hood. The RNA pellet

was dissolved in 20-50µl RNase-free water and incubated at 55-60°C for 10-15 minutes to ensure RNA dissolution. cDNA was obtained by reverse transcription using the 5X All-In-One RT MasterMix cDNA synthesis system (abm, #G592). Gene expression data was obtained from RT-qPCR analysis using the fluorescent dye, SYBR Green, (Biorad, #1725271) and primers, as described in **Table 4**, by combining 1µl of 5mM forward primer, 1µl 5mM of the reverse primer and 5µl SYBR Green to make the PCR mix. This mix was used to generate a final plated mix of 3µl of 30ng cDNA and 7µl PCR mix that was run on the QuantStudioTM 7 Flex Real-Time PCR System (Applied Biosystems). mRNA expression levels were normalized to one of two housekeeping genes: beta-glucuronidase (*GUSB*) or beta-Actin (*ACTB*). Table 4 describes all the primers that were used.

Table 4: qPCR primers used to assess gene expression

Gene	**Forward Primer Sequence**	**Reverse Primer sequence**
GUSB	GCGTTCCTTTTGCGAGGAGA	GGTGGTATCAGTCTTGCTCAA
ACTB	CAGCAGATGTGGATCAGCAAG	GCATTTGCGGTGGACGAT
OSMR	ACTGGAACCTGCCACAGAGT	TCCAAGCTCACAATTCTCCA
CLIC1	ACCGCAGGTCGAATTCTTC	ACGGTGGTAACATTGAAGGTG

B.5 Immunoblotting and antibodies

Total protein from samples was harvested from a minimum of $5x10^5$ cells using 1x RIPA Buffer (Thermo Fisher Scientific, #89900) supplemented with protease and phosphatase inhibitors (Thermo Fisher Scientific, #A32959). Following cell lysis, protein concentration was assessed using the Bradford Assay (Bio-Rad), after which samples were run on a 10-15% SDS-PAGE gel and transferred to a Nitrocellulose Membrane 0.45um (Bio-Rad, #1620115) for 1 hour and 30 minutes at 100 volts. Membranes were blocked for non-specific binding using 5% bovine serum albumin (BSA) in 1X TBST for 1-2 hours. Membranes were then probed using primary antibodies overnight at 4°C followed by Horseradish peroxidase (HRP) -conjugated secondary antibodies in

5% BSA blocking solution. Proteins of interest were visualised by ClarityTM Western ECL Subtrate (BioRad, 170-5060) using the ChemiDoc Imaging System (Biorad). The antibodies used for immunoblotting include, anti-OSMR (1:100, Santa Cruz Biotechnology, sc-271695, mouse), anti-CLIC1 (1:200, Santa Cruz Biotechnology, sc-81873, mouse), α-Tubulin (1:5000, Abcam, ab4074, mouse), HRP-conjugated secondary antibody (1:5000, BioRad, 1706516, mouse).

B.6 Duolink Proximity Ligation Assay (PLA)

Proximity Ligation Assay was performed following the manufacturer's protocol using the Duolink *In Situ* Red Starter Kit (Sigma, #DUO92101) but optimized by our group (Sharanek & Raco et al., 2022) for use in BTSCs. Briefly, single cell BTSC suspension was plated on a Nunc Lab-Tek, II CC2 Chamber Slide System (Thermo Scientific, #154941) that was coated overnight with a poly-d-lysine (PDL) coating. The working PDL solution (10 μg/mL) was made from a 2 mg/mL stock (Fisher Scientific, # CB-40210) using sterile water and incubated on the chamber slide overnight at 37 °C and washed thoroughly (3 times) with sterile water prior to addition of the single cell suspension. Following Accumax (Innovative Cell Technologies, #AM105) dissociation, the single cell suspension was plated at a density of ~$2.5x10^4$ cells in media containing 10% FBS for 1 to 6 hours; until cells had visible projections. Following incubation, cells were quickly washed with 1x PBS and fixed using 4% paraformaldehyde for 15 min at room temperature (22-25°C). Next, samples were washed with 1x PBS and permeabilized using 0.5% Triton X-100 for 25 min and subsequently blocked for non-specific binding for 1 hour using the Duolink Blocking Solution provided in the starter kit with agitation at 37°C. Samples were then incubated overnight at 4°C in a humid chamber with primary antibodies against the protein of interest: anti-OSMR (1:200, Abnova, H00009180-D01P, rabbit) and anti-CLIC1 (1:200, Santa Cruz Biotechnology, sc-81873, mouse). Following overnight incubation, samples were washed with Wash Buffer A (available in the Starter Kit) and incubated with the PLUS and MINUS oligonucleotide probes conjugated to secondary antibodies for 1 hour at 37 °C in a humid chamber. Samples were subsequently washed with Wash Buffer A and incubated with ligation Buffer with ligase (available in the Starter Kit) for 30 min at 37°C in a humid chamber. Rolling circle amplification (RCA) was achieved by washing samples with Wash Buffer A and incubating with polymerase and amplification solution (available in the Starter Kit) containing nucleotides for 100 min at 37 °C in

a humid chamber and protected from light. Following RCA, samples were washed with Wash Buffer B and mounted with Duolink *In Situ* Mounting Medium with DAPI (DUO82040, Sigma). PLA signals were visualized and captured by a scanning microscope (Olympus LS, IXplore Pro Automated Microscope system) equipped with the adjoining imaging software (Olympus LS, cellSens Version 1.12) at 40-60x objective magnification.

B.7 Cell population growth assay

BTSC spheres were processed into a single cell suspension using Accumax dissociation solution (Innovative Cell Technologies, #AM105). Single cells were plated at a density of 30,000 or 50,000 cells per well (6 well plate) in 2mL BTSC media for CRISPR-CAS9 clones and siRNA experiments, respectively. 1 day (24 hours), 3 days (72 hours) and 7 days (168 hours) following plating, cells were collected, and live cells were assessed using trypan blue exclusion dye (Gibco #15250-061). This dye differentiates live and dead cells by the uptake or lack of uptake of a blue dye. Counts were done using an automated cell counter (Countess II FL Automated Cell Counter).

B.8 Sphere size assessment

Sphere size assessment was used to determine any differences in size between BTSC wild type (WT) spheres, or spheres generated from either siRNA transient knockdown or CRISPR-CAS9 stable knockdown, or knockout. BTSC spheres were collected and processed into a single cell suspension using Accumax dissociation solution (Innovative Cell Technologies, #AM105). Cells were plated as follows: 3 to 6 well containing 500, 250 and 125 cells respectively, in 100µl of BTSC media in a 96 well plate. This was done in order to ensure that sphere size was not impacted by the density of plating. 72 hours following plating and incubation, sphere size was assessed, and visualization was captured using a scanning microscope (Olympus LS, IXplore Pro Automated Microscope system) equipped with the adjoining imaging software (Olympus LS, cellSens Version 1.12) using the ‘Measure’ feature at 10-20x objective magnification.

B.9 Extreme Limiting Dilution Assay (ELDA)

ELDA was performed by first generating a single cell suspension and followed by dilution using BTSC media containing serum free NeuroCult NS-A medium (StemCell Technologies, Inc., #05750), supplemented with 100 U/mL penicillin, 100 µg/mL streptomycin (Sigma Aldrich, P4333), heparin (2 µg/mL, StemCell Technologies, Inc., #07980), human EGF (20 ng/mL, Miltenyi Biotec, #130-093-825), and human FGF (10 ng/mL, Miltenyi Biotec, #130-093-838) to generate a final plated density of 25, 12, 6, 3 and 1 cell per well. 100µl of the diluted single cell suspensions was plated in a 96 well plate as follows: 12 wells plated for dilution 25, 12, 6 and 3 cells per well and 48 wells (4 replicates of 12 wells) plated for 1 cell per well dilution. This was done for 1 cell per well plating to achieve comparable results as many times single cell death can occur following plating. Plates were incubated at 37°C and 5% CO_2 for 7 days after which sphere formation was assessed. Analysis of the responding wells as a function of the plated wells was undertaken and data (**Table 5**) was input into an online software available at https://bioinf.wehi.edu.au/software/elda/. Using these data provided by the software, the number of cells required to generate a positive well (having a sphere) was determined for each condition. Stem cell frequency (SCF) or the probability of finding a stem cell in the bulk sample of cells was also given as a value of 1/stem cell frequency. To determine percent stem cell frequency (SCF) 1/stem cell frequency was multiplied by 100.

Table 5: ELDA data recording for input into software

Cell dilution	Number of wells plated	Number of response wells	Condition
25	12	12	CTL
12	12	12	CTL
6	12	12	CTL
3	12	12	CTL
1	12 x 4	22	CTL
25	12	12	CRISPR8
12	12	9	CRISPR8
6	12	7	CRISPR8
3	12	6	CRISPR8
1	12 x 4	14	CRISPR8

B.10 Mammalian Membrane Two Hybrid – High Throughput Screen (MaMTH-HTS)

To identify binding partners of OSMR in the presence and absence of EGFRvIII, Mammalian Membrane Two Hybrid (MaMTH) High Throughput Screen (HTS) technology was used as described by (Lim et al., 2022; Petschnigg et al., 2014). Briefly, a plasmid expressing OSMR 'Bait' protein with a C-terminus fused MaMTH-HTS Bait tag (Cub-GAL4TF-P2A-tagBFP) alone or a plasmid expressing EGFRvIII (fused with 3xFLAG at its N-terminus) was transfected alongside the OSMR 'Bait' plasmid into a pooled 'Prey' library of HEK293T MaMTH-HTS reporter cell lines. The library of reporter cell lines stably expressed members of the Human ORFemon V8.1 collection (~8000 open reding frames - ORF's) fused to MaMTH-HTS Prey tag (Nub) at their N-terminus and P2A-mCherry at their C-Terminus and contained a chromosomally integrated GFP reporter under the control of the GAL4 transcription factor (GAL4TF) promoter. Transfections were performed using X-tremeGene™ 9 Transfection Reagent (Roche, XTG9-RO) as specified by the manufacturer's protocol. In order to induce Bait and Prey expression, cells were grown for 2-3 days in the presence of 0.5ug/mL Tetracycline in the following conditions: 37°C, 5% CO_2 in DMEM containing 10% FBS and 1% Penicillin/Streptomycin media. Cells were then harvested by trypsinization and resuspended at a concentration of 1-2x10^6 cell/mL in Basic Sorting

Buffer (1xPBS, 5 mM EDTA, 25 mM HEPES pH 7.0, 1% BSA) and subjected to sorting by Flow Cytometry using BD FACs Melody (BD Biosciences). Cells were sequentially selected according to the following: tag-BFP fluorescence indicating 'Bait' expression, mCherry fluorescence indicating 'Prey' expression and GFP fluorescence indicating Bait-Prey interaction. Cells were collected for analysis in DMEM containing 25% FBS and centrifuged pellets were processed in Phire Tissue Direct Dilution Buffer (ThermoFisher Scientific). Amplification of ORF's was done using Phire Tissue Direct PCR Master Mix (ThermoFisher Scientific) and products were purified using QIAquick PCR Purification Kit (Qiagen). Purified PCR products were subjected to Nextera XT library preparation and deep sequencing using IlluminaHiSeq2500 system (150 bp single read). Sequencing data was processed and hits identified using a custom software developed using the R programming language and integrated Bowtie2 alignment tool (Langmead & Salzberg, 2012).

B.11 Statistical analysis

Statistical analysis between conditions was performed using a Student *t*-test in which the mean of n=3 replicates were compared between two conditions to assess significance. Analysis was undertaken with the aid of GraphPad software 7. Data is shown as a mean with standard deviation (mean ± SD). p-values less than 0.05 were considered significant and were marked with an asterisk as follows, $p < 0.05$ *; $p < 0.01$ **; $p < 0.001$ ***.

C. Results

C.1 Analysis of Mammalian Membrane Two-Hybrid High Throughput Screen

Recent studies have led to the identification of OSMR as a key oncogenic player in glioblastoma, specifically in EGFRvIII-expressing tumour cells. Genome-wide studies revealed that OSMR shares a common gene network with EGFRvIII as part of the same receptor complex and yet OSMR possesses unique downstream targets not shared by EGFRvIII (Jahani-Asl et al., 2016). This led to the question of how OSMR interacts with other key oncogenic players to maintain its signalling in the absence and presence of EGFRvIII. To address this question, we performed a Mammalian Membrane Two-Hybrid High Throughput Screen (MaMTH-HTS) to unravel the possible interactions of OSMR in the presence and absence of EGFRvIII. Specifically, the aim of this screen was to identify how OSMR regulates glioblastoma tumorigenesis beyond its role in maintaining EGFRvIII/STAT3 signalling. High-Throughput Sequencing was carried out to identify target hits. This screening led to the identification of 750 hits for OSMR in the absence of EGFRvIII (OSMR-unique), 166 hits for OSMR in complex with EGFRvIII (OSMR/EGFRvIII) and 80 common hits between the two groups (**Figure 8**). Additional, analyses revealed 11 biological functional clusters of proteins for OSMR in the absence of EGFRvIII, and 7 biological clusters for the OSMR/EGFRvIII condition (**Figure 9**) (Mi et al., 2021). To begin to dissect membrane specific binding partners of OSMR and potential pathways that are activated in the absence and presence of EGFRvIII, candidate hits were categorized based on their location and function. Priorities were given to membrane associated candidates, integral membrane candidates and a co-receptor candidates for each group (**Table 6 - 7**).

Although detailed functional analysis of each of these clusters will lead to uncovering underlying molecular mechanisms of OSMR signalling in different subtypes of glioblastoma, we focused on the 80 common hits (**Table 8)** that were shared between cells expressing OSMR alone and cells expressing OSMR/EGFRvIII, and perhaps being implicated in a larger subset of glioma tumours (Abou-Fayçal et al., 2017; Gan et al., 2009). Using bioinformatic tools such as DAVID Functional Annotation analysis (Huang et al., 2009; Sherman et al., 2022) embedded with the clustering function, 37 out of the 80 (~46%) candidate interacting proteins were identified to be

associated with the membrane (**Table 8**). These candidates include proteins that are integral to the membrane as well as proteins that are associated with the membrane itself or interact with proteins embedded in the membrane. We focused specifically on 27 proteins that were integral to the membrane (**Table 9**). These 27 hits were of high interest because they, as well as OSMR, are embedded directly in the membrane and were seen as potential targets for therapeutic interventions that do not require uptake by the cell. Prior to follow-up validation, we set out to gain further insights into the identified 27 integral membrane proteins via employing various criteria pertaining to the known role of these proteins in regulation of glioblastoma and other human cancers, as well as our current knowledge of how these proteins impact different hallmarks of cancer, including proliferation, cell cycle, and stemness. In addition to the above criteria, MaMTH-HTS screening 'frequent flyers' were identified in the hit list from both conditions. This list of frequent flyers was generated from repeated MaMTH-HTS result from 10 individual 'bait' protein control experiments (Lim et al., 2022), and thus excluded from our analysis. This refining led to a total of 17 candidate hits from which the top 7 were chosen. The top 7 hits included: Cluster of Differentiation CD79A (CD79a), Synaptic Vesicle 2 Related Protein (SVOP), Adenosine A2a Receptor (ADORA2A), Chloride Intracellular Channel 1 (CLIC1), Lysophosphatidylcholine Acyltransferase 1 (LPCAT1), Presenilin 1 (PSEN1), and Teratocarcinoma-Derived Growth Factor 1 (TDGF1). Through additional literature analysis, Chloride Intracellular Channel 1 (CLIC1) was one of the candidate proteins selected for follow-up analysis. CLIC1 met several criteria including high expression in BTSCs and glioblastoma tumours (**Figure 10**).

CLIC1 is a member of the chloride intracellular family (CLIC1-6) in which it exists in both a soluble and a membrane bound form where it has the ability to act as an ion channel (Ashley, 2003; Gururaja Rao et al., 2020). It has been proposed that this protein is highly expressed in various cancers, including highly aggressive solid tumours such as glioblastoma (Setti et al., 2013) compared to surrounding tissues. Interestingly, CLIC1 has been identified as a potential target for therapy as its transition to the cellular membrane, where it acts as a chloride channel, is mediated by specific cellular conditions that are not favoured in normal healthy surrounding tissue (Littler et al., 2004). Additionally, CLIC1 is reported to mediate and/or enhance cellular resistance to standard of care cancer therapies. Together, these data suggest that CLIC1 may prove to be an interesting avenue of study considering that it has been linked to key events that enhance cancer

progression, aggressiveness and resistance to therapy on a cellular level. Different glioblastoma cellular subtypes have been identified including the proneural, classical, and mesenchymal subtypes, of which the mesenchymal subtype is thought to be the most aggressive in terms of recurrence and metastasis (Olar & Aldape, 2014; Sidaway, 2017; Zhang et al., 2020). Interestingly, similar to OSMR, which is found to be highly expressed in the mesenchymal subtype (Natesh et al., 2015), CLIC1 is also highly expressed in this subtype (Setti et al., 2013). In addition to these two proteins being identified as binding partners, their overall expression in the mesenchymal subtype may suggest that together they may have some role in mediating the aggressiveness of this subtype, potentially through intersecting pathways or mechanisms.

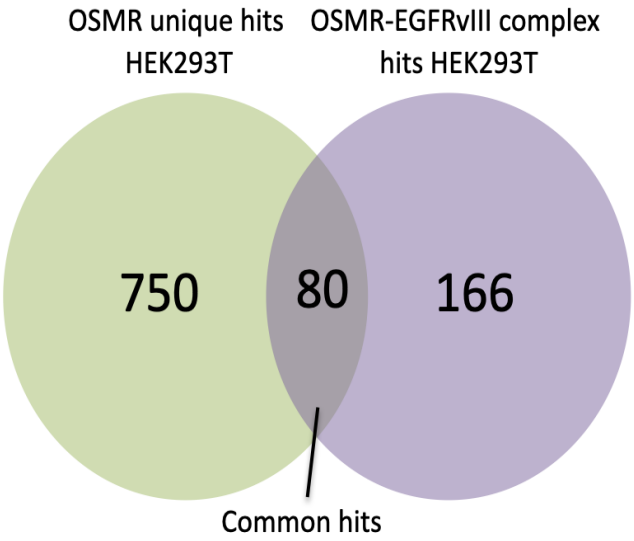

Figure 8. Protein-protein interaction hits in OSMR unique and OSMR/EGFRvIII complex in HEK293T cells. 750 hits were identified for OSMR in the absence of EGFRvIII while there were 166 hits identified in OSMR/EGFRvIII conditions. 80 hits were common between the two groups.

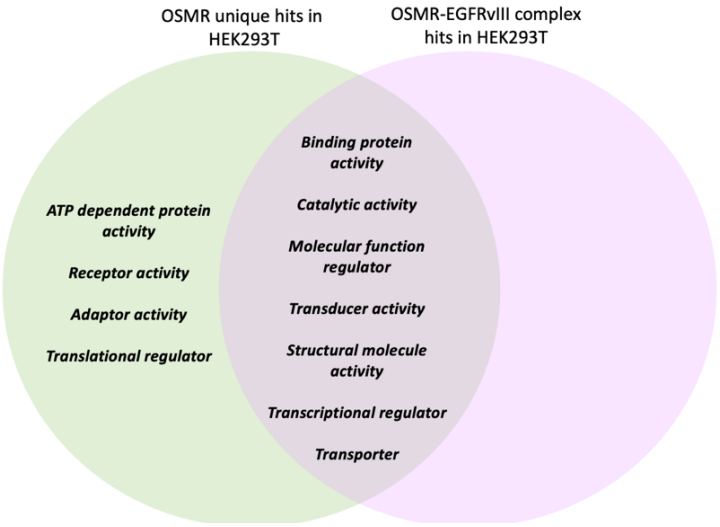

Figure 9. Biological functional clusters identified from OSMR unique and OSMR in complex with EGFRvIII. All functional clusters identified for OSMR/EGFRvIII complex were present in the OSMR unique grouping. Four functional categorizations were distinctive for OSMR unique.

Table 6. OSMR unique candidates for membrane associated proteins, integral membrane proteins and co-receptors

OSMR unique membrane associated candidates						*OSMR unique integral membrane candidates*					*OSMR unique co-receptor candidates*
DHCR24	NOX4	CLDN19	IFI27L1	PFDN4	SYNPR	DHCR24	ACVR1	IL20RB	RHBDD2	TMEM167B	HTR1E
HMGCLL1	ORMDL3	CLU	IL2RG	PRRG3	SYBU	ALG8	A4GALT	IL27RA	SERAC1	TMEM182	CLEC12A
HTR1E	PQLC2	CCDC136	IL20RB	PSCA	STX17	ATCAY	AOC3	KIR3DL2	SHISA5	TMEM220	CLEC12B
ARFGAP3	RAB5C	COG3	IL27RA	PDIA6	STX8	ABCA8	AIG1	KLRK1	SLAMF1	TMEM31	CLEC7A
ALG8	RAB9B	CRB3	KIR3DL2	PLP1	TAS2R38	BCAP29	AGTR1	LEPROT	SLC14A1	TMEM45B	CD36
ATCAY	REPS1	CYP1A1	KLRK1	PLP2	TEX261	BIK	ANKRD46	LRRC15	SLC18A1	TMEM56	F2RL1
ABCA8	RFT1	CYP19A1	LEPROT	P2RX6	TSPAN16	BCL2L2	ANTXR1	LHFPL1	SLC19A3	TMEM92	FCGR3B
ATP5C1	ARHGAP15	CYP51A1	LRRC15	QRFPR	TXNDC15	BSCL2	AIFM1	LHFPL5	SLC22A14	TPRA1	GPR12
ATP5L2	SEC22C	DYM	LHFPL1	RFTN2	TBXAS1	CXCL16	BTC	LPCAT4	SLC22A2	TNFSF13	GPR160
ATP1B4	ST3GAL1	DNTBP1	LHFPL5	RAMP3	TRPM1	CLEC10A	CHST15	LAMP1	SLC22A23	TTYH1	GPR161
BCAP29	ST6GAL1	ELMO1	LPCAT4	RAPSN	TOMM34	CLEC12A	CHST9	HLA-DQB1	SLC24A5	UCP2	GPR173
BCAP31	SUN3	EPHX1	LPGAT1	RTP3	TM4SF20	CLEC12B	CLN8	MALL	SLC25A32	VAMP4	ACVR1
BIK	SEC61A2	ERMAP	LAMP1	RDH11	TM9SF1	CLEC7A	CH25H	MAN1B1	SLC29A3	VKORC1L1	AGTR1
BCL2L2	TIMD4	EXT1	HLA-DQB1	RHBDD2	TMIGD1	CD36	C19orf12	MS4A4A	SLC30A2	VKORC1	ANTXR1
BSCL2	TMD3	EXT2	MALL	SERAC1	TMED2	CD48	C19orf39	MPPE1	SLC33A1	ZDHHC11	FFAR3
CXCL16	B3GNT2	FAM26E	MAN1B1	SHISA5	TMPRSS11E	CD68	C4orf3	MAOB	SLC35D1	ZDHHC17	GABRB2
CLEC10A	VSIG2	FIS1	MS4A4A	SCOC	TMEM106C	CD70	CLDN14	NRSN2	SLC37A2	ZDHHC19	GYPA
CLEC12A	VAPB	FMO2	MPPE1	SLAMF1	TMEM107	DRAM2	CLDN18	OR1L3	SLC39A7	ZDHHC4	HRH2
CLEC12B	VPS29	FFAR3	MAP1LC3B	SLC10A6	TMEM120A	DNAJB14	CLDN19	OR13J1	SLCA41	HTR1E	IL2RG
CLEC7A	YIPF2	FUT3	MAOB	SLC14A1	TMEM167B	DNAJC15	CCDC136	OR3A1	SLC44A5		IL20RB
CD36	ACVR1	FUT9	MYLIP	SLC19A3	TMEM116	DNAJC19	CRB3	OR4D1	SLC5A12		IL27RA
CD48	AP1S2	GABRB2	NRSN2	SLC22A14	TMEM182	ELOVL6	CYP19A1	OR5F1	SLC5A9		KIR3DL2
CD68	ADORA2	GABRG2	OR1L3	SLC22A2	TMEM220	ERCC5	CYP51A1	OR52B2	SLC6A14		KLRK1
CD70	CAP1	GABRR1	OR13J1	SLC22A23	TMEM31	ERGIC3	EPHX1	OR8B4	SCD		LAMP1
CAMKV	AIF1	GJA1	OR3A1	SLC24A5	TMEM45B	F2RL1	ERMAP	OR8H1	SFTPC		OR1L3
DDX19A	A4GALT	G6PC	OR4D1	SLC25A32	TMEM56	FCGR3B	EXT1	OLR1	SYPL1		OR13J1
DDX19B	AOC3	GBA	OR5F1	SLC29A3	TMEM92	GPR12	EXT2	PIGO	SYNPR		OR3A1
DRAM2	AIG1	GPAM	OR52B2	SLC30A2	TPRA1	GPR160	FMO2	PIGY	SYBU		OR4D1
DNAJB14	AGTR1	GPD2	OR8B4	SLC33A1	TNFSF13	GPR161	FFAR3	PLD3	STX17		OR5F1
DNAJC15	ANK1	GYPA	OR8H1	SLC35D1	TTYH1	GPR173	FUT3	PKD1L2	STX8		OR52B2
DNAJC19	ANKRD46	GLT8D2	OLR1	SLC37A2	USP32	HRASLS	FUT9	GALNT12	TAS2R38		OR8B4
EHBP1	ANTXR1	GLT8D1	PIGO	SLC39A7	UCP2	KIAA1524	GABRB2	GALNT5	TSPAN16		OR8H1
ELOVL3	AIFM1	HHATL	PIGY	SLC4A1	VAMP4	NOX4	GABRG2	GALNT8	TXNDC15		OLR1
ELOVL6	BTC	HMOX2	PISD	SLC44A5	VAMP5	ORMDL3	G6PC	PORCN	TBXAS1		PRAME
ERCC5	CACNG5	HK1	PDE4D	SLC18A1	VKORC1L1	PQLC2	GPAM	KCNJ15	TRPM1		P2RX6
ERGIC3	CHST15	HRH2	PLD3	SLC5A12	VKORC1	RFT1	GPD2	KCNJ5	TOMM34		QRFPR
F2RL1	CHST9	HOMER1	PKD1L2	SLC5A9	ZDHHC11	SEC22C	GYPA	PRAME	TM4SF20		RAMP3
FCGR3B	CLN8	HERPUD1	GALNT12	SLC6A14	ZDHHC17	ST3GAL1	GLT8D1	PFDN4	TM9SF1		SLAMF1
GNAO1	CH25H	HADHB	GALNT5	SNX12	ZDHHC19	ST6GAL1	GLT8D2	PRRG3	TMIGD1		TAS2R38
GPR12	C19ORF12	HSD17B2	GALNT8	SPG21	ZDHHC4	SUN3	HHATL	PLP1	TMED2		TRPM1
GPR160	C19ORF38	IRGM	PORCN	SPA17	ZYMND19	SEC61A2	HMOX2	PLP2	TMPRSS11E		
GPR161	C19ORF70	IGKC	KCNMB4	SPRY1		TIMD4	HERPUD1	QRFPR	TMEM106C		
GPR173	C4ORF3	IGKV1-5	KCNJ15	SCD		B3GNT2	HSD17B2	RAMP3	TMEM107		
HRASLS	CLDN14	IKBKB	KCNJ5	SFTPC		VAPB	IFI27L1	RTP3	TMEM116		
KIAA1524	CLDN18	IDE	PRAME	SYPL1		YIPF2	IL2RG	RDH11	TMEM120A		

OSMR/EGFRvIII complex memebrane asociated candidates	*OSMR/EGFRvIII complex intergral membrane candidates*	*OSMR/EGFRvIII complex co-receptos*
BCL2L1	BCL2L1	DGCR2
CD207	CD207	ANTXR2
DGCR2	DGCR2	LPAR6
GNAS	ANTXR2	MARCO
APBB1IP	CRAB3	MSR1
ANTXR2	EXTL3	OR2T33
CAMK1G	FADS2	CD207
CRAT	GPM6B	BCL2L1
EXTL3	LHFPL4	
FADS2	LPAR6	
GPM6B	MARCO	
LRRC57	MSR1	
LHFPL4	OR2T33	
LPAR6	SLC25A6	
MARCO	SLC35B3	
MSR1	TMEM174	
MGRN1	TMEM211	
OR2T33	ZP1	
PIGK		
KCNJ6		
SLC25A6		
SLC35B3		
SLC5A8		
TMEM174		
TMEM211		
ZC4H2		
ZP1		

Table 7. OSMR/EGFRvIII candidates for membrane associated proteins, integral membrane proteins and co-receptors

Table 8. All 80 OSMR unique and OSMR/EGFRvIII common candidates followed by the 37 OSMR unique and OSMR/EGFRvIII common membrane associate candidate binding partners

OSMR unique and OSMR/EGFRvIII complex common - all common candidates			OSMR unique and OSMR/EGFRvIII complex common - membrane associated candidates	
BCAP31	SPATA7	RGS13	ATK2	PGAP2
CLEC2B	PSEN1	FAM71C	BCAP31	KCNS2
GC	NFE2	TDGF1	BCL2L14	PSEN1
CLIC1	DCT	BCMO1	CLEC2B	RHBDD1
CXorf1	FKBPL	VAC14	CD79A	TDGF1
LRRIQ1	KCNS2	C11orf74	NAT8	TMPRSS6
NRM	LPCAT1	PBXIP1	PBXIP1	ZDHHC9
PTDSS1	C9orf80	ZUFSP	RAB1B	ZP1
IMMP2L	MAPK10	ADORA2A	ST3GAL4	
ST3GAL4	DIMT1L	HAUS8	SVOP	
ZP1	MRAS	LOC285074	VAC14	
RAB1B	PGAP2	NDUFAF1	ADORA2A	
CREB3	OXSM	PYGB	B3GALT2	
PIGK	PSD4	STRADA	CREB3	
C18orf62	SVOP	CGB	CLIC1	
TANK	B3GALT2	CGB2	CSGALNACT2	
DCN	IZUMO1	CGB5	CYYR1	
BCL2L14	CD79A	CGB8	DCT	
MAP4	LEPROTL1	RHBDD1	IMMP2L	
GLRX	BBS10	ZDHHC9	IZUMO1	
C8orf44	AKT2		LEPROTL1	
SLC35B3	MORC2		LPCAT1	
HIST1H3F	CYYR1		MAPK10	
SETD7	PEX16		MRAS	
CSGALNACT2	ZNF468		NRM	
NAT8	GEMIN8		PEX16	
EIF2C3	PYCR2		PIGK	
GPBP1	RDH12		PTDSS1	
TMPRSS6	CHCHD5		PSD4	
SRGAP1	LOC285735			

Table 9. Integral membrane hits identified from OSMR unique and OSMR in complex with EGFRvIII

OSMR unique and OSMR/EGFRvIII complex common - integral membrane candidates	
Candidate	**Description**
BCAP31	B Cell Receptor Associated Protein 31, chaperone protein of the ER with anterograde transport activity
CD79A	CD79a Molecule, B lymphocyte antigen receptor
NAT8	N-Acetyltransferase 8 (Putative), N-acetyltransferase
PBXIP1	PBX Homeobox Interacting Protein 1,transcriptional co-repressor by inhibiting PBX1homeodomain from being transcriptionally expressed
ST3GAL4	ST3 Beta-Galactoside Alpha -2,3-Sialytransferase 4, terminal sialylation on glycoproteins and glycolipids
SVOP	SV2 Related Protein, transmembrane transporter activity
ADORA2A	Adenosine A2a Receptor, G protein coupled receptor superfamily with activity in multiple intracellular signaling pathways
B3GALT2	Beta-1,3-Galactosyltransferase 2, part of the beta-1,3-galactosyltransferase (beta3GalT) gene family with membrane bound enzymatic activity
CREB3	CAMP Responsive Element Binding Protein 3, trascription factor activity
CLIC1	Chloride Intracellular Channel 1, chloride ion channel activity when inserted in the membrane
CSGALNACT2	Chondroitin Sulfate N-Acetygalactosaminyltransferase2, enzymatic activity
CYYR1	Cysteine and tyrosine Rich 1, type 1 transmembrane protein contaning a central cysteine and tyrosine domain - function not clear
DCT	Dopachrome Tautomerase, isomerase activity - blue light response
IMMP2L	Inner Mitochondrial Membrane Peptidase Subunit 2, enzymatic activity for processing signal peptides of proteins destined to the mitochondria
IZUMO1	Izumo Sperm-Egg Fusion 1, sperm cell surface ligand required for fertilization with receptor siganling activity
LEPROTL1	Leptin Receptor Overlapping Transcript Like 1, negative regulation of growth hormone receptor signaling
LPCAT1	Lysophosphatidylcholine Acyltransferase 1, enzymatic activity with a role in phospholipid metabolism
NRM	Nurim, homologous to isoprenylcysteine carboxymethyltransferase enzymes and has tight nuclear association
PTDSS1	Phosphatidylserine Synthase 1, enzymatic activity to catalyze the formation of phosphatidylserine
PGAP2	Post-GPI Attachment to Protein 2, protein involved in maturation of glycosylphosphatidylinositol (GPI) anchors on GPI-anchored proteins
KCNS2	Potassium Voltage Gated Channel Modifier Subfamily S Member 2, potassium channel activity when in complex with KCNB1 and KCNB2
PSEN1	Presenilin1, catalytic subunit of the gamma-secretase complex
RHBDD1	Rhomboid Domain Containing 1, intramembrane-cleaving serine protease
TDGF1	Teratocarcinoma-Derived Growth Factor 1, Nodal co-receptor activity
TMPRSS6	Transmembrane Serine Protease 6, membrane-bound serine protease
ZDHHC9	Zinc Finger DHHC-Type Palmitoyltransferase 9, Palmitoyltransferase for H- and N-RAS
ZP1	Zona Pellucida Glycoprotein 1, structual protein of the zona pellucida

C.2 Analysis of CLIC1 expression in BTSCs

Previous work with CLIC1 in glioblastoma has suggested that CLIC1 is highly expressed in GB and specifically highly expressed in glioma stem cells of the mesenchymal subtype (Setti et al., 2013). Gene expression analysis revealed that CLIC1 is highly expressed in BTSC147 and BTSC73, both harbouring the EGFRvIII mutation (**Figure 10**) in relation to a moderately expressed stable housekeeping gene, GUSB (Valente et al., 2009).

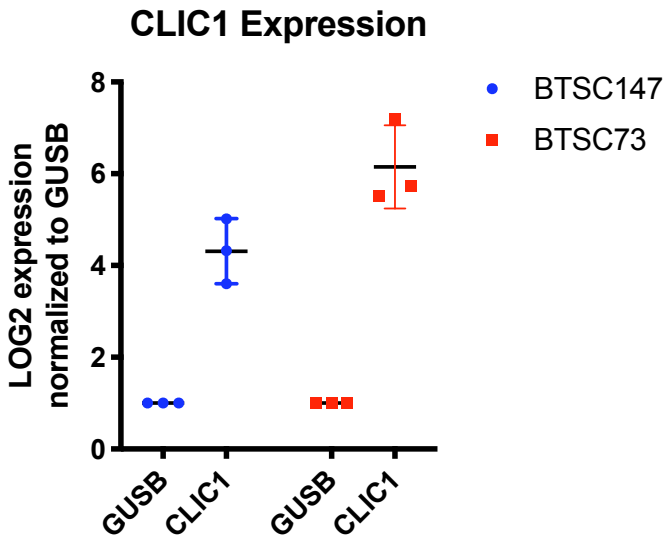

Figure 10. CLIC1 mRNA expression in patient-derived BTSCs

mRNA expression of CLIC1 with respect to GUSB quantified by RT-qPCR. Expression analysis was performed in two patient-derived cell lines (BTSC147, BTSC73). n=3 biological replicates.

C.3 Investigate if OSMR and CLIC1 interact endogenously in BTSCs

The MaMTH-HTS was developed and performed in mammalian HEK293T cells. Therefore, to validate the interaction in BTSCs in situ, proximity ligation assay (PLA) was employed. This method utilizes antibody recognition to the target antigen and subsequent probe hybridization. The hybridized probes are conjugated to oligonucleotides that can be ligated together if the proteins in question are less than 40 nm apart, indicative of an interaction. Following ligation, polymerase is added to generate a rolling circle amplification (RCA) of the ligated product that contains an integrated fluorescent mark, which can be visualized by microscopy (Fredriksson et al., 2002) (**Figure 11**). Fluorescent signals were identified in BTSC147, and PLA puncta were confirmed to be specific to BTSC147 using two independent controls. First, primary antibodies (OSMR and CLIC1) were omitted, providing an indication of the precision of the assay to samples that received antibody, and second, a CRISPR-CAS9-CLIC1 clone was generated and used as additional control to establish the specificity of the signal. Quantification of the PLA signal was then carried out to assess the signal in BTSC147WT compared to a CRISPR-CAS9 CLIC1 clone.

This data revealed that there was a significant reduction in PLA signal in CRISPR-CAS9 CLIC1 compared to control (**Figure 12**).

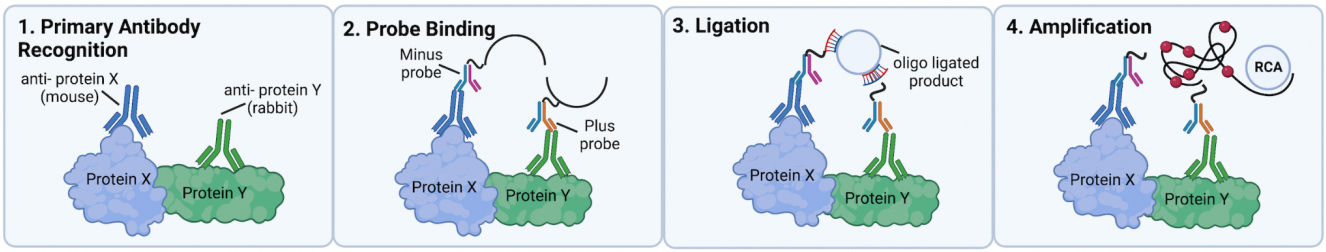

Figure adapted from Fredriksson et al., 2002 in Nature Biotechnology using Biorender.com

Figure 11. Proximity ligation assay (PLA) allows for the detection of a possible protein-protein interaction using four steps that can be done using minimal cellular material; **1.** Primary antibodies from each of the proteins of interest are incubated with the sample to generate an antibody-antigen reaction. For this assay a primary antibody of mouse and rabbit origin is required. **2.** Oligonucleotide probes containing secondary antibodies are incubated with the sample to generate a primary and secondary antibody reaction. One PLUS and one MINUS probe are required as the PLUS probe contains the template for amplification. **3.** Using a ligation reaction the probe oligonucleotides are ligated together if the proteins are suspected to interact. **4.** Rolling circle amplification (RCA) in the presence of polymerase is subsequently completed to generate a product that contains a fluorescent signal that can be visualised by fluorescent microscopy.

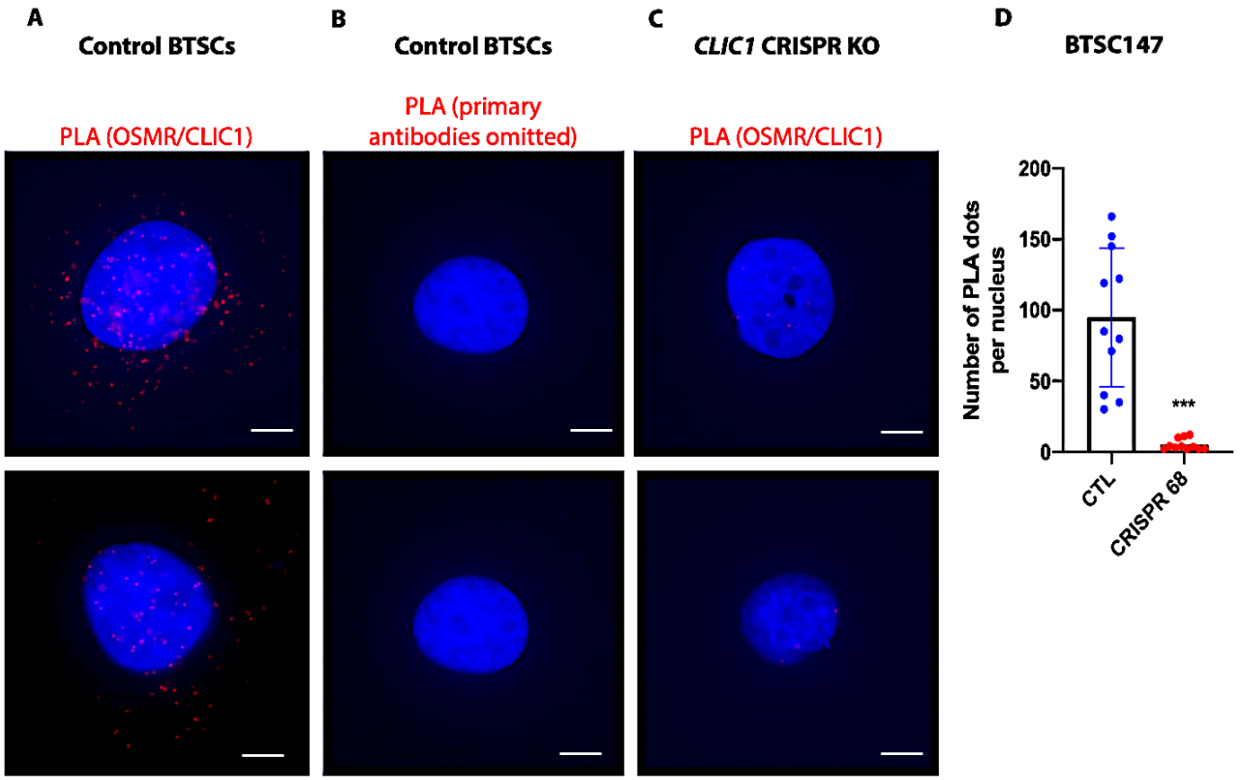

Figure 12. Detection of OSMR and CLIC1 interaction by PLA in patient-derived BTSC147

Control BTSC147 and CRISPR-CAS9 CLIC1 in the background of BTSC147 were subject to PLA analysis. (**A**) Each red puncta indicates an interaction between OSMR and CLIC1. Two representative images. (**B**) Primary antibodies omitted were used as control for the assay. One representative image. (**C**) PLA in CLIC1 CRISPR KO clone was used as a negative control for the specificity of the antibodies. Two representative images. (**D**) The number of PLA puncta per nucleus was determined based on BTSC147WT and CLIC1 CRISPR KO line. Data are presented as the mean ± SD, n = 3 biological replicates from which 14 nuclei were counted for BTSC147WT and 16 nuclei were counted for CLIC1 CRISPR KO. Statistical analysis was performed using a student t-test. *** $p<0.001$. Nuclei were stained with DAPI. Scale bar, 10 µm.

C.4 Pilot experiments: Impact of transient knockdown (KD) of CLIC1 on BTSCs

OSMR has previously been identified to be a driving force in BTSC growth and self-renewal *in vitro* and tumorigenesis *in vivo*. Mechanistically, this is driven in part via its interaction with the oncogenic protein, EGFRvIII (Jahani-Asl et al., 2016). Thus, to assess the impact of a novel OSMR binding partner in BTSC growth and self-renewal, we first employed short

interfering RNA (siRNA) targeting CLIC1 in pilot experiments. Following electroporation with a pool of 4 siRNA targeting CLIC1 and control (siCTL) non-targeting RNAi, samples were incubated for 48 to a maximum of 72 hours prior to analysis. This was done in order to ensure maximal efficiency of the siRNA to degrade the mRNA CLIC1 transcript. Validation using RTq-PCR and immunoblotting analyses showed that the siRNA mediated knockdown of CLIC1 was efficient, resulting in greater than 85% decrease in mRNA level and a significant decline in CLIC1 protein expression level (**Figure 13**). Cells treated with siRNA CLIC1, or control were then subjected to a cell population growth assay. This was accomplished by counting the number of live cells using trypan blue exclusion dye after a designated period of incubation following electroporation. This data revealed a significant decrease in the BTSC growth upon knockdown of CLIC1(**Figure 14**).

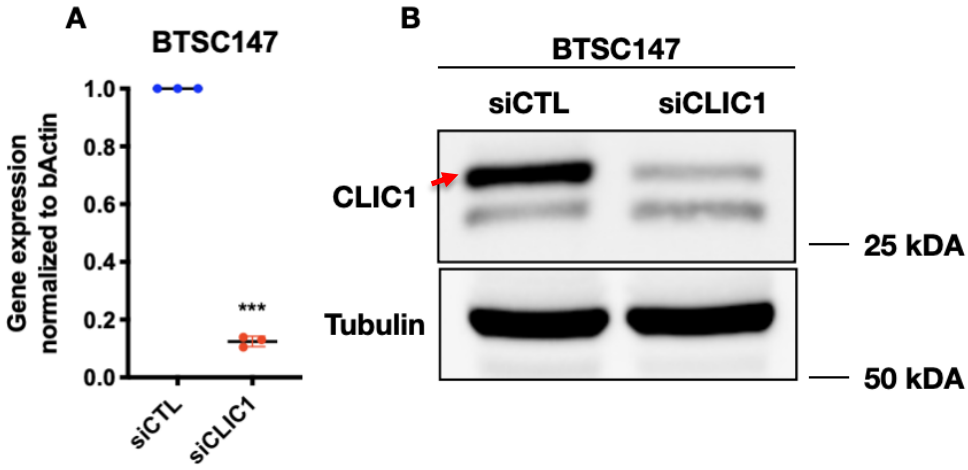

Figure 13. Validation of siRNA mediated knockdown in patient-derived BTSC147

(**A**) mRNA CLIC1 expression data following electroporation with siRNA targeting CLIC1 or control. Data are presented as the mean ± SD, n=3 biological replicates, ***p<0.001. (**B**) CLIC1 protein expression assessed by immunoblotting following electroporation with siRNA targeting CLIC1 or control, n=2 biological replicates.

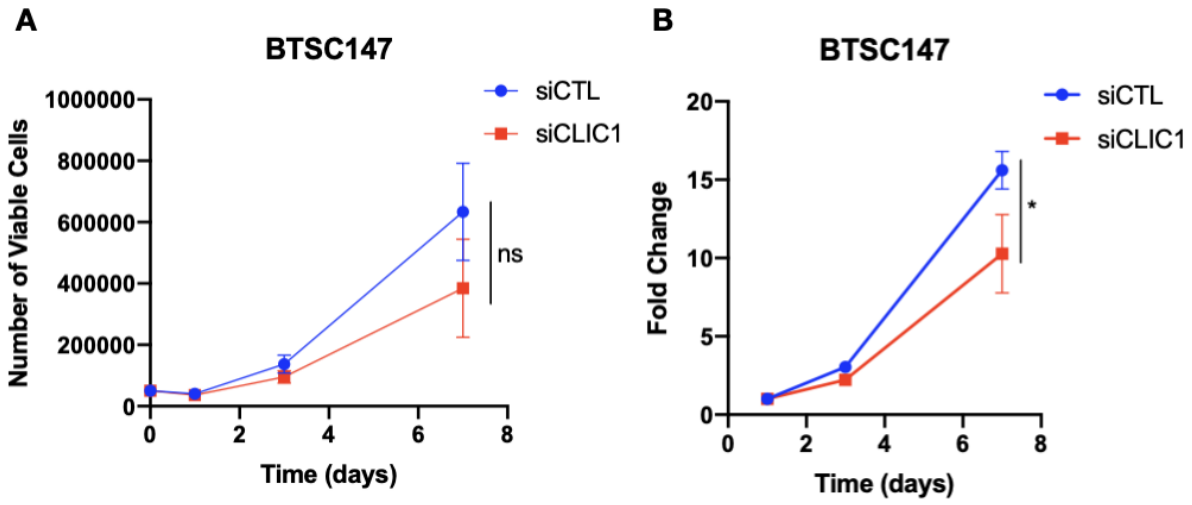

Figure 14. CLIC1 knockdown on proliferation in patient-derived BTSC147

Knockdown of CLIC1 using siRNA decreased the proliferation capabilities of BTSC147. (**A**) Proliferation ability plotted based on the number of viable cells counted using trypan blue exclusion dye. (**B**) Proliferation capability plotted as fold change based on the initial count on day 1 for each condition. A student-t test was used to compare two conditions at day 7 for both **A** and **B**. Data are presented as mean ± SD, n = 3 biological replicates, non-significant (ns), **p<0.01.

Next, since proliferation was found to be reduced in cells treated with short interfering RNA targeting CLIC1, we asked how this proliferation reduction may be taking place. To begin to look at this, we employed a simple experiment in which we measured the size of the spheres that were formed following 3 days of incubation at 37°C and 5% CO_2. The results suggest that spheres generated from cells treated with siRNA targeting CLIC1 are significantly smaller (~5%) than those treated with control siRNA (**Figure 15**).

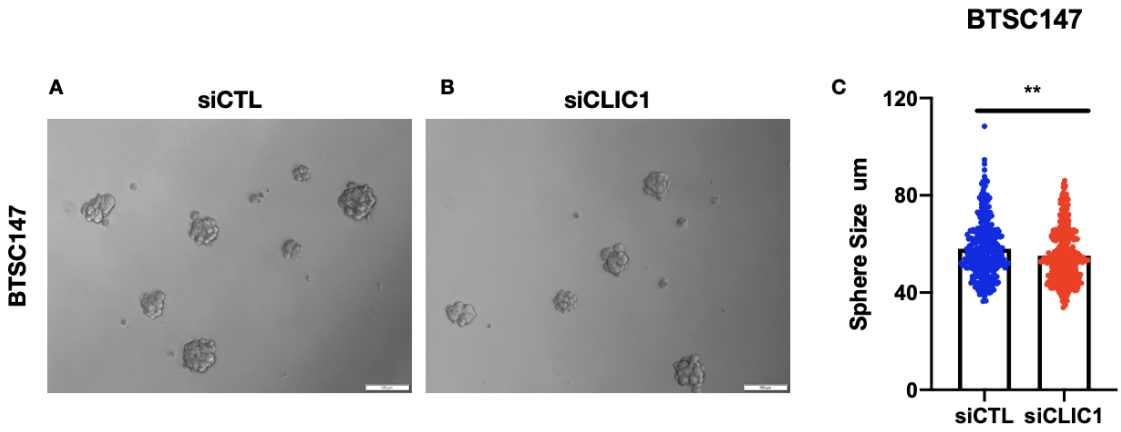

Figure 15. CLIC1 knockdown on sphere size in patient derived BTSC147

(**A-B**) Representative images of BTSC spheres following 3 days of incubation at 37°C and 5% CO_2. Scale bar 100 µm. (**C**) Sphere size assessment in cells treated with siCLIC1 or siCTL. A minimum of 100 spheres were measured from each biological replicate and data was plotted as a mean ± SD. All sphere measurements are shown. A student-t test was used to identify significance, **p<0.01.

Self-renewal is the process by which a stem cell divides and gives rise to one or two daughter cells that can also self-renew or commit to become a progenitor (Shenghui et al., 2009). Maintaining the stem cell pool requires the activation and suppression of multiple signalling pathways (cell intrinsic mechanisms) that are regulated by the niche or microenvironment (extrinsic mechanisms) in which the stem cell resides (Shenghui et al., 2009). These cell extrinsic signals include but are not limited to ligand binding to specific receptor such as LIF/LIFR/gp130 (Shenghui et al., 2009; Williams et al., 1988), BMP (Shenghui et al., 2009; Ying et al., 2003), and OSMR/EGFRvIII in BTSCs (Jahani-Asl et al., 2016). Thus, we asked whether CLIC1 impairs self-renewal capacity of BTSCs. An extreme limiting dilution assay (ELDA) (Hu & Smyth, 2009) was used to determine BTSC self-renewal following their electroporation with siCLIC1 or siCTL. Using this strategy, it is possible to determine the number of biologically active particles, or cells that are able to undergo self-renewal, from those that are not (Hu & Smyth, 2009; Rasool et al., 2022). Following electroporation, cells from each condition were plated at varying concentrations starting at 25 cells per well to 1 cell per well. After 7 days, wells were recorded as either a positive well (having a sphere) or a negative well (not having a sphere). The results suggest that siCLIC1

reduced self-renewal capacity of BTSC147 with the number of biologically active particles or stem cells frequency (SCF) being reduced by ~15% (**Figure 16**).

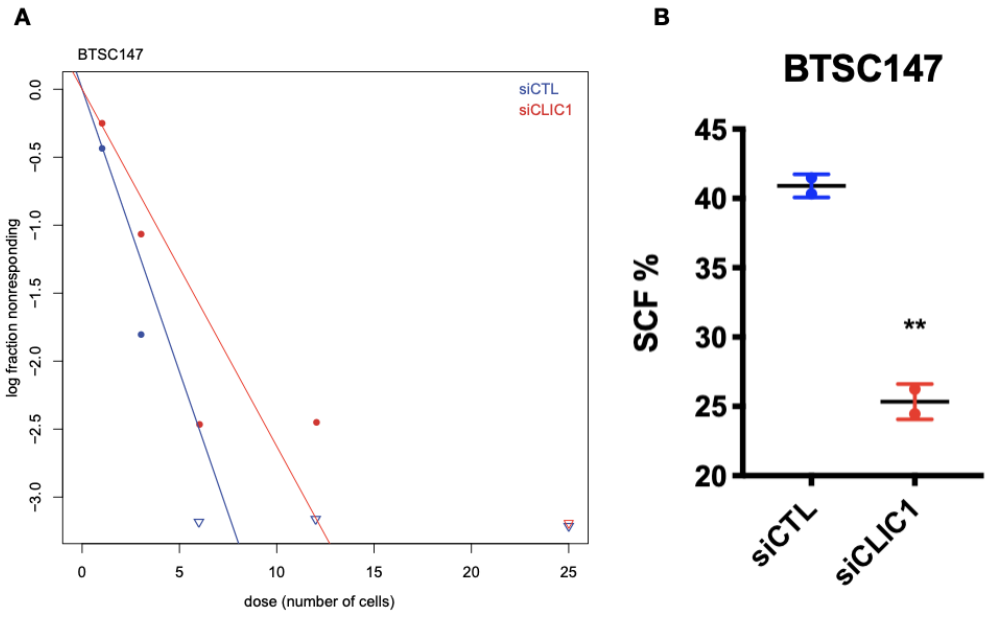

Figure 16. CLIC1 knockdown on self-renewal capacity in patient-derived BTSC147

(**A**) ELDA was performed following electroporation with siRNA targeting CLIC1 or CTL in BTSC147. Representative image for n=2 biological replicates (**B**) Percent stem cell frequency (SCF %) in siRNA targeting CLIC1 or CTL. Data are presented as mean ± SD, n = 2 biological replicates, **p<0.01.

C.5 Generation of transgenic BTSC lines using CRISPR-CAS9 technology

To pursue future experiments in understanding the role of CLIC1 in BTSCs and glioblastoma tumorigenesis, CRISPR-CAS9 technology was employed to generate CLIC1 KO cell line. Following *in vitro* assembly of the CRISPR-CAS9 constructs, plasmids were expanded and verified to contain the desired guide RNA (gRNA) sequences through plasmid sequencing. The plasmids contained either gRNA1 or gRNA2 with GFP or RFP markers, respectively. Electroporation was used to introduce the CRISPR-CAS9 CLIC1 construct to patient-derived BTSCs and subsequent fluorescence activated cell sorting (FACS) was employed to determine

singlet cells that had received both plasmids (**Figure 17A-H, I-P**). Singlet live cells for BTSC147 wild type (WT), BTSC73WT as well as BTSC147 or BTSC73 electroporated with guide RNAs were determined based on light scattering for parameters of size and granulation (**Figure 17A-C, E-G, I-K, M-O**). The top 20% of singlet double positive cells (**Figure 17D, H, L, P**) were seeded at a density of 1 cell per well in order to generate a colony of CRISPR-CAS9 CLIC1 clones. A clonal model of expansion was used for the culturing of BTSC CRISPR-CAS9 CLIC1 clones.

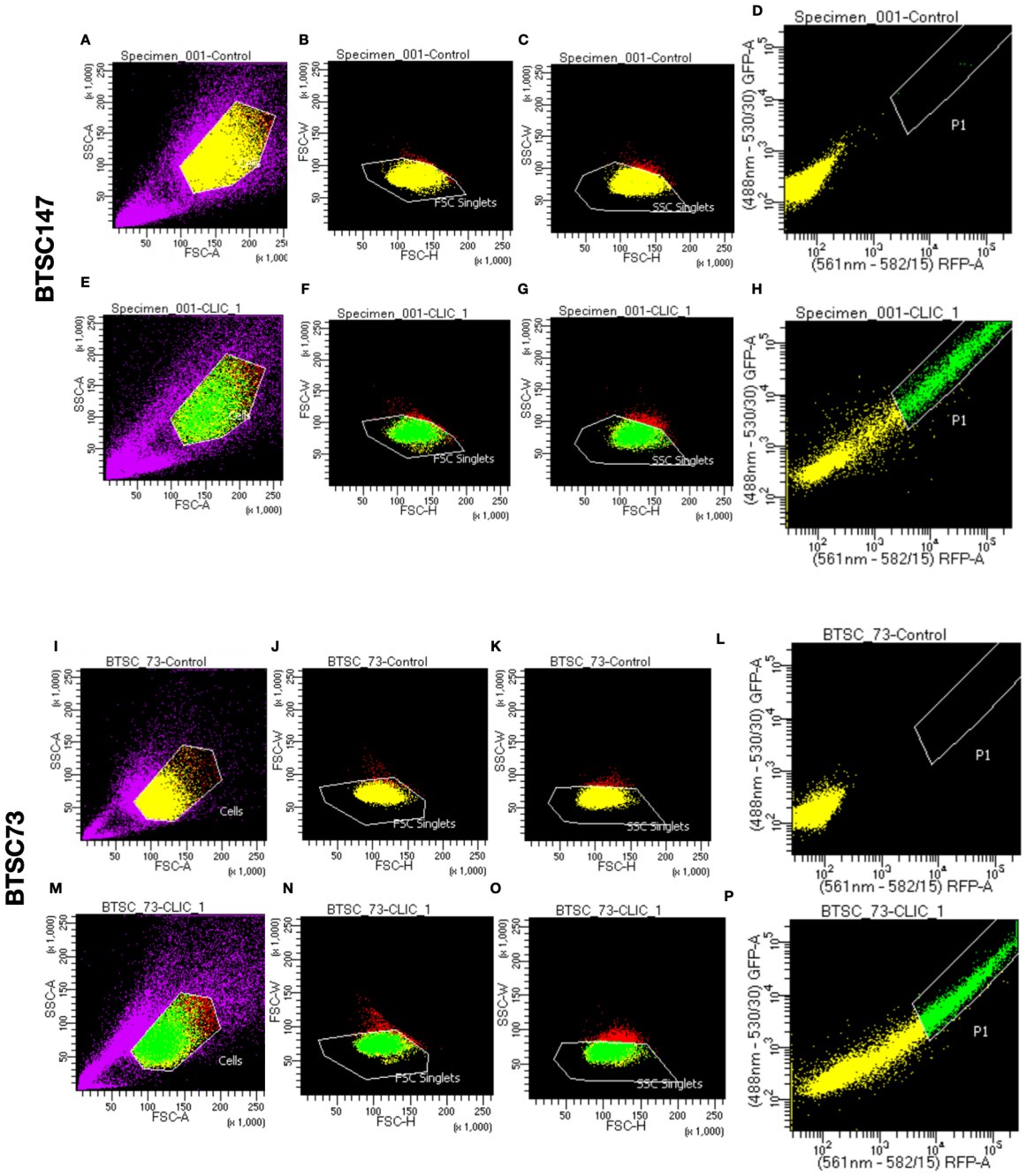

Figure 17. Fluorescence activated cell sorting plots in control and CRISPR-CAS9 CLIC1 patient-derived BTSCs

(**A-C, I-K**) Control and electroporated BTSC147 and BTSC73 were subjected to FACS following dissemination of spheres into a single cell suspension. Yellow colour used to denote selected cells and red colour used to denote cells that were omitted. (**D,L**) Control BTSC147 and BTSC73 were used as a baseline for identification of singlet live cells and autofluorescence signal with the suspected top 20% denoted by **P1**. (**A, E, I, M**) Using forward scatter (FSC-A) and side scatter (SSC-A) to determine singlet cells from dead cells, debris or doublet cells in CTL or electroporated BTSC147 and BTSC73 using light scattering patterns to assess size and granularity respectively. (**B-C, F-G, J-K, N-O**) Using alternate parameters of forward scatter (FSC-H/W) and side scatter (SSC-W) to further define the population of singlet cells in CTL or electroporated BTSC73 and BTSC147. (**H, P**) Defining the subset of double positive cells of which the top 20% were chosen (**P1** in green) based on baseline autofluorescence defined in CTL (**D, L**).

Following clonal expansion, clones were assessed for mono- or bi-allelic deletion using internal and external primers to cut sites generated by the CAS9 protein following gRNA recognition (**Figure 18A**). A mono-allelic deletion supports the hypothesis that the clone in question has undergone a cut event in one allele in the desired location by the CAS9 protein, suggestive of a knockdown phenotype, whereas a bi-allelic deletion suggests that both alleles were cut, generating a possible complete knockout of the gene of interest. Among multiple positive clones from both BTSC147 and BTSC73 electroporated cells, we selected one clone with a mono-allelic deletion and one clone with a bi-allelic deletion for each to conduct follow up analysis (**Table 10**). Validation of mono- and bi-allelic clones was completed using RT-qPCR analysis of CLIC1 mRNA expression in the chosen clones and immunoblotting of protein expression relative to parental wild type control BTSC147 or BTSC73 which had not undergone any form of CRISPR-CAS9 mediated alterations. Both chosen clones from each of the parental lines (BTSC147 or BTSC73) demonstrated to have a significant silencing of CLIC1 with respect to the mRNA expression and protein expression (**Figure 18B-E**). This suggests that CRISPR-CAS9 mediated deletion of CLIC1 was successful and could be used for subsequent experimentation to assess the role of CLIC1 in BTSCs.

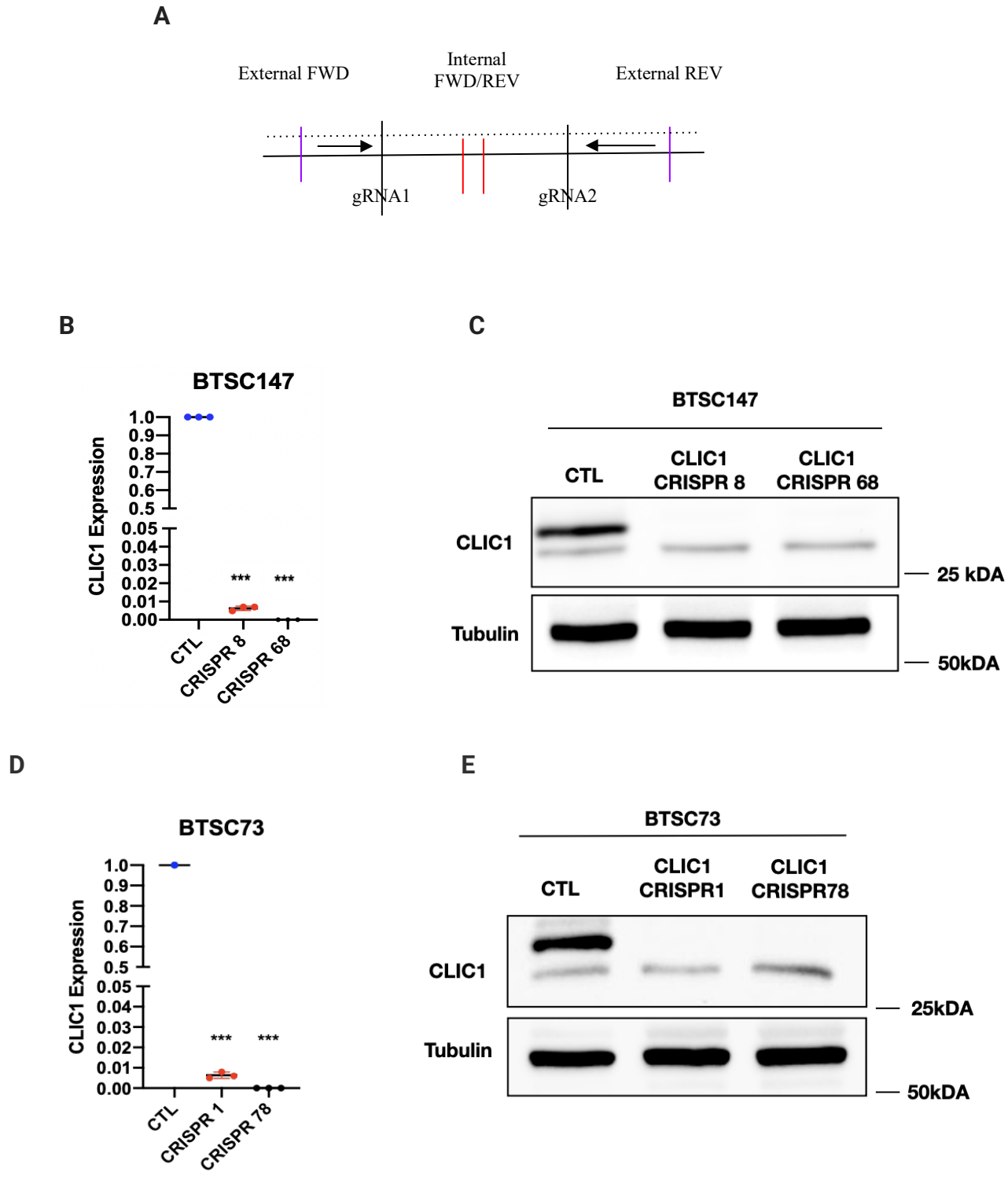

Figure 18. Validation of CRISPR-CAS9 CLIC1 clones in patient-derived BTSCs

(**A**) Schematic of primers used for identification of mono- and bi-allelic deletions. Internal primers (red; forward -FWD and reverse -REV) and external primer (purple; forward -FWD and reverse -REV) sequences were generated based on the location of the guide RNA sequences. Arrows indicate the direction of primer sequences. Solid and dotted lines represent one allele respectively. If a mono-allelic deletion were to take place, one allele would remain intact leading to amplification of the internal primer sequence only while the other would generate a product based on the external primer sequence. If a bi-allelic deletion takes place, only products based on external primers will be observed. (**B**) mRNA CLIC1 expression in two CRISPR-CAS9 CLIC1 clones compared to parental BTSC147WT. Data are presented as the mean ± SD, n=3 biological replicates, ***p<0.001. (**C**) CLIC1 protein expression assessed by immunoblotting in two CRISPR-CAS9 CLIC1 clones compared to parental BTSC147WT, n=2 biological replicates. (**D**) mRNA CLIC1 expression data in two CRISPR-CAS9 CLIC1 clones compared to parental BTSC73WT. Data are presented as the mean ± SD, n=3 biological replicates, ***p<0.001. (**E**) CLIC1 protein expression assessed by immunoblotting in two CRISPR-CAS9 CLIC1 clones compared to parental BTSC73WT, n=2 biological replicates.

Table 10. Description of CLIC1 clones selected for follow up analysis

Parental BTSC line	Clone	Type of deletion	Suggested phenotype
BTSC147	CRISPR8	Mono-allelic	Knockdown
BTSC147	CRISPR68	Bi-allelic	Knockout
BTSC73	CRISPR1	Mono-allelic	Knockdown
BTSC73	CRISPR78	Bi-allelic	Knockout

C.6 Effect of CLIC1 genetic deletion in BTSCs

Having established CRISPR-CAS9 CLIC1 clones, we next investigated if the clones presented the same or similar phenotype for proliferation, sphere size and stemness as observed in siRNA CLIC1 pilot experiments in patient-derived BTSC147. BTSC147WT and each CRISPR-CAS9 CLIC1 clone (CRISPR8 and CRISPR68) were plated at a density of 30,000 cells per well in a 6 well plate with 2mL of BTSC growth media respectively and assessed for proliferation following 1, 3 and 7 days of incubation at 37°C and 5% CO_2 using trypan blue exclusion dye. The

results showed that the proliferation of both CRISPR-CAS9 CLIC1 clones was significantly decreased by over 50% compared to BTSC147WT control (**Figure 19)**. Interestingly, although CRISPR-CAS9 CLIC1 clones exhibited ~10-fold decline in proliferation compared to controls, there was no significant difference between the CRISPR-CAS9 CLIC1 clones (**Figure 19B**). Along with reduced proliferation, the sphere size of CRISPR-CAS9 CLIC1 clone 8 was found to be significantly smaller than control cells by ~20% (**Figure 20**). Interestingly, however, CRISPR-CAS9 CLIC1 clone 68 (bi-allelic deletion) appeared to be unable to form spheres following 3 days of incubation at 37°C and 5% CO_2 (**Figure 20C**) compared to control or CRISPR-CAS9 CLIC1 clone 8 (mono-allelic deletion) (**Figure 20A-B**).

Next, CRISPR-CAS9 CLIC1 clones were subject to extreme limiting dilution assay in which self-renewal and stemness capacity was assessed. Following 7 days of incubation at 37°C and 5% CO_2 the experiment was completed, and it was determined that both CRISPR-CAS9 CLIC1 clones showed a significant decrease in self renewal capacity (**Figure 21**). This data is consistent with that observed for proliferation, sphere size and stemness in siRNA CLIC1 pilot experiments (**Figure 14-16**) but to a greater extent, suggesting that the effects of CLIC1 silencing using CRISPR-CAS9 technology in patient-derived BTSCs is dose dependent.

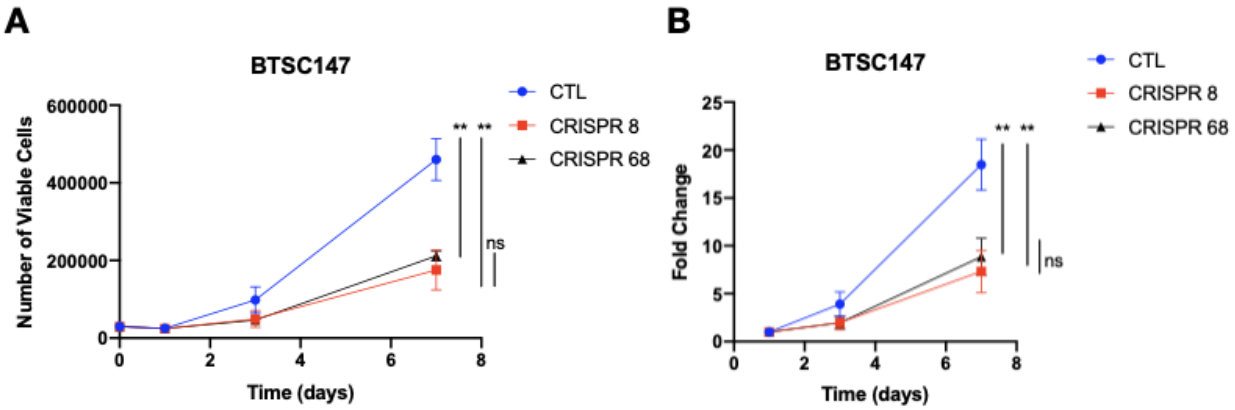

Figure 19. CRISPR-CAS9 CLIC1 on proliferation in patient-derived BTSC147

Silencing of CLIC1 using CRISPR-CAS9 technology significantly decreases proliferation capabilities of BTSC147. (**A**) Proliferation capability plotted based on the number of viable cells

counted using trypan blue exclusion dye. (**B**) Proliferation capability plotted as fold change based on the initial count on day 1 for each condition. A student-t test was used to compare two conditions at day 7 for both **A** and **B**. Data are presented as mean ± SD, n = 3 biological replicates, **p<0.01.

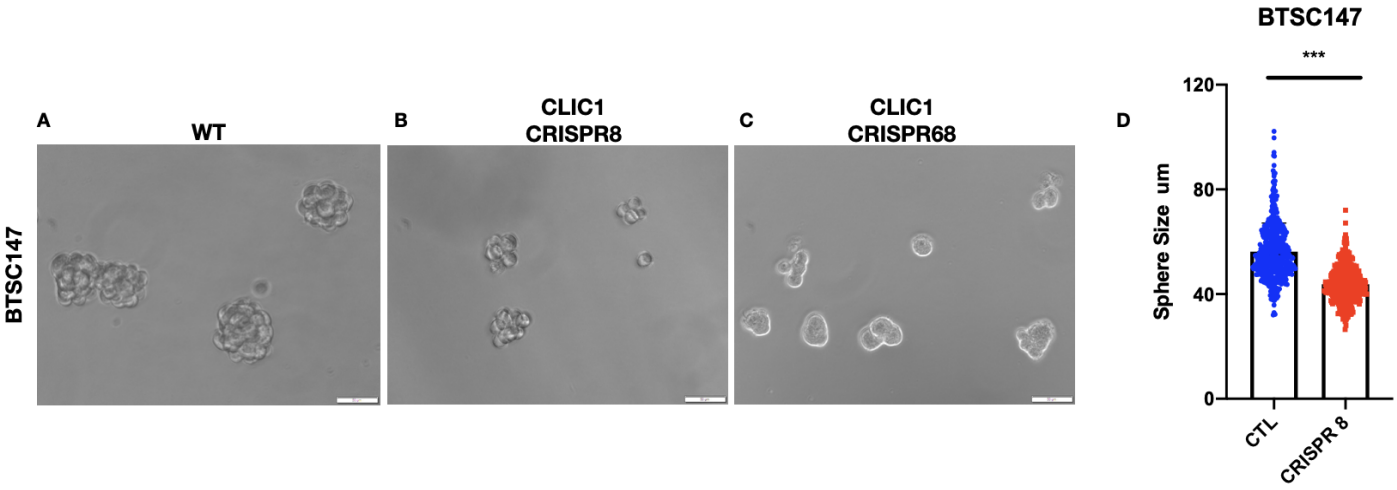

Figure 20. CRISPR-CAS9 CLIC1 on sphere size in patient-derived BTSC147

Silencing of CLIC1 significantly reduces the size of BTSC spheres following 3 days of incubation at 37°C and 5% CO_2. (**A-C**) Representative images of BTSC spheres following 3 days of incubation at 37°C and 5% CO_2. Scale bar 50 µm. (**D**) Sphere size assessment in CTL BTSC147WT and CRISPR 8 clone. A minimum of 100 spheres were measured from each biological replicate and data was plotted as a mean ± SD. All sphere measurements are shown. A student-t test was used to identify significance, ***p<0.001.

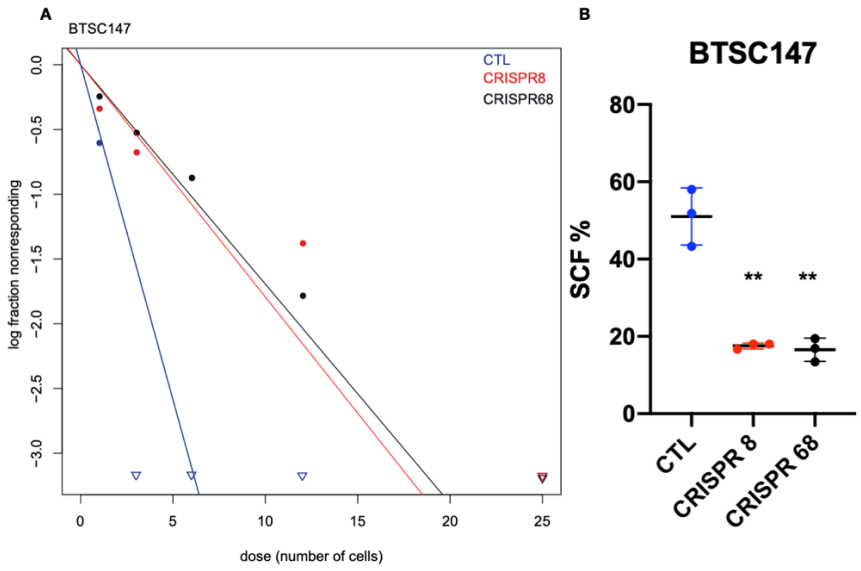

Figure 21. CRISPR-CAS9 CLIC1 on self-renewal capacity in patient-derived BTSC147
(**A**) ELDA was performed on control BTSC147 and two CRISPR-CAS9 CLIC1 clones (CRISPR 8 and CRISPR 68). Representative image for n=3 biological replicates. (**B**) Percent stem cell frequency (SCF %) in control BTSC147 and two CRISPR-CAS9 CLIC1 clones (CRISPR 8 and CRISPR 68). Data are presented as a mean ± SD, n = 3 biological replicates, **p<0.01.

D. Discussion and future directions

Glioblastoma is one of the most aggressive brain cancers in adults. Its aggressive nature is brought on by cancer cells that are able to metastasize and evade standard of care therapy (Gilard et al., 2021; Shergalis et al., 2018). Research over the past decade has suggested that one of the reasons for glioblastoma recurrence and lack of response to therapy is due to a small subset of brain tumour stem cells (BTSCs) that are able to give rise to new cancerous populations following even the most intense therapeutic interventions (Singh et al., 2003; Singh et al., 2004). This has led to the hypothesis that to effectively treat glioblastoma, a combined approach must be employed, one that targets slower dividing BTSCs and those that are supporting these cells (Yang et al., 2020). In order to target BTSCs for therapy, patient specific-driver mutations or gene amplifications must be identified. Importantly, these genetic alterations can also be modulating the tumour microenvironment, which is of high importance (Gimple et al., 2019). For instance, the epidermal growth factor receptor (EGFR) is frequently amplified in BTSCs, however there is also

a mutant variant of EGFR in the form of an EGFR variant (EGFRvIII) that is constitutively active in almost 30% of GB patients (Rutkowska et al., 2019). This mutation contributes to BTSC functioning, but it is not acting alone. Recent discoveries have revealed that EGFRvIII forms a complex with the oncostatin M receptor (OSMR) to generate a positive feedback loop to induce the activation of STAT3 and the subsequent expression of OSMR as a direct target of STAT3 (Jahani-Asl et al., 2016). Interestingly, although OSMR is an EGFRvIII co-receptor, recent evidence has suggested that it too may be considered a driver because of its multifaceted role in BTSC maintenance and glioblastoma tumorigenesis. A mitochondrial OSMR has been discovered which is targeted to complex 1 of the mitochondrial electron transport chain (ETC) and interacts with NADH ubiquinone oxidoreductase 1 (NDUFS1) and NADH ubiquinone oxidoreductase 2 (NDUFS2) of the ETC. This interaction was found to increase oxidative phosphorylation (OXPHOS) thus generating a highly resistant tumour phenotype to ionizing radiation (Sharanek et al., 2020). OSMR has also been identified to be modulating the transition to mesenchymal-like states and impacting surrounding immune responses to either promote or suppress tumour growth (Guo et al., 2019; Hara et al., 2021; Masjedi et al., 2021), suggesting that this pathway can switch roles depending on multiple other factors. Thus, we hypothesized that OSMR signalling can be influenced by its binding partners in different genetic backgrounds and that it may regulate different aspects of GB tumorigenesis.

D1. MaMTH-HTS validation and other binding partners

In the present study, we employed a MaMTH-HTS screen in the goal of identifying a novel OSMR binding partner in the absence and presence of EGFRvIII. Through careful screen analysis and extensive literature review, I selected to investigate the role of a candidate binding partner, Chloride Intracellular Channel 1 (CLIC1) in BTSCs. This partner was chosen as CLIC1 is highly expressed in glioma cancer stem cells specifically those of the mesenchymal subtype, of which OSMR is also found to be highly expressed (Natesh et al., 2015). CLIC1 is shown to play a significant role in GB tumorigenesis in cancer stem cells (CSC) (Setti et al., 2013) and it has been identified as a possible target for therapeutic intervention because of its dichotomous structure (Barbieri et al., 2022; Barbieri et al., 2018; Gritti et al., 2014). Importantly, upon mRNA expression analyses in patient-derived BTSCs (BTSC147 and BTSC73), CLIC1 appeared to be

highly expressed (Valente et al., 2009). This suggests that CLIC1 may be a viable target for further experimentation.

Interestingly, analysis of the hits identified in the MaMTH-HTS did not identify gp130 or EGFRvIII as OSMR binding partners, although both have been proven to bind with OSMR (Heinrich et al., 1998; Jahani-Asl et al., 2016). For gp130, one possible reason is that heterodimerization of OSMR and gp130 takes place in the presence of its ligand, which suggests that if the ligand is not present then the dimerization to form the OSMR/gp130 complex would not take place (Heinrich et al., 1998). Since OSM was not introduced as part of the screen, it is not surprising the gp130 did not come up as a possible binding partner. As for EGFRvIII, one possible explanation for its lack of identity in the screen could be environmental. This means that the tumour BTSC microenvironment may be favouring this interaction, but once this environment is removed the interaction may not occur or it may occur at a very low frequency. For this reason, once CLIC1 was identified as a possible candidate binding partner, validation was undertaken to assess if this interaction was in fact taking place endogenously in BTSCs as opposed to exogenously in HEK293T cells in which the screen was run. Proximity ligation assay (PLA) in patient-derived BTSC147 was used to validate CLIC1 and OSMR interaction in situ. Using this method, we confirmed that OSMR and CLIC1 are novel binding partners in situ.

Although CLIC1 was chosen as the focus of this project, various other binding partners identified through the MaMTH-HTS may be equally viable targets for experimentation, such as kinases or DNA-binding proteins (**Table 11-12**). For example, looking at the kinase candidate interacting partners in the presence and absence of EGFRvIII may shed light on whether OSMR is post-translationally modified in each condition and how this modification may be impacting its ability to maintain BTSCs or its translocation to mitochondria. Previously, OSMR has been identified to either take a role as a tumour suppressor or a oncogenic player through signal modulation by c-myc (Kan et al., 2011). In this manner, c-myc acts as a molecular switch dictating the pathways activated by OSMR to either support tumour growth or inhibit it (Kan et al., 2011). However, post translational modification to OSMR by different kinases may help further identify how OSMR signalling is acting in such a dichotomous manner sometimes even in the same cancer type. Additionally, the numerous possible co-receptor candidates

identified in OSMR unique versus OSMR/EGFRvIII may suggest that in addition to EGFRvIII, OSMR may generate feedback loops with other receptors to modulate different aspects of tumorigenesis. This may take the form of enhancing metastasis or even modulating the activity of neighbouring non-cancerous cells to support the growth of the tumour. Finally, four distinct functional categorisations were identified from the OSMR unique hits that were not identified in the OSMR/EGFRvIII complex grouping. These functional categorizations include ATP dependent protein activity, receptor activity, adaptor activity and translational regulator activity (**Figure 9**). This data again points to OSMR as an active player in pathways other than those identified when it is in complex with EGFRvIII. Future studies can focus on these pathways to potentially identify new targets and complexes that contribute to glioblastoma tumorigenesis.

Table 11. Hits identified to be functional kinases or kinase-related proteins. The identification of the hit in OSMR unique, OSMR in complex with EGFRvIII or both is denoted by an **X** next to the indicated hit.

Kinases/Kinase related			
Candidate hits	**OSMR unique**	**OSMR/EGFRvIII complex**	**Description**
DCK	X		Deoxycytidine Kinase, phosphorylation of many deoxyribonuclosides and analogs related to drug resistance in cancer
MST4	X		Serine/Theronine Kinase 26, kinase involved in cell growth and apoptosis
MAPK1IP1L	X		Mitogen-Activated Protein Kinase 1 Interacting Protein 1 like, MAPK pathway
CLK4	X		CDC Like Kinase 4, dual specificity to phosphorylate serine/threonine and tyrosine containing subtrates
AURKB		X	Aurora Kinase B, serine/threonine kinase involved in cell cycle
PRKRIR		X	Known as THAP Domain Containing 12, upsteam regulator of Protein Kinase R
HTATIP2		X	HIV- Tat Interactive Protein 2, enables kinase activity (serine/threonine) and has oxidoreductase activity
CAMK1G		X	Calcium/Calmodulin Dependent Protein Kinase IG, phosphorylation of CREB1
MAPK10	X	X	Mitogen-Activated Protein Kinase 10, serine/threonine kinase involved in many cuellular processes of the MAPK pathway
AKT2	X	X	AKT Serine/Threonine Kinase 2, regulation of multiple pathways
STRADA	X	X	STE20 Related Adaptor Alpha, pseudokinase that has activity when in a complex
HK1	X		Hexokinase 1, phosphorylation of hexose sugars involved in glucose metabolism
PRKAG1	X		Protein Kinase AMP-Activated Non-Catalytic Subunit Gamma 1, regulation of AMP-activated protein kinase (AMPK)
ULK3	X		Unc-51 Like Kinase 3, serine/threonine kinase activity acting on multiple proteins and pathways
PRKACG	X		Protein Kinase CAMP-Activated Catalytic subunit Gamma, catalytic subunit of the PKA kinase
IKBKB	X		Inhibitor of Nuclear Factor Kappa B Subunit Beta, serine phosphotylation of inhibitor protein activates NF-kappa-B
C9orf98	X		Adenylate kinase 8, ternimal transfer of phosphate groups between tri and monophosphates
PRKRA	X		Protein Activator of Interferon Induced Protein Kinase, activation leads to viral reponse pathways activity
TK1	X		Thymidine Kinase 1, addition of phosphate to thymidine involved in DNA replication
CAMKV	X		CaM Kinase like Vesicle Associated, Calmodulin-dependent protein kinase (predicted - not proven)

Table 12. Hits identified as protein involved in DNA processes: DNA/chromatin binding proteins and transcription factors. The identification of the hit in OSMR unique, OSMR in complex with EGFRvIII or both is denoted by an **X** next to the indicated hit.

			DNA/Chromatin binidng and TF
Candidate hits	**OSMR unique**	**OSMR/EGFRvIII complex**	**Description**
MLLT10	X		MLLT10 Histone Lysine Methyltransferase DOT1L Cofactor, transcription factor activity
ZNF770	X		Zinc Finger Protein 770, transcriptional activator and regulator (predicted)
ZBTB43	X		Zinc Finger and BTB Damoin Containing 43, transcriptional regulator (predicted)
PHF17	X		PHD finger Protein 17 or Jade Family PDH finger (JADE1), transcriptional cofactor and involved in Wnt signaling and cell cycle
TCF19	X		Transcription factor 19, transcription factor with a PHD-type zing finger domain
PYHIN1	X		Pyrin and HIN Domain Family Member 1, transcriptional regulation and tumor supressor activity
ELF4	X		E74 Like ETS Transcription Factor 4, transcriptional activator for hematopoetic growth factor, immune and lysozyme genes
TGIF2	X		TGFB Induced Factor Homeobox 2, transcriptional repressor
ZNF468	X	X	Zinc Finger Protein 468, transcriptional regulation (predicted)
IKZF2	X		IKAROS Family Zinc Finger 2, hematopoetic specific transcription factors
DLX4	X		Distal-Less Homeobox 4, related to Drasophila developmnetal genes for head a limb development
NFIL3	X		Nuclear Factor Interleukin 3 Regulated, transcriptional reguulation as a activator and repressor with immune related activities and cicadian rhythm roles
HEYL	X		Hes Related Family BHLH Trascription factor with YRPw Motif like, involved in Notch siganling and cell fate decision
ZFP112	X		Zinc Finger Protein 112, transcriptional regulator (predicted)
THAP1	X		THAP Domain Containing 1, transcriptional regulator for cell cycle and proliferation and associated with apoptosis
NFE2	X	X	Nuclear Factor Erythoid 2, maturation and differentiation of erythoid amd megakaryocytes
ZNF660	X		Zinc Finger Protein 660, transcriptional regulation (predicted)
ZNF595	X		Zinc Finger Protein 595, transcription factor for developmental and cellular processes
ZSCAN2	X		Zinc Finger and SCAN Doamin Containing 2, transcriptional regulation in germ cells (spermatogenesis)
ZNF776	X		Zinc Finger Protein 776, transcriptional regulation (predicted)
MYF6	X		Myogenic Factor 6, DNA binding protein involved cellular differentiation (muscle)
DACH2	X		Dachshund Family Transcription factor 2, transcripton factor regulating developmnetal and differentiation genes
MLX	X		MAX Dimerization Protein MLX, transcription factor involved in cell fate and proliferation
ZNF34		X	Zinc Finger Protein 34, transcriptional regulation (predicted)
ZNF350		X	Zinc Finger Protein 350, transcriptional repressor
PITX2		X	Paired Like Homeodomain 2, transcription factor in developmental pathways
ZNF256		X	Zinc Finger Protein 256, transcriptional repressor acting on proliferation
HESX1		X	HESX Homeobox 1, transcriptional repressor in the development of brain structures
ZNF22	X		Zinc Finger Protein 22, transcriptional regulation (predicted)
HMGB4	X		High Mobility Group Box 4, transcriptional regulation (predicted) involved in cellular differentiation
SETD7	X	X	SET Domain Containing 7, Histone Lysine Methyltransferase, epigenetic regulation and action on non histone proteins such as P53
DPF1	X		Double PHD Fingers 1, neurospecific transcription factor involved in cell fate (stem/progenitors to adult commitment) and neural development
GPBP1	X	X	GC-Rich Promoter Binding Protein 1, trans-activating transcription factor
CREB3	X	X	CAMP Responsive Element Binding Protein 3, transcription factor involved in multiple processes including proliferation, tumour supression, unfolded protrein response etc...
ERCC1	X		ERCC Excision Repair 1 Endonuclease Non-catalytic Subunit, nuceotide excision base repair pathway
ERCC5	X		ERCC Excision Repair 5 Endonuclease, DNA specific endonuclease involved in DNA excision repair pathway
AIFM1	X		Apoptosis Inducing Factor Mitochondria Associated 1, translocation to the nucleus where it binds DNA on in a sequence independent manner to induce chromosomal fragmentation
HP1BP3	X		Heterochromatin Protein 1 Binding Protein 3, DNA and nucleosome bindicativity to maintain stbility of heterochromatin
MCM7	X		Minichromosome Maintenance Complex Component 7, inititation of genome replication in Eukaryotes
MSH5	X		MutS Homolog 5, DNA mismatch repair and meiotic recombination events by facilitating cross-over
PDS5B	X		PDS5 Cohesin Associated Factor B, regulation of sister chromatid cohesion
PRAME	X		PRAME Nuclear Receptor Trascriptional Regulator, transcriptional repressor for retionic acid signaling by mediating receptor expression
NR3C1		X	Nuclear Receptor Subfamily 3 Group C Member 1, dual role as a receptor and transcription factor to promote GRE gene expression
TIGD6		X	Tigger Transposable Element Derived 6, enable DNA binding activity (predicted)
POLI		X	DNA Polymease Iota, error prone DNA polymease invoved in DNA repair

D2. Silencing of CLIC1 impacts BTSC proliferation, sphere size and stemness

Following validation that CLIC1 and OSMR are endogenous binding partners in BTSC73 and BTSC147. We next set out to determine the impact of CLIC1 silencing on patient-derived BTSCs. OSMR has been shown to have a significant impact on BTSC and astrocyte proliferation both *in vitro* and *in vivo*. Mechanistically, this is driven in part via interaction with EGFRvIII to induce the constitutive phosphorylation of STAT3 (Jahani-Asl et al., 2016). Thus, to begin to unravel how the interaction of OSMR with CLIC1 is involved in BTSC maintenance, we first employed short interfering RNA as a pilot experiment to assess the impact of KD in patient-derived BTSC147. In previous studies, CLIC1 KD in glioma cancer stem cells (CSC) was found to induce a significant reduction in proliferation, viability and stemness specifically in glioma CSC of the mesenchymal

subtype (Setti et al., 2013). Studies using siRNA targeting of CLIC1 versus a non-targeting - CTL were conducted to analyse population growth assay, BTSC sphere size and self-renewal via extreme limiting dilution assay (ELDA).

We first confirmed that the siRNA induced an 85-90% KD of CLIC1 mRNA and a significant decrease in CLIC1 protein expression. We found that KD of CLIC1 induced an approximate 5-fold decrease in proliferation growth of BTSC147. Of note, fold change was used to determine significance and correct for any discrepancies in initial plating. Additionally, using siRNA targeting CLIC1, it was observed that there was a significant decrease in sphere size and ability to self-renew. Of note, this effect was found to be dose dependent, such that deletion of CLIC1 using CRISPR-CAS9 technology more profoundly impaired self-renewal and growth. This was especially evident when looking at fold change for the population growth assay in which an approximate 5-fold change was observed between siCTL and siCLIC1 groups compared to an upwards of around 10-fold proliferation difference between control BTSC147 and both CRISPR-CAS9 CLIC1 clones, respectively. Additionally, using extreme limiting dilution assay (ELDA), knockdown of CLIC1 by siRNA yielded a decrease in self renewal capacity by ~15.6% between siCTL and siCLIC1 while CRISPR-CAS9 silencing of CLIC1 yielded a ~33.5% to ~34.6% decrease in self-renewal capacity between control BTSC147 and CRISPR-CAS9 CLIC1 clones. In follow up analyses, I conducted sphere size assessment of CRISPR-CAS9 CLIC1 clones and the data revealed that silencing of CLIC1 impairs the ability of the cells to form spheres. Upon identification of the clone that was not able to form spheres (clone 68), it was found that this clone is generated from a biallelic deletion of CLIC1 whereas clone 8, which was able to form spheres after 3 days of incubation, presented a mono-allelic deletion of CLIC1 (**Table 10**). This again, may point to the dose dependent effect of CLIC1 KD or silencing. There are, however, some limitations to experimentation that could be addressed in future work with the CRISPR-CAS9 CLIC1 clones such as the use of a negative control. In this thesis, the parental cell line which had not been edited by the CRISPR-CAS9 construct was used as the wild-type control. Using this type of control may fail to determine additional phenotypic changes that occur in the cells as a result of the editing system. Thus, to properly adjust for such a limitation, future experimentation may use a control non targeting gRNA sequence in the CRISPR-CAS9 construct. Although additional studies must be conducted on the mechanistic intersection of OSMR and CLIC1 in patient-derived BTSC and

in a murine model, the dose dependent effect of silencing CLIC1 may suggest that targeting channel activity with a CLIC1 specific inhibitor such as IAA-94 combined with inhibiting OSMR signalling may prove to have a significant therapeutic potential. To elucidate this, future experiments can begin with performing extreme limiting dilution assay (ELDA) with IAA-94 treatment in in control or OSMR knockout lines.

Additionally future experiments to understand how and if OSMR is impacting the functionality of CLIC1 and therefore impacting glioblastoma progression must be undertaken. It has been suggested that the cytoplasmic domain of membrane receptors can activate intracellular proteins such as ion channels and transporters (Yeagle, 2016). Thus, based on preliminary data collected, perhaps OSMR is additionally impacting the localization of CLIC1 to the membrane to activate its function as an ion channel. In order to begin to understand the possible role of OSMR in the regulation of CLIC1 functioning and CLIC1 localization, dimerization to form a channel and phosphorylation status can be investigated in control BTSCs and OSMR KO lines.

D2.1 Impact of CLIC1 silencing on cell fate

Using the population growth assay, it was determined that silencing of CLIC1 induced a significant decrease in the number of viable cells, however, a reduction in the number of cells can take the form of increased cell death or slower cell cycling. Sphere size was found to be significantly reduced in both siRNA and CRISPR-CAS9 mediated silencing of CLIC1 suggesting that the cell cycle processes might be impaired. Additional experiments are, however, required to support this hypothesis. Interestingly, there has been considerable evidence that CLIC1 impairs the cell cycle and slows progression through various stages, (Peretti et al., 2018; Valenzuela et al., 2000) but it has also been suggested that silencing of CLIC1 leads to increased cell death in the form of apoptosis (Kobayashi et al., 2018; Li et al., 2018). To determine which process or if both processes are at play upon silencing of CLIC1 in BTSCs, future experiments should be conducted to explore the various possibilities including Ki-67 staining or 5-Ethynyl-2′-deoxyuridine (EdU) incorporation assay along with Annexin V and Propidium Iodide (PI) staining followed by flow cytometry analysis. Ki-67 is a nuclear protein that has been widely used as a marker for active proliferation (Gerdes et al., 1983), as it has been identified to have an active role in the cell cycle

at multiple stages (Gerdes et al., 1983; Sun & Kaufman, 2018). Additionally EdU incorporation assay can be used. This chemical additive is a nucleoside analogue of thymidine, and thus will be incorporated upon DNA synthesis. These experiments will provide an indication of if a reduced number of viable cells is a result of impaired cell cycling. However, to identify if the number of viable cells decreases as a result of cell death, PI staining can be used, but to specifically look at if cell death is a result of apoptosis, Annexin V staining can be employed. Annexin V is able to bind phosphatidylserine that has been transitioned to the outside of the cell during the process of apoptosis (Van Engeland et al., 1998). By combining both Annexin V and PI staining followed by FACS analysis, both necrotic cells as well as early and late-stage apoptosis can be ascertained. This will help elucidate the mechanism by which cell death is occurring in CLIC1 silenced cells. For instance, cells stained with PI only indicate necrosis is taking place whereas cells stained with Annexin V only will be indicative of early-stage apoptosis. However, late stage apoptosis is defined by both Annexin and PI staining (Rieger et al., 2011).

D2.2 Intersection of oncogenic pathways between CLIC1 and OSMR

CRISPR-CAS9 technology was employed to generate a constitutive silencing CLIC1 in two patient-derived BTSC lines (BTSC147 and BTSC73). Validation of the two clones in both cell lines demonstrated to have a significant impact on proliferation, sphere size and stemness of BTSCs, leading to the conclusion that the phenotypes presented by the silencing of CLIC1 in the chosen clones phenocopies that of silencing OSMR in BTSCs (Jahani-Asl et al., 2016; Sharanek et al., 2020). Using the clones generated in this study, future experiments can be undertaken to determine the mechanistic intersection of OSMR and CLIC1 in BTSCs. An important question that requires more attention is how OSMR is regulated to determine its pro or anti-tumorigenic capabilities and how novel binding partners may influence its oncogenic role in cancer cells. One group attempting to answer this question has suggested that c-myc acts as a molecular switch to modulate the activity of OSMR/gp130 through downstream targets (Kan et al., 2011). C-myc belongs to the MYC oncogene family and it, like many of its members, has been identified to play a significant role in different hallmarks of cancer. Specifically, c-myc has been identified to be a master regulator in metabolic and proliferative pathways (Chen et al., 2018; Miller et al., 2012). The expression of c-myc, itself, is regulated by the binding of STAT3 to its promoter region which

has been shown to be induced by the activity of IL-6 family receptors of which OSMR is a member (Hirano et al., 2000). Interestingly, CLIC1 has been previously identified to be a transcriptional target of c-myc. In addition, CLIC1 expression was found to regulate the expression of downstream c-myc related genes (Jiang et al., 2020). This data, along with validation that CLIC1 and OSMR are endogenous binding partners suggests that these two proteins may mechanistically converge on c-myc or c-myc related pathways. Additionally, this could suggest that CLIC1 may be playing a larger role, perhaps in additional signalling to regulate the activity of OSMR in patient-derived BTSCs toward its pro- or anti-tumorigenic capabilities. To investigate this, experiments can first be devised to look at activity of downstream c-myc targets in the absence of CLIC1, OSMR or both.

D2.3 CLIC1 and immune function

The immune system is a complex system in which the innate and adaptive systems play a significant role in ensuring health of the individual. Although differentiated by two names, the innate and adaptive immune systems present coordinated and sometimes overlapping activities in the goal of protecting the host from pathogen, foreign substances, and compromised self-cells, such as the ones encountered in cancer (Chaplin, 2010). The innate immune system is composed of elements such as mucosal barriers, enzymatic proteins/bioactive molecules, and membrane receptors or proteins that bind specific molecular patterns. This branch also includes specific cell types including basophils, eosinophils, neutrophils, mast cells and natural killer (NK) cells (Chaplin, 2010; Marshall et al., 2018). The adaptive immune system, on the other hand, is composed of specialized cells that will generate a tailored response. This includes B and T cells that can be further divided into plasma cells, cytotoxic T cells, regulatory T cells, and natural killer T cells to name a few. Additionally, there are cell types that mediate the interaction between the innate and adaptive systems, this includes cells such as macrophages, other antigen-presenting cells (APC) and dendritic cells which are also known as professional phagocytic cells (Chaplin, 2010; Marshall et al., 2018). The cells that can present antigen must also be able to uptake material in a process known as phagocytosis. These cells are known as professional phagocytes as they have specific pathogen-associated molecular patterns on their plasma membrane to effectively phagocytize foreign material. Once engulfment takes place there is a series of pinching off events

that leads to the formation of a nascent phagosome within the APC. Phagosomes then go through a period of maturation in which the phagosome becomes increasingly acidic to degrade the particle engulfed (Kinchen & Ravichandran, 2008; Lee et al., 2020) (**Figure 22**).

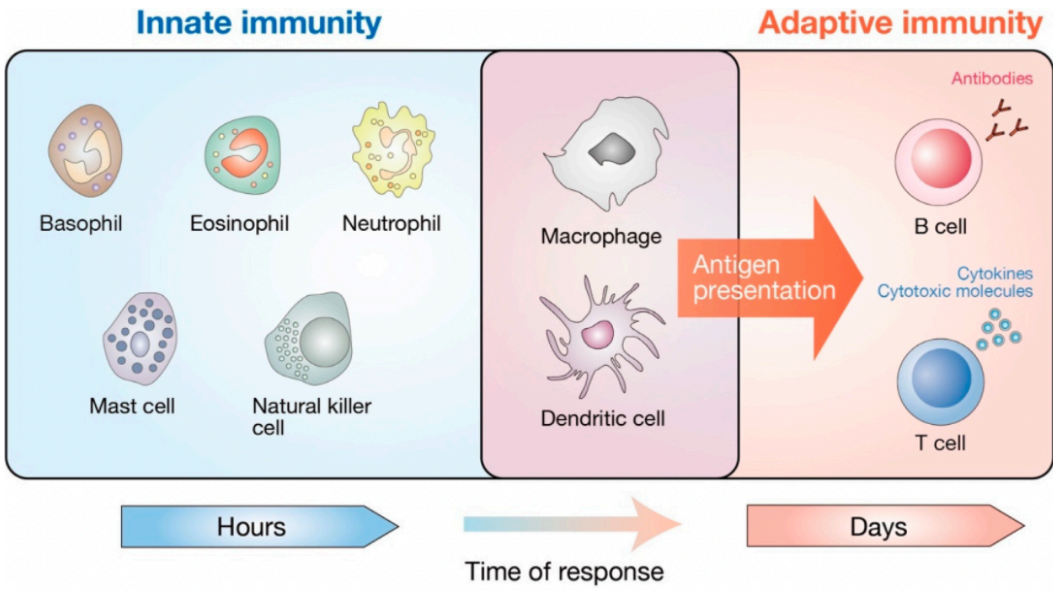

Figure retrieved from (Yamauchi & Moroishi, 2019) in Cell

Figure 22. Innate and adaptive immune cells with cells that overlap in both systems to generate a coordinated response against pathogens or hijacked self-cells. The innate immune system is the first line of defence of the body with cells taking action hours after infection, while the adaptive system is active days after infection to generate a tailored response.

The role of ion channels has been widely characterised for their importance in immunology such that they have been associated with lymphocyte function and development, as well as in innate immune function (Feske et al., 2012). Specifically, chloride channels play a key role in regulating the innate and adaptive immune pathways through the acquisition of intracellular chloride (Wang, 2016). The acquisition of chloride ions is highly essential to cells that can take up antigen or antigen-presenting cells; cells such as macrophages and dendritic cells that are the bridge between the two systems (Wang, 2016; Westman & Grinstein, 2021). This is because the change in pH, which is accomplished by chloride ion currents among others, is required for phagosome maturation. For instance, luminal acidification is essential in recycling receptors on

phagosomes, facilitating microbial responses by activating degrading enzymes, limiting microbial replication and enabling proteolysis for antigen presentation (Westman & Grinstein, 2021). Specifically, proteolysis capabilities of antigen presenting cells is accomplished by lysosomal proteinases one of which is cathepsin C. Interestingly, this proteinase has been identified to be activated in a chloride-dependent manner (Gorter & Gruber, 1970; Wang, 2016). This suggests that chloride is a key element in determining the efficiency of antigen presentation to other immune cells, thus mediating activities of the adaptive immune system (Wang, 2016). Similarly, to classical chloride channels, CLIC1, particularly, has been found to mediate immune function through phagosomal acidification (Jiang et al., 2012; Salao et al., 2016; Westman & Grinstein, 2021). In 2012, researchers concluded that upon phagocytosis of a serum-opsonized zymosan, CLIC1 localised to the phagosomal membrane in macrophages where it had an impact on acidification of these phagosomes. Although silencing of CLIC1 decreased acidification by a pH value of 0.2, this small difference was sufficient to produce an apparent change in macrophage proteolysis capabilities (Jiang et al., 2012). Similarly, the role of CLIC1 has also been characterised in antigen presenting cells such as dendritic cells. Impairment in acidification by silencing of CLIC1 significantly reduced $CD4^+$ T cell activation by mediating antigen processing pathways in bone marrow derived dendritic cells (BMDCs) (Salao et al., 2016). Furthermore, CLIC1 has been implicated in the activation and induction of secretory products such as IL-1β. This discovery highlights the role of this protein in the innate immune system through its involvement in the activation of the NOD-, LRR- and pyrin domain-containing protein 3 (NLRP3) inflammasome (Domingo-Fernández et al., 2017). Importantly, aberrant activity of the NLRP3 inflammasome has been implicated in the progression of several cancers including GB (Hamarsheh & Zeiser, 2020; Kelley et al., 2019). Finally, CLIC1 has also been identified to be translocated to the cell membrane where it mediates Cl^- current in activated microglia upon stimulation by β-amyloid protein (Aβ) (Novarino et al., 2004). Microglia are the immune effectors of the central nervous system which become activated upon stimulation by bacterial assault, trauma-related damage and inflammation (Block et al., 2007). Once activated these cells travel to the site of infection or damage and begin a series of events including secretion and production of pro-inflammatory molecules such as ROS/ tumour necrosis factor alpha (TNF-alpha) and begin to proliferate. This activation has been characterized to be mediated by alerted ion currents including chloride currents (Block et al., 2007). Interestingly, inhibition of CLIC1 in microglia reduced proliferative capacity as well as

reduced microglia capacity to express TNF-alpha thereby protecting neurons from neurotoxicity associated with Aβ protein (Novarino et al., 2004). This data points to the possibility of CLIC1 chloride currents having a direct and profound impact on immune function, hence it is important to conduct future studies on the intersection of OSMR and CLIC1 in terms of immune functioning. This is especially important since OSM, the natural ligand of OSMR is a critical mediator of inflammation, and immunity as well as plays a role in disease progression.

D2.4 Future studies of impact on ROS and ion conductance

Since CLIC1 presents a dichotomous structure, one in which it functions as a chloride channel (Gururaja Rao et al., 2020), looking at how chloride current is impacted by binding OSMR and how this current impacts other cellular processes can prove to be further avenues of study. Chloride currents are highly important in health and disease as chloride itself is known to be the principal anion of the body (Berend et al., 2012; Verkman & Galietta, 2009). In connection with other chloride channels that mediate the role of chloride currents in the cell cycle and the immune response, CLIC1 has also been identified to be an additional mediator of chloride currents in cancer cells (Francisco et al., 2020; Jia et al., 2016; Li et al., 2018; Miyazaki et al., 2008; Setti et al., 2013; Singha et al., 2018; L. Wang et al., 2012; Wang et al., 2011). Of note, chloride currents by CLIC1 have been previously identified as a mediator of intracellular ROS production in cancer cells. Interestingly, some research has suggested that CLIC1 is involved in suppressing ROS production while others claim it increases ROS generation, thus moulding the fate of the cell towards death or survival (Peretti et al., 2018; Shen & Liu, 2006). This is an area of interest and future study as there has been considerable evidence suggesting a bidirectional relationship between ROS, other ions and ion channels. This includes channels responsible for Ca^{2+} release or uptake (Görlach et al., 2015; Kiselyov & Muallem, 2016). This may suggest that CLIC1 could have a role in the regulation of intracellular ions. For instance, CLIC1 may be impacting ions such as Ca^{2+} through the regulation of ROS in the cell. Another hypothesis can be that CLIC1 is regulating Ca^{2+} currents in a more direct manner. In this manner, the impact of CLIC1 on calcium currents may be modulating the bidirectional effect of calcium and subsequently ROS as a second messengers. In support of this hypothesis, although the mechanism remains unclear, in 2019 Lee et al., published an article suggesting that CLIC1 regulates Ca^{2+} by controlling the activity of L-Type Calcium

Channels (LTCC) (Görlach et al., 2015; Hempel & Trebak, 2017; Lee et al., 2019). The mechanism by which this occurs is still under investigation, but one hypothesis proposed is environmental (Lee et al., 2019). Nonetheless, the potential intersection of ROS, chloride currents generated by CLIC1, and intracellular calcium currents suggests that CLIC1 may play a role in wide scale processes such as mitochondrial activity and metabolic functions of which both are critical in cancer progression. To begin to investigate these hypotheses the first step would be to examine how chloride currents are impacted by OSMR KO in BTSCs. This can be done using patch clamp experiments in OSMR KO and control BTSC lines. Next, calcium content studies can be undertaken in both OSMR and CLIC1 KO/KD lines using a calcium sensitive fluorescent radiometric dye, such as fura-2 (Zanin et al., 2019), to understand how calcium is affected by KO or KD of one or both interacting proteins. Finally, by looking at ROS production in control BTSCs and OSMR or CLIC1 KO lines important conclusions can be made about the intersection of these critical elements in the progression of glioblastoma.

D3. Conclusion

The data presented in this study identified a novel OSMR binding partner, Chloride Intracellular Channel 1 (CLIC1), in patient-derived brain tumour stem cells. This protein was identified through analysis of a Mammalian Membrane Two-Hybrid High Throughput Screen (MaMTH-HTS) and through in situ validation in BTSCs. siRNA or CRISPR-CAS9 mediated silencing of CLIC1 proved to have a significant impact on proliferation, sphere size and self-renewal capacity of BTSCs in a dose-dependent manner, suggesting an important role of CLIC1 in glioblastoma tumorigenesis. This work lays the foundation for future studies specifically aimed at understanding the mechanistic intersection of OSMR and CLIC1 in BTSCs at the level of resistance to therapy, metastasis and progression. The findings of this study put OSMR and CLIC1 at an important inspection point, one that places ions and ion conductance at the forefront of cancer progression in glioblastoma.

References

Abou-Fayçal, C., Hatat, A.-S., Gazzeri, S., & Eymin, B. (2017). Splice variants of the RTK family: their role in tumour progression and response to targeted therapy. *International journal of molecular sciences*, *18*(2), 383.

Adams, J. M., & Strasser, A. (2008). Is tumor growth sustained by rare cancer stem cells or dominant clones? *Cancer research*, *68*(11), 4018-4021.

Al Khamici, H., Brown, L. J., Hossain, K. R., Hudson, A. L., Sinclair-Burton, A. A., Ng, J. P. M., Daniel, E. L., Hare, J. E., Cornell, B. A., & Curmi, P. M. (2015). Members of the chloride intracellular ion channel protein family demonstrate glutaredoxin-like enzymatic activity. *PloS one*, *10*(1), e115699.

Araujo, A. M., Abaurrea, A., Azcoaga, P., López-Velazco, J. I., Manzano, S., Rodriguez, J., Rezola, R., Egia-Mendikute, L., Valdés-Mora, F., & Flores, J. M. (2022). Stromal oncostatin M cytokine promotes breast cancer progression by reprogramming the tumor microenvironment. *The Journal of clinical investigation*, *132*(7).

Ashley, R. (2003). Challenging accepted ion channel biology: p64 and the CLIC family of putative intracellular anion channel proteins. *Molecular membrane biology*, *20*(1), 1-11.

Bagal, S. K., Brown, A. D., Cox, P. J., Omoto, K., Owen, R. M., Pryde, D. C., Sidders, B., Skerratt, S. E., Stevens, E. B., & Storer, R. I. (2013). Ion channels as therapeutic targets: a drug discovery perspective. *Journal of medicinal chemistry*, *56*(3), 593-624.

Barbieri, F., Bosio, A. G., Pattarozzi, A., Tonelli, M., Bajetto, A., Verduci, I., Cianci, F., Cannavale, G., Palloni, L. M., & Francesconi, V. (2022). Chloride intracellular channel 1 activity is not required for glioblastoma development but its inhibition dictates glioma stem cell responsivity to novel biguanide derivatives. *Journal of Experimental & Clinical Cancer Research*, *41*(1), 1-27.

Barbieri, F., Verduci, I., Carlini, V., Zona, G., Pagano, A., Mazzanti, M., & Florio, T. (2019). Repurposed biguanide drugs in glioblastoma exert antiproliferative effects via the inhibition of intracellular chloride channel 1 activity. *Frontiers in Oncology*, *9*, 135.

Barbieri, F., Würth, R., Pattarozzi, A., Verduci, I., Mazzola, C., Cattaneo, M. G., Tonelli, M., Solari, A., Bajetto, A., & Daga, A. (2018). Inhibition of chloride intracellular channel 1 (CLIC1) as biguanide class-effect to impair human glioblastoma stem cell viability. *Frontiers in pharmacology*, *9*, 899.

Barnum, K. J., & O'Connell, M. J. (2014). Cell cycle regulation by checkpoints. In *Cell cycle control* (pp. 29-40). Springer.

Berend, K., van Hulsteijn, L. H., & Gans, R. O. (2012). Chloride: the queen of electrolytes? *European journal of internal medicine*, *23*(3), 203-211.

Block, M. L., Zecca, L., & Hong, J.-S. (2007). Microglia-mediated neurotoxicity: uncovering the molecular mechanisms. *Nature Reviews Neuroscience*, *8*(1), 57-69.

Board, P. G., Coggan, M., Watson, S., Gage, P. W., & Dulhunty, A. F. (2004). CLIC-2 modulates cardiac ryanodine receptor Ca2+ release channels. *The international journal of biochemistry & cell biology*, *36*(8), 1599-1612.

Böing, I., Stross, C., Radtke, S., Lippok, B. E., Heinrich, P. C., & Hermanns, H. M. (2006). Oncostatin M-induced activation of stress-activated MAP kinases depends on tyrosine 861 in the OSM receptor and requires Jak1 but not Src kinases. *Cellular signalling*, *18*(1), 50-61.

Brennan, C. W., Verhaak, R. G., McKenna, A., Campos, B., Noushmehr, H., Salama, S. R., Zheng, S., Chakravarty, D., Sanborn, J. Z., & Berman, S. H. (2013). The somatic genomic landscape of glioblastoma. *Cell*, *155*(2), 462-477.

Burke Jr, K. J., & Bender, K. J. (2019). Modulation of ion channels in the axon: mechanisms and function. *Frontiers in cellular neuroscience*, *13*, 221.

Chaplin, D. D. (2010). Overview of the immune response. *Journal of allergy and clinical immunology*, *125*(2), S3-S23.

Chen, D., Chu, C. Y., Chen, C. Y., Yang, H. C., Chiang, Y. Y., Lin, T. Y., Chiang, I. P., Chuang, D. Y., Yu, C. C., & Chow, K. C. (2008). Expression of short-form oncostatin M receptor as a decoy receptor in lung adenocarcinomas. *The Journal of Pathology: A Journal of the Pathological Society of Great Britain and Ireland*, *215*(3), 290-299.

Chen, H., Liu, H., & Qing, G. (2018). Targeting oncogenic Myc as a strategy for cancer treatment. *Signal transduction and targeted therapy*, *3*(1), 1-7.

Chen, M., Ren, R., Lin, W., Xiang, L., Zhao, Z., & Shao, B. (2021). Exploring the oncostatin M (OSM) feed-forward signaling of glioblastoma via STAT3 in pan-cancer analysis. *Cancer cell international*, *21*(1), 1-19.

Dang, C. V. (2012). MYC on the path to cancer. *Cell*, *149*(1), 22-35.

David, E., Guihard, P., Brounais, B., Riet, A., Charrier, C., Battaglia, S., Gouin, F., Ponsolle, S., Bot, R. L., & Richards, C. D. (2011). Direct anti-cancer effect of oncostatin M on chondrosarcoma. *International Journal of Cancer*, *128*(8), 1822-1835.

David, E., Tirode, F., Baud'Huin, M., Guihard, P., Laud, K., Delattre, O., Heymann, M. F., Heymann, D., Redini, F., & Blanchard, F. (2012). Oncostatin M is a growth factor for Ewing sarcoma. *The American journal of pathology*, *181*(5), 1782-1795.

Dey, G., Radhakrishnan, A., Syed, N., Thomas, J. K., Nadig, A., Srikumar, K., Mathur, P. P., Pandey, A., Lin, S.-K., & Raju, R. (2013). Signaling network of Oncostatin M pathway. *Journal of Cell Communication and Signaling*, *7*(2), 103-108.

Djuric, U., Lam, K. B., Kao, J., Batruch, I., Jevtic, S., Papaioannou, M.-D., & Diamandis, P. (2019). Defining Protein Pattern Differences Among Molecular Subtypes of Diffuse Gliomas Using Mass Spectrometry*[S]. *Molecular & Cellular Proteomics*, *18*(10), 2029-2043.

Domingo-Fernández, R., Coll, R. C., Kearney, J., Breit, S., & O'Neill, L. A. (2017). The intracellular chloride channel proteins CLIC1 and CLIC4 induce IL-1β transcription and activate the NLRP3 inflammasome. *Journal of Biological Chemistry*, *292*(29), 12077-12087.

Dubyak, G. R. (2004). Ion homeostasis, channels, and transporters: an update on cellular mechanisms. *Advances in physiology education*, *28*(4), 143-154.

Engler, C., Gruetzner, R., Kandzia, R., & Marillonnet, S. (2009). Golden gate shuffling: a one-pot DNA shuffling method based on type IIs restriction enzymes. *PloS one*, *4*(5), e5553.

Feng, J., Xu, J., Xu, Y., Xiong, J., Xiao, T., Jiang, C., Li, X., Wang, Q., Li, J., & Li, Y. (2019). CLIC1 promotes the progression of oral squamous cell carcinoma via integrins/ERK pathways. *American Journal of Translational Research*, *11*(2), 557.

Fernandes, C., Costa, A., Osório, L., Lago, R. C., Linhares, P., Carvalho, B., & Caeiro, C. (2017). Current standards of care in glioblastoma therapy. *Exon Publications*, 197-241.

Feske, S., Skolnik, E. Y., & Prakriya, M. (2012). Ion channels and transporters in lymphocyte function and immunity. *Nature Reviews Immunology*, *12*(7), 532-547.

Feske, S., Wulff, H., & Skolnik, E. Y. (2015). Ion channels in innate and adaptive immunity. *Annual review of immunology*, *33*, 291.

Francisco, M. A., Wanggou, S., Fan, J. J., Dong, W., Chen, X., Momin, A., Abeysundara, N., Min, H.-K., Chan, J., & McAdam, R. (2020). Chloride intracellular channel 1 cooperates with potassium channel EAG2 to promote medulloblastoma growth. *Journal of Experimental Medicine*, *217*(5).

Fredriksson, S., Gullberg, M., Jarvius, J., Olsson, C., Pietras, K., Gústafsdóttir, S. M., Östman, A., & Landegren, U. (2002). Protein detection using proximity-dependent DNA ligation assays. *Nature biotechnology*, *20*(5), 473-477.

Friedrich, M., Höss, N., Stögbauer, F., Senner, V., Paulus, W., Ringelstein, E. b., & Halfter, H. (2001). Complete inhibition of in vivo glioma growth by oncostatin M. *Journal of neurochemistry*, *76*(5), 1589-1592.

Gabrusiewicz, K., Rodriguez, B., Wei, J., Hashimoto, Y., Healy, L. M., Maiti, S. N., Thomas, G., Zhou, S., Wang, Q., & Elakkad, A. (2016). Glioblastoma-infiltrated innate immune cells resemble M0 macrophage phenotype. *JCI insight*, *1*(2).

Galli, R., Binda, E., Orfanelli, U., Cipelletti, B., Gritti, A., De Vitis, S., Fiocco, R., Foroni, C., Dimeco, F., & Vescovi, A. (2004). Isolation and characterization of tumorigenic, stem-like neural precursors from human glioblastoma. *Cancer research*, *64*(19), 7011-7021.

Gan, H. K., Kaye, A. H., & Luwor, R. B. (2009). The EGFRvIII variant in glioblastoma multiforme. *Journal of Clinical Neuroscience*, *16*(6), 748-754.

Gangemi, R. M. R., Griffero, F., Marubbi, D., Perera, M., Capra, M. C., Malatesta, P., Ravetti, G. L., Zona, G. L., Daga, A., & Corte, G. (2009). SOX2 silencing in glioblastoma tumor-initiating cells causes stop of proliferation and loss of tumorigenicity. *Stem cells*, *27*(1), 40-48.

Gerdes, J., Schwab, U., Lemke, H., & Stein, H. (1983). Production of a mouse monoclonal antibody reactive with a human nuclear antigen associated with cell proliferation. *International Journal of Cancer*, *31*(1), 13-20.

Gilard, V., Tebani, A., Dabaj, I., Laquerrière, A., Fontanilles, M., Derrey, S., Marret, S., & Bekri, S. (2021). Diagnosis and management of glioblastoma: A comprehensive perspective. *Journal of Personalized Medicine*, *11*(4), 258.

Gimple, R. C., Bhargava, S., Dixit, D., & Rich, J. N. (2019). Glioblastoma stem cells: lessons from the tumor hierarchy in a lethal cancer. *Genes & development*, *33*(11-12), 591-609.

Giorgi, C., Marchi, S., & Pinton, P. (2018). The machineries, regulation and cellular functions of mitochondrial calcium. *Nature reviews Molecular cell biology*, *19*(11), 713-730.

Gordeeva, A., Zvyagilskaya, R., & Labas, Y. A. (2003). Cross-talk between reactive oxygen species and calcium in living cells. *Biochemistry (Moscow)*, *68*(10), 1077-1080.

Görlach, A., Bertram, K., Hudecova, S., & Krizanova, O. (2015). Calcium and ROS: A mutual interplay. *Redox biology*, *6*, 260-271.

Gorter, J., & Gruber, M. (1970). Cathepsin C: an allosteric enzyme. *Biochimica et Biophysica Acta (BBA)-Enzymology*, *198*(3), 546-555.

Gottesman, M. M., Fojo, T., & Bates, S. E. (2002). Multidrug resistance in cancer: role of ATP–dependent transporters. *Nature Reviews Cancer*, *2*(1), 48-58.

Gritti, M., Würth, R., Angelini, M., Barbieri, F., Peretti, M., Pizzi, E., Pattarozzi, A., Carra, E., Sirito, R., & Daga, A. (2014). Metformin repositioning as antitumoral agent: selective antiproliferative effects in human glioblastoma stem cells, via inhibition of CLIC1-mediated ion current. *Oncotarget*, *5*(22), 11252.

Gumz, M. L., Rabinowitz, L., & Wingo, C. S. (2015). An integrated view of potassium homeostasis. *New England journal of medicine*, *373*(1), 60-72.
Guo, D., Xie, W., Xiong, P., Li, H., Wang, S., Chen, G., Gao, Y., Zhou, J., Zhang, Y., & Bu, G. (2018). Cyclin-dependent kinase 5-mediated phosphorylation of chloride intracellular channel 4 promotes oxidative stress-induced neuronal death. *Cell death & disease*, *9*(10), 1-13.
Guo, Q., Guan, G. f., Cao, J. y., Zou, C. y., Zhu, C., Cheng, W., Xu, X. y., Lin, Z. g., Cheng, P., & Wu, A. h. (2019). Overexpression of oncostatin M receptor regulates local immune response in glioblastoma. *Journal of Cellular Physiology*, *234*(9), 15496-15509.
Gurski, L. A., Knowles, L. M., Basse, P. H., Maranchie, J. K., Watkins, S. C., & Pilch, J. (2015). Relocation of CLIC1 Promotes Tumor Cell Invasion and Colonization of FibrinCLIC1 Promotes Fibrin Invasion and Colonization. *Molecular Cancer Research*, *13*(2), 273-280.
Gururaja Rao, S., Patel, N. J., & Singh, H. (2020). Intracellular chloride channels: novel biomarkers in diseases. *Frontiers in physiology*, *11*, 96.
Habela, C. W., & Sontheimer, H. (2007). Cytoplasmic volume condensation is an integral part of mitosis. *Cell cycle*, *6*(13), 1613-1620.
Hale, J. S., Sinyuk, M., Rich, J. N., & Lathia, J. D. (2013). Decoding the cancer stem cell hypothesis in glioblastoma. *CNS oncology*, *2*(4), 319-330.
Halfter, H., Friedrich, M., Resch, A., Kullmann, M., Stögbauer, F., Ringelstein, E. B., & Hengst, L. (2006). Oncostatin M induces growth arrest by inhibition of Skp2, Cks1, and cyclin A expression and induced p21 expression. *Cancer research*, *66*(13), 6530-6539.
Hamarsheh, S. a., & Zeiser, R. (2020). NLRP3 inflammasome activation in cancer: a double-edged sword. *Frontiers in immunology*, *11*, 1444.
Hara, T., Chanoch-Myers, R., Mathewson, N. D., Myskiw, C., Atta, L., Bussema, L., Eichhorn, S. W., Greenwald, A. C., Kinker, G. S., & Rodman, C. (2021). Interactions between cancer cells and immune cells drive transitions to mesenchymal-like states in glioblastoma. *Cancer cell*, *39*(6), 779-792. e711.
Harrop, S. J., DeMaere, M. Z., Fairlie, W. D., Reztsova, T., Valenzuela, S. M., Mazzanti, M., Tonini, R., Qiu, M. R., Jankova, L., & Warton, K. (2001). Crystal structure of a soluble form of the intracellular chloride ion channel CLIC1 (NCC27) at 1.4-Å resolution. *Journal of Biological Chemistry*, *276*(48), 44993-45000.
Hartwell, L. H., & Weinert, T. A. (1989). Checkpoints: controls that ensure the order of cell cycle events. *Science*, *246*(4930), 629-634.
Heinrich, P. C., Behrmann, I., Haan, S., Hermanns, H. M., Müller-Newen, G., & Schaper, F. (2003). Principles of interleukin (IL)-6-type cytokine signalling and its regulation. *Biochemical journal*, *374*(1), 1-20.
Heinrich, P. C., Behrmann, I., Müller-Newen, G., Schaper, F., & Graeve, L. (1998). Interleukin-6-type cytokine signalling through the gp130/Jak/STAT pathway. *Biochemical journal*, *334*(2), 297-314.
Hempel, N., & Trebak, M. (2017). Crosstalk between calcium and reactive oxygen species signaling in cancer. *Cell Calcium*, *63*, 70-96.
Hermanns, H. M. (2015). Oncostatin M and interleukin-31: cytokines, receptors, signal transduction and physiology. *Cytokine & growth factor reviews*, *26*(5), 545-558.
Hermanns, H. M., Radtke, S., Schaper, F., Heinrich, P. C., & Behrmann, I. (2000). Non-redundant signal transduction of interleukin-6-type cytokines: the adapter protein Shc is

specifically recruited to the oncostatin M receptor. *Journal of Biological Chemistry*, *275*(52), 40742-40748.
Hernandez-Fernaud, J. R., Ruengeler, E., Casazza, A., Neilson, L. J., Pulleine, E., Santi, A., Ismail, S., Lilla, S., Dhayade, S., & MacPherson, I. R. (2017). Secreted CLIC3 drives cancer progression through its glutathione-dependent oxidoreductase activity. *Nature communications*, *8*(1), 1-17.
Hirano, T., Ishihara, K., & Hibi, M. (2000). Roles of STAT3 in mediating the cell growth, differentiation and survival signals relayed through the IL-6 family of cytokine receptors. *Oncogene*, *19*(21), 2548-2556.
Holohan, C., Van Schaeybroeck, S., Longley, D. B., & Johnston, P. G. (2013). Cancer drug resistance: an evolving paradigm. *Nature Reviews Cancer*, *13*(10), 714-726.
Hu, Y., & Smyth, G. K. (2009). ELDA: extreme limiting dilution analysis for comparing depleted and enriched populations in stem cell and other assays. *Journal of immunological methods*, *347*(1-2), 70-78.
Huang, D. W., Sherman, B. T., & Lempicki, R. A. (2009). Systematic and integrative analysis of large gene lists using DAVID bioinformatics resources. *Nature protocols*, *4*(1), 44-57.
Hübner, C. A., & Jentsch, T. J. (2002). Ion channel diseases. *Human molecular genetics*, *11*(20), 2435-2445.
Iyer, K., Burkle, L., Auerbach, D., Thaminy, S., Dinkel, M., Engels, K., & Stagljar, I. (2005). Utilizing the split-ubiquitin membrane yeast two-hybrid system to identify protein-protein interactions of integral membrane proteins. *Science's STKE*, *2005*(275), pl3-pl3.
Jahani-Asl, A., Yin, H., Soleimani, V. D., Haque, T., Luchman, H. A., Chang, N. C., Sincennes, M.-C., Puram, S. V., Scott, A. M., & Lorimer, I. A. (2016). Control of glioblastoma tumorigenesis by feed-forward cytokine signaling. *Nature neuroscience*, *19*(6), 798-806.
Jentsch, T. J., Hübner, C. A., & Fuhrmann, J. C. (2004). Ion channels: function unravelled by dysfunction. *Nature cell biology*, *6*(11), 1039-1047.
Jia, N., Dong, S., Zhao, G., Gao, H., Li, X., & Zhang, H. (2016). CLIC1 overexpression is associated with poor prognosis in pancreatic ductal adenocarcinomas. *Journal of cancer research and therapeutics*, *12*(2), 892.
Jiang, L., Salao, K., Li, H., Rybicka, J. M., Yates, R. M., Luo, X. W., Shi, X. X., Kuffner, T., Tsai, V. W.-W., & Husaini, Y. (2012). Intracellular chloride channel protein CLIC1 regulates macrophage function through modulation of phagosomal acidification. *Journal of cell science*, *125*(22), 5479-5488.
Jiang, X., Liu, Y., Wang, G., Yao, Y., Mei, C., Wu, X., Ma, W., & Yuan, Y. (2020). Up-regulation of CLIC1 activates MYC signaling and forms a positive feedback regulatory loop with MYC in Hepatocellular carcinoma. *American journal of cancer research*, *10*(8), 2355.
Junk, D. J., Bryson, B. L., Smigiel, J. M., Parameswaran, N., Bartel, C. A., & Jackson, M. W. (2017). Oncostatin M promotes cancer cell plasticity through cooperative STAT3-SMAD3 signaling. *Oncogene*, *36*(28), 4001-4013.
Kagiali, Z. C. U., Saner, N., Akdag, M., Sanal, E., Degirmenci, B. S., Mollaoglu, G., & Ozlu, N. (2020). CLIC4 and CLIC1 bridge plasma membrane and cortical actin network for a successful cytokinesis. *Life science alliance*, *3*(2).
Kalkan, R. (2015). Glioblastoma stem cells as a new therapeutic target for glioblastoma. *Clinical Medicine Insights: Oncology*, *9*, CMO. S30271.

Kan, C. E., Cipriano, R., & Jackson, M. W. (2011). c-MYC functions as a molecular switch to alter the response of human mammary epithelial cells to oncostatin M. *Cancer research*, *71*(22), 6930-6939.

Kang, M.-K., & Kang, S.-K. (2008). Pharmacologic blockade of chloride channel synergistically enhances apoptosis of chemotherapeutic drug-resistant cancer stem cells. *Biochemical and Biophysical Research Communications*, *373*(4), 539-544.

Kelley, N., Jeltema, D., Duan, Y., & He, Y. (2019). The NLRP3 inflammasome: an overview of mechanisms of activation and regulation. *International journal of molecular sciences*, *20*(13), 3328.

Kim, M. S., Louwagie, J., Carvalho, B., Terhaar sive Droste, J. S., Park, H. L., Chae, Y. K., Yamashita, K., Liu, J., Ostrow, K. L., & Ling, S. (2009). Promoter DNA methylation of Oncostatin M receptor-β as a novel diagnostic and therapeutic marker in colon cancer. *PloS one*, *4*(8), e6555.

Kim, Y., Varn, F. S., Park, S.-H., Yoon, B. W., Park, H. R., Lee, C., Verhaak, R. G., & Paek, S. H. (2021). Perspective of mesenchymal transformation in glioblastoma. *Acta neuropathologica communications*, *9*(1), 1-20.

Kinchen, J. M., & Ravichandran, K. S. (2008). Phagosome maturation: going through the acid test. *Nature reviews Molecular cell biology*, *9*(10), 781-795.

Kiselyov, K., & Muallem, S. (2016). ROS and intracellular ion channels. *Cell Calcium*, *60*(2), 108-114.

Knowles, L. M., Malik, G., Hood, B. L., Conrads, T. P., & Pilch, J. (2012). CLT1 targets angiogenic endothelium through CLIC1 and fibronectin. *Angiogenesis*, *15*(1), 115-129.

Kobayashi, T., Shiozaki, A., Nako, Y., Ichikawa, D., Kosuga, T., Shoda, K., Arita, T., Konishi, H., Komatsu, S., & Kubota, T. (2018). Chloride intracellular channel 1 as a switch among tumor behaviors in human esophageal squamous cell carcinoma. *Oncotarget*, *9*(33), 23237.

Kucia-Tran, J. A., Tulkki, V., Smith, S., Scarpini, C. G., Hughes, K., Araujo, A. M., Yan, K. Y. M., Botthof, J., Pérez-Gómez, E., & Quintanilla, M. (2016). Overexpression of the oncostatin-M receptor in cervical squamous cell carcinoma is associated with epithelial–mesenchymal transition and poor overall survival. *British journal of cancer*, *115*(2), 212-222.

Kullmann, D. M., & Waxman, S. G. (2010). Neurological channelopathies: new insights into disease mechanisms and ion channel function. *The Journal of physiology*, *588*(11), 1823-1827.

Langmead, B., & Salzberg, S. L. (2012). Fast gapped-read alignment with Bowtie 2. *Nature methods*, *9*(4), 357-359.

Lee, B. Y., Hogg, E. K., Below, C. R., Kononov, A., Blanco-Gomez, A., Heider, F., Xu, J., Hutton, C., Zhang, X., & Scheidt, T. (2021). Heterocellular OSM-OSMR signalling reprograms fibroblasts to promote pancreatic cancer growth and metastasis. *Nature communications*, *12*(1), 1-20.

Lee, H.-J., Woo, Y., Hahn, T.-W., Jung, Y. M., & Jung, Y.-J. (2020). Formation and maturation of the phagosome: a key mechanism in innate immunity against intracellular bacterial infection. *Microorganisms*, *8*(9), 1298.

Lee, J.-R., Lee, J.-Y., Kim, H.-J., Hahn, M.-J., Kang, J.-S., & Cho, H. (2019). The inhibition of chloride intracellular channel 1 enhances Ca2+ and reactive oxygen species signaling in A549 human lung cancer cells. *Experimental & molecular medicine*, *51*(7), 1-11.

Levy, J. B., Schindler, C., Raz, R., Levy, D. E., Baron, R., & Horowitz, M. C. (1996). Activation of the JAK-STAT signal transduction pathway by oncostatin-M cultured human and mouse osteoblastic cells. *Endocrinology*, *137*(4), 1159-1165.

Li, B.-p., Mao, Y.-t., Wang, Z., Chen, Y.-y., Wang, Y., Zhai, C.-y., Shi, B., Liu, S.-y., Liu, J.-l., & Chen, J.-q. (2018). CLIC1 promotes the progression of gastric cancer by regulating the MAPK/AKT pathways. *Cellular Physiology and Biochemistry*, *46*(3), 907-924.

Li, C., Ahlborn, T. E., Kraemer, F. B., & Liu, J. (2001). Oncostatin M–induced growth inhibition and morphological changes of MDA-MB231 breast cancer cells are abolished by blocking the MEK/ERK signaling pathway. *Breast cancer research and treatment*, *66*(2), 111-121.

Liebelt, B. D., Shingu, T., Zhou, X., Ren, J., Shin, S. A., & Hu, J. (2016). Glioma stem cells: signaling, microenvironment, and therapy. *Stem cells international*, *2016*.

Lim, S. H., Snider, J., Birimberg-Schwartz, L., Ip, W., Serralha, J. C., Botelho, H. M., Lopes-Pacheco, M., Pinto, M. C., Moutaoufik, M. T., & Zilocchi, M. (2022). CFTR interactome mapping using the mammalian membrane two-hybrid high-throughput screening system. *Molecular systems biology*, *18*(2), e10629.

Litan, A., & Langhans, S. A. (2015). Cancer as a channelopathy: ion channels and pumps in tumor development and progression. *Frontiers in cellular neuroscience*, *9*, 86.

Littler, D. R., Harrop, S. J., Fairlie, W. D., Brown, L. J., Pankhurst, G. J., Pankhurst, S., DeMaere, M. Z., Campbell, T. J., Bauskin, A. R., & Tonini, R. (2004). The intracellular chloride ion channel protein CLIC1 undergoes a redox-controlled structural transition. *Journal of Biological Chemistry*, *279*(10), 9298-9305.

Littler, D. R., Harrop, S. J., Goodchild, S. C., Phang, J. M., Mynott, A. V., Jiang, L., Valenzuela, S. M., Mazzanti, M., Brown, L. J., & Breit, S. N. (2010). The enigma of the CLIC proteins: Ion channels, redox proteins, enzymes, scaffolding proteins? *FEBS letters*, *584*(10), 2093-2101.

Liu, Y., Wang, Z., Li, M., Ye, Y., Xu, Y., Zhang, Y., Yuan, R., Jin, Y., Hao, Y., & Jiang, L. (2017). Chloride intracellular channel 1 regulates the antineoplastic effects of metformin in gallbladder cancer cells. *Cancer science*, *108*(6), 1240-1252.

Lu, C., Rak, J. W., Kobayashi, H., & Kerbel, R. S. (1993). Increased resistance to oncostatin M-induced growth inhibition of human melanoma cell lines derived from advanced-stage lesions. *Cancer research*, *53*(12), 2708-2711.

Malik, N., Kallestad, J., Gunderson, N., Austin, S., Neubauer, M., Ochs, V., Marquardt, H., Zarling, J., Shoyab, M., & Wei, C. (1989). Molecular cloning, sequence analysis, and functional expression of a novel growth regulator, oncostatin M. *Molecular and Cellular Biology*, *9*(7), 2847-2853.

Marchi, S., Patergnani, S., Missiroli, S., Morciano, G., Rimessi, A., Wieckowski, M. R., Giorgi, C., & Pinton, P. (2018). Mitochondrial and endoplasmic reticulum calcium homeostasis and cell death. *Cell Calcium*, *69*, 62-72.

Mariathasan, S., Turley, S. J., Nickles, D., Castiglioni, A., Yuen, K., Wang, Y., Kadel III, E. E., Koeppen, H., Astarita, J. L., & Cubas, R. (2018). TGFβ attenuates tumour response to PD-L1 blockade by contributing to exclusion of T cells. *nature*, *554*(7693), 544-548.

Marshall, J. S., Warrington, R., Watson, W., & Kim, H. L. (2018). An introduction to immunology and immunopathology. *Allergy, Asthma & Clinical Immunology*, *14*(2), 1-10.

Martin, T. A., Ye, L., Sanders, A. J., Lane, J., & Jiang, W. G. (2013). Cancer invasion and metastasis: molecular and cellular perspective. In *Madame Curie Bioscience Database [Internet]*. Landes Bioscience.

Masjedi, A., Hajizadeh, F., Dargani, F. B., Beyzai, B., Aksoun, M., Hojjat-Farsangi, M., Zekiy, A., & Jadidi-Niaragh, F. (2021). Oncostatin M: a mysterious cytokine in cancers. *International Immunopharmacology*, *90*, 107158.

Matsui, W. H. (2016). Cancer stem cell signaling pathways. *Medicine*, *95*(Suppl 1).

Matsumoto, Y., Ichikawa, T., Kurozumi, K., Otani, Y., Fujimura, A., Fujii, K., Tomita, Y., Hattori, Y., Uneda, A., & Tsuboi, N. (2020). Annexin A2–STAT3–Oncostatin M receptor axis drives phenotypic and mesenchymal changes in glioblastoma. *Acta neuropathologica communications*, *8*(1), 1-13.

McLendon, R., Friedman, A., Bigner, D., Van Meir, E. G., Brat, D. J., M. Mastrogianakis, G., Olson, J. J., Mikkelsen, T., Lehman, N., Aldape, K., Alfred Yung, W. K., Bogler, O., VandenBerg, S., Berger, M., Prados, M., Muzny, D., Morgan, M., Scherer, S., Sabo, A., . . . National Human Genome Research, I. (2008). Comprehensive genomic characterization defines human glioblastoma genes and core pathways. *nature*, *455*(7216), 1061-1068. https://doi.org/10.1038/nature07385

Menon, S., & Goswami, P. (2007). A redox cycle within the cell cycle: ring in the old with the new. *Oncogene*, *26*(8), 1101-1109.

Mi, H., Ebert, D., Muruganujan, A., Mills, C., Albou, L.-P., Mushayamaha, T., & Thomas, P. D. (2021). PANTHER version 16: a revised family classification, tree-based classification tool, enhancer regions and extensive API. *Nucleic acids research*, *49*(D1), D394-D403.

Miller, D. M., Thomas, S. D., Islam, A., Muench, D., & Sedoris, K. (2012). c-Myc and cancer metabolism. *Clinical cancer research*, *18*(20), 5546-5553.

Miltiadous, G., Christidis, D., Kalogirou, M., & Elisaf, M. (2008). Causes and mechanisms of acid–base and electrolyte abnormalities in cancer patients. *European journal of internal medicine*, *19*(1), 1-7.

Miyazaki, H., Shiozaki, A., Niisato, N., Ohsawa, R., Itoi, H., Ueda, Y., Otsuji, E., Yamagishi, H., Iwasaki, Y., & Nakano, T. (2008). Chloride ions control the G1/S cell-cycle checkpoint by regulating the expression of p21 through a p53-independent pathway in human gastric cancer cells. *Biochemical and Biophysical Research Communications*, *366*(2), 506-512.

Mongin, A. A., & Orlov, S. N. (2001). Mechanisms of cell volume regulation and possible nature of the cell volume sensor. *Pathophysiology*, *8*(2), 77-88.

Mosley, B., De Imus, C., Friend, D., Boiani, N., Thoma, B., Park, L. S., & Cosman, D. (1996). Dual oncostatin M (OSM) receptors: cloning and characterization of an alternative signaling subunit conferring OSM-specific receptor activation. *Journal of Biological Chemistry*, *271*(51), 32635-32643.

Mount, D. B., & Zandi-Nejad, K. (2012). Disorders of potassium balance. *The kidney. 9th ed. Philadelphia: Elsevier*, *2012*, 640-688.

Natesh, K., Bhosale, D., Desai, A., Chandrika, G., Pujari, R., Jagtap, J., Chugh, A., Ranade, D., & Shastry, P. (2015). Oncostatin-M differentially regulates mesenchymal and proneural signature genes in gliomas via STAT3 signaling. *Neoplasia*, *17*(2), 225-237.

Neftel, C., Laffy, J., Filbin, M. G., Hara, T., Shore, M. E., Rahme, G. J., Richman, A. R., Silverbush, D., Shaw, M. L., & Hebert, C. M. (2019). An integrative model of cellular states, plasticity, and genetics for glioblastoma. *Cell*, *178*(4), 835-849. e821.

Ng, G., Winder, D., Muralidhar, B., Gooding, E., Roberts, I., Pett, M., Mukherjee, G., Huang, J., & Coleman, N. (2007). Gain and overexpression of the oncostatin M receptor occur frequently in cervical squamous cell carcinoma and are associated with adverse clinical outcome. *The Journal of Pathology: A Journal of the Pathological Society of Great Britain and Ireland*, *212*(3), 325-334.

Novarino, G., Fabrizi, C., Tonini, R., Denti, M. A., Malchiodi-Albedi, F., Lauro, G. M., Sacchetti, B., Paradisi, S., Ferroni, A., & Curmi, P. M. (2004). Involvement of the intracellular ion channel CLIC1 in microglia-mediated β-amyloid-induced neurotoxicity. *Journal of Neuroscience*, *24*(23), 5322-5330.

Nowell, P. C. (1976). The Clonal Evolution of Tumor Cell Populations: Acquired genetic lability permits stepwise selection of variant sublines and underlies tumor progression. *Science*, *194*(4260), 23-28.

Ohgaki, H., Dessen, P., Jourde, B., Horstmann, S., Nishikawa, T., Di Patre, P.-L., Burkhard, C., Schüler, D., Probst-Hensch, N. M., & Maiorka, P. C. (2004). Genetic pathways to glioblastoma: a population-based study. *Cancer research*, *64*(19), 6892-6899.

Ohgaki, H., & Kleihues, P. (2013). The Definition of Primary and Secondary GlioblastomaDefinition of Primary and Secondary Glioblastomas. *Clinical cancer research*, *19*(4), 764-772.

Okada, Y., Maeno, E., Shimizu, T., Dezaki, K., Wang, J., & Morishima, S. (2001). Receptor-mediated control of regulatory volume decrease (RVD) and apoptotic volume decrease (AVD). *The Journal of physiology*, *532*(1), 3-16.

Olar, A., & Aldape, K. D. (2014). Using the molecular classification of glioblastoma to inform personalized treatment. *The Journal of pathology*, *232*(2), 165-177.

Orecchioni, M., Ghosheh, Y., Pramod, A. B., & Ley, K. (2019). Macrophage polarization: different gene signatures in M1 (LPS+) vs. classically and M2 (LPS–) vs. alternatively activated macrophages. *Frontiers in immunology*, *10*, 1084.

Palmer, B. F. (2015). Regulation of potassium homeostasis. *Clinical Journal of the American Society of Nephrology*, *10*(6), 1050-1060.

Pan, C.-M., Wang, M.-L., Chiou, S.-H., Chen, H.-Y., & Wu, C.-W. (2016). Oncostatin M suppresses metastasis of lung adenocarcinoma by inhibiting SLUG expression through coordination of STATs and PIASs signalings. *Oncotarget*, *7*(37), 60395.

Panyi, G., Beeton, C., & Felipe, A. (2014). Ion channels and anti-cancer immunity. *Philosophical Transactions of the Royal Society B: Biological Sciences*, *369*(1638), 20130106.

Peng, J.-M., Lin, S.-H., Yu, M.-C., & Hsieh, S.-Y. (2021). CLIC1 recruits PIP5K1A/C to induce cell-matrix adhesions for tumor metastasis. *The Journal of clinical investigation*, *131*(1).

Peretti, M., Angelini, M., Savalli, N., Florio, T., Yuspa, S. H., & Mazzanti, M. (2015). Chloride channels in cancer: Focus on chloride intracellular channel 1 and 4 (CLIC1 AND CLIC4) proteins in tumor development and as novel therapeutic targets. *Biochimica et Biophysica Acta (BBA)-Biomembranes*, *1848*(10), 2523-2531.

Peretti, M., Raciti, F. M., Carlini, V., Verduci, I., Sertic, S., Barozzi, S., Garré, M., Pattarozzi, A., Daga, A., & Barbieri, F. (2018). Mutual Influence of ROS, pH, and CLIC1 Membrane Protein in the Regulation of G1–S Phase Progression in Human Glioblastoma Stem CellsCLIC1 Activity Controls Glioblastoma Stem Cell Proliferation. *Molecular cancer therapeutics*, *17*(11), 2451-2461.

Petschnigg, J., Groisman, B., Kotlyar, M., Taipale, M., Zheng, Y., Kurat, C. F., Sayad, A., Sierra, J. R., Usaj, M. M., & Snider, J. (2014). The mammalian-membrane two-hybrid assay (MaMTH) for probing membrane-protein interactions in human cells. *Nature methods*, *11*(5), 585-592.

Ponnalagu, D., Rao, S. G., Farber, J., Xin, W., Hussain, A. T., Shah, K., Tanda, S., Berryman, M., Edwards, J. C., & Singh, H. (2016). Molecular identity of cardiac mitochondrial chloride intracellular channel proteins. *Mitochondrion*, *27*, 6-14.

Queen, M. M., Ryan, R. E., Holzer, R. G., Keller-Peck, C. R., & Jorcyk, C. L. (2005). Breast cancer cells stimulate neutrophils to produce oncostatin M: potential implications for tumor progression. *Cancer research*, *65*(19), 8896-8904.

Raffaello, A., Mammucari, C., Gherardi, G., & Rizzuto, R. (2016). Calcium at the center of cell signaling: interplay between endoplasmic reticulum, mitochondria, and lysosomes. *Trends in biochemical sciences*, *41*(12), 1035-1049.

Rasool, D., Soleimani, V. D., & Jahani-Asl, A. (2022). Isolation of Adult Mouse Neural Stem Cells and Assessment of Self-Renewal by ELDA. In *Neuronal Cell Death* (pp. 343-354). Springer.

Reya, T., Morrison, S. J., Clarke, M. F., & Weissman, I. L. (2001). Stem cells, cancer, and cancer stem cells. *nature*, *414*(6859), 105-111.

Rieger, A. M., Nelson, K. L., Konowalchuk, J. D., & Barreda, D. R. (2011). Modified annexin V/propidium iodide apoptosis assay for accurate assessment of cell death. *JoVE (Journal of Visualized Experiments)*(50), e2597.

Rose, T. M., & Bruce, A. G. (1991). Oncostatin M is a member of a cytokine family that includes leukemia-inhibitory factor, granulocyte colony-stimulating factor, and interleukin 6. *Proceedings of the National Academy of Sciences*, *88*(19), 8641-8645.

Rose-John, S., Scheller, J., & Schaper, F. (2015). "Family reunion"–A structured view on the composition of the receptor complexes of interleukin-6-type and interleukin-12-type cytokines. *Cytokine and Growth Factor Reviews*, *5*(26), 471-474.

Rosendo-Pineda, M. J., Moreno, C. M., & Vaca, L. (2020). Role of ion channels during cell division. *Cell Calcium*, *91*, 102258.

Rutkowska, A., Stoczyńska-Fidelus, E., Janik, K., Włodarczyk, A., & Rieske, P. (2019). EGFRvIII: an oncogene with ambiguous role. *Journal of Oncology*, *2019*.

Salao, K., Jiang, L., Li, H., Tsai, V. W.-W., Husaini, Y., Curmi, P. M., Brown, L. J., Brown, D. A., & Breit, S. N. (2016). CLIC1 regulates dendritic cell antigen processing and presentation by modulating phagosome acidification and proteolysis. *Biology open*, *5*(5), 620-630.

Saraon, P., Grozavu, I., Lim, S. H., Snider, J., Yao, Z., & Stagljar, I. (2017). Detecting membrane protein-protein interactions using the mammalian membrane two-hybrid (MaMTH) assay. *Current protocols in chemical biology*, *9*(1), 38-54.

Schneider, M., Johnson, J. R., Krogan, N. J., & Chanda, S. K. (2016). The virus–host interactome: Knowing the players to understand the game. In *Viral Pathogenesis* (pp. 157-167). Elsevier.

Setti, M., Osti, D., Richichi, C., Ortensi, B., Del Bene, M., Fornasari, L., Beznoussenko, G., Mironov, A., Rappa, G., & Cuomo, A. (2015). Extracellular vesicle-mediated transfer of CLIC1 protein is a novel mechanism for the regulation of glioblastoma growth. *Oncotarget*, *6*(31), 31413.

Setti, M., Savalli, N., Osti, D., Richichi, C., Angelini, M., Brescia, P., Fornasari, L., Carro, M. S., Mazzanti, M., & Pelicci, G. (2013). Functional role of CLIC1 ion channel in glioblastoma-derived stem/progenitor cells. *Journal of the National Cancer Institute*, *105*(21), 1644-1655.

Shackleton, M., Quintana, E., Fearon, E. R., & Morrison, S. J. (2009). Heterogeneity in cancer: cancer stem cells versus clonal evolution. *Cell*, *138*(5), 822-829.

Sharanek, A., Burban, A., Laaper, M., Heckel, E., Joyal, J.-S., Soleimani, V. D., & Jahani-Asl, A. (2020). OSMR controls glioma stem cell respiration and confers resistance of glioblastoma to ionizing radiation. *Nature communications*, *11*(1), 1-16.

Sharanek, A., Raco, L., Soleimani, V. D., & Jahani-Asl, A. (2022). In situ detection of protein-protein interaction by proximity ligation assay in patient derived brain tumor stem cells. *STAR protocols*, *3*(3), 101554.

Shen, H.-M., & Liu, Z.-g. (2006). JNK signaling pathway is a key modulator in cell death mediated by reactive oxygen and nitrogen species. *Free Radical Biology and Medicine*, *40*(6), 928-939.

Shenghui, H., Nakada, D., & Morrison, S. J. (2009). Mechanisms of stem cell self-renewal. *Annual Review of Cell and Developmental*, *25*, 377-406.

Shergalis, A., Bankhead, A., Luesakul, U., Muangsin, N., & Neamati, N. (2018). Current challenges and opportunities in treating glioblastoma. *Pharmacological reviews*, *70*(3), 412-445.

Sherman, B. T., Hao, M., Qiu, J., Jiao, X., Baseler, M. W., Lane, H. C., Imamichi, T., & Chang, W. (2022). DAVID: a web server for functional enrichment analysis and functional annotation of gene lists (2021 update). *Nucleic Acids Res*, *10*.

Shien, K., Papadimitrakopoulou, V. A., Ruder, D., Behrens, C., Shen, L., Kalhor, N., Song, J., Lee, J. J., Wang, J., & Tang, X. (2017). JAK1/STAT3 Activation through a Proinflammatory Cytokine Pathway Leads to Resistance to Molecularly Targeted Therapy in Non–Small Cell Lung CancerProinflammatory Cytokines and Drug Resistance. *Molecular cancer therapeutics*, *16*(10), 2234-2245.

Shiozaki, A., Otsuji, E., & Marunaka, Y. (2011). Intracellular chloride regulates the G1/S cell cycle progression in gastric cancer cells. *World journal of gastrointestinal oncology*, *3*(8), 119.

Sidaway, P. (2017). Glioblastoma subtypes revisited. *Nature reviews Clinical oncology*, *14*(10), 587-587.

Singh, S. K., Clarke, I. D., Terasaki, M., Bonn, V. E., Hawkins, C., Squire, J., & Dirks, P. B. (2003). Identification of a cancer stem cell in human brain tumors. *Cancer research*, *63*(18), 5821-5828.

Singh, S. K., Hawkins, C., Clarke, I. D., Squire, J. A., Bayani, J., Hide, T., Henkelman, R. M., Cusimano, M. D., & Dirks, P. B. (2004). Identification of human brain tumour initiating cells. *nature*, *432*(7015), 396-401.

Singha, B., Harper, S. L., Goldman, A. R., Bitler, B. G., Aird, K. M., Borowsky, M. E., Cadungog, M. G., Liu, Q., Zhang, R., & Jean, S. (2018). CLIC1 and CLIC4 complement CA125 as a diagnostic biomarker panel for all subtypes of epithelial ovarian cancer. *Scientific reports*, *8*(1), 1-14.

Sjöstedt, E., Zhong, W., Fagerberg, L., Karlsson, M., Mitsios, N., Adori, C., Oksvold, P., Edfors, F., Limiszewska, A., & Hikmet, F. (2020). An atlas of the protein-coding genes in the human, pig, and mouse brain. *Science*, *367*(6482), eaay5947.

Sorscher, S. M. (2004). EGFR mutations and sensitivity to gefitinib. *The New England journal of medicine*, *351*(12), 1260-1261; author reply 1260.
Strange, K. (2004). Cellular volume homeostasis. *Advances in physiology education*, *28*(4), 155-159.
Stupp, R., Mason, W. P., Van Den Bent, M. J., Weller, M., Fisher, B., Taphoorn, M. J., Belanger, K., Brandes, A. A., Marosi, C., & Bogdahn, U. (2005). Radiotherapy plus concomitant and adjuvant temozolomide for glioblastoma. *New England journal of medicine*, *352*(10), 987-996.
Sun, X., & Kaufman, P. D. (2018). Ki-67: more than a proliferation marker. *Chromosoma*, *127*(2), 175-186.
Talks, M. MRM Insights: Targeting OXPHOS in Glioma Stem Cells.
Tan, A. C., Ashley, D. M., López, G. Y., Malinzak, M., Friedman, H. S., & Khasraw, M. (2020). Management of glioblastoma: State of the art and future directions. *CA: a cancer journal for clinicians*, *70*(4), 299-312.
Tan, B. T., Park, C. Y., Ailles, L. E., & Weissman, I. L. (2006). The cancer stem cell hypothesis: a work in progress. *Laboratory investigation*, *86*(12), 1203-1207.
Tanaka, T., Narazaki, M., Ogata, A., & Kishimoto, T. (2014). A new era for the treatment of inflammatory autoimmune diseases by interleukin-6 blockade strategy. Seminars in immunology,
Tawara, K., Scott, H., Emathinger, J., Wolf, C., LaJoie, D., Hedeen, D., Bond, L., Montgomery, P., & Jorcyk, C. (2019). HIGH expression of OSM and IL-6 are associated with decreased breast cancer survival: synergistic induction of IL-6 secretion by OSM and IL-1β. *Oncotarget*, *10*(21), 2068.
Thoma, B., Bird, T. A., Friend, D. J., Gearing, D. P., & Dower, S. K. (1994). Oncostatin M and leukemia inhibitory factor trigger overlapping and different signals through partially shared receptor complexes. *Journal of Biological Chemistry*, *269*(8), 6215-6222.
Thuringer, D., Chanteloup, G., Winckler, P., & Garrido, C. (2018). The vesicular transfer of CLIC1 from glioblastoma to microvascular endothelial cells requires TRPM7. *Oncotarget*, *9*(70), 33302.
Tung, J. J., & Kitajewski, J. (2010). Chloride intracellular channel 1 functions in endothelial cell growth and migration. *Journal of angiogenesis research*, *2*(1), 1-13.
Turkewitz, D. R., Moghaddasi, S., Alghalayini, A., D'Amario, C., Ali, H. M., Wallach, M., & Valenzuela, S. M. (2021). Comparative study of His-and Non-His-tagged CLIC proteins, reveals changes in their enzymatic activity. *Biochemistry and biophysics reports*, *26*, 101015.
Turner, K. L., & Sontheimer, H. (2014). Cl− and K+ channels and their role in primary brain tumour biology. *Philosophical Transactions of the Royal Society B: Biological Sciences*, *369*(1638), 20130095.
Uphoff, C. C., & Drexler, H. G. (2011). Cell culture mycoplasmas. *From the*, *65*.
Urbani, A., Prosdocimi, E., Carrer, A., Checchetto, V., & Szabò, I. (2021). Mitochondrial ion channels of the inner membrane and their regulation in cell death signaling. *Frontiers in cell and developmental biology*, *8*, 620081.
Valente, V., Teixeira, S. A., Neder, L., Okamoto, O. K., Oba-Shinjo, S. M., Marie, S. K., Scrideli, C. A., Paçó-Larson, M. L., & Carlotti, C. G. (2009). Selection of suitable housekeeping genes for expression analysis in glioblastoma using quantitative RT-PCR. *BMC molecular biology*, *10*(1), 1-11.

Valenzuela, S. M., Martin, D. K., Por, S. B., Robbins, J. M., Warton, K., Bootcov, M. R., Schofield, P. R., Campbell, T. J., & Breit, S. N. (1997). Molecular cloning and expression of a chloride ion channel of cell nuclei. *Journal of Biological Chemistry*, *272*(19), 12575-12582.

Valenzuela, S. M., Mazzanti, M., Tonini, R., Qiu, M. R., Warton, K., Musgrove, E. A., Campbell, T. J., & Breit, S. N. (2000). The nuclear chloride ion channel NCC27 is involved in regulation of the cell cycle. *The Journal of physiology*, *529*(Pt 3), 541.

Van Engeland, M., Nieland, L. J., Ramaekers, F. C., Schutte, B., & Reutelingsperger, C. P. (1998). Annexin V-affinity assay: a review on an apoptosis detection system based on phosphatidylserine exposure. *Cytometry: The Journal of the International Society for Analytical Cytology*, *31*(1), 1-9.

Verbon, E. H., Post, J. A., & Boonstra, J. (2012). The influence of reactive oxygen species on cell cycle progression in mammalian cells. *Gene*, *511*(1), 1-6.

Verkman, A. S., & Galietta, L. J. (2009). Chloride channels as drug targets. *Nature reviews Drug discovery*, *8*(2), 153-171.

Walker, E. C., McGregor, N. E., Poulton, I. J., Solano, M., Pompolo, S., Fernandes, T. J., Constable, M. J., Nicholson, G. C., Zhang, J.-G., & Nicola, N. A. (2010). Oncostatin M promotes bone formation independently of resorption when signaling through leukemia inhibitory factor receptor in mice. *The Journal of clinical investigation*, *120*(2), 582-592.

Wang, G. (2016). Chloride flux in phagocytes. *Immunological reviews*, *273*(1), 219-231.

Wang, J.-W., Peng, S.-Y., Li, J.-T., Wang, Y., Zhang, Z.-P., Cheng, Y., Cheng, D.-Q., Weng, W.-H., Wu, X.-S., & Fei, X.-Z. (2009). Identification of metastasis-associated proteins involved in gallbladder carcinoma metastasis by proteomic analysis and functional exploration of chloride intracellular channel 1. *Cancer letters*, *281*(1), 71-81.

Wang, L., He, S., Tu, Y., Ji, P., Zong, J., Zhang, J., Feng, F., Zhao, J., Zhang, Y., & Gao, G. (2012). Elevated expression of chloride intracellular channel 1 is correlated with poor prognosis in human gliomas. *Journal of Experimental & Clinical Cancer Research*, *31*(1), 1-7.

Wang, P., Zhang, C., Yu, P., Tang, B., Liu, T., Cui, H., & Xu, J. (2012). Regulation of colon cancer cell migration and invasion by CLIC1-mediated RVD. *Molecular and Cellular Biochemistry*, *365*(1), 313-321.

Wang, Q., Hu, B., Hu, X., Kim, H., Squatrito, M., Scarpace, L., DeCarvalho, A. C., Lyu, S., Li, P., & Li, Y. (2017). Tumor evolution of glioma-intrinsic gene expression subtypes associates with immunological changes in the microenvironment. *Cancer cell*, *32*(1), 42-56. e46.

Wang, W., Xu, X., Wang, W., Shao, W., Li, L., Yin, W., Xiu, L., Mo, M., Zhao, J., & He, Q. (2011). The expression and clinical significance of CLIC1 and HSP27 in lung adenocarcinoma. *Tumor Biology*, *32*(6), 1199-1208.

Watkins, S., & Sontheimer, H. (2011). Hydrodynamic cellular volume changes enable glioma cell invasion. *Journal of Neuroscience*, *31*(47), 17250-17259.

Weiner, I. D., Linas, S. L., Wingo, C. S., Floege, J., Johnson, R., & Feehally, J. (2010). Disorders of potassium metabolism. *Comprehensive clinical nephrology*, *4*, 118-129.

West, N. R., Owens, B. M., & Hegazy, A. N. (2018). The oncostatin M-stromal cell axis in health and disease. *Scandinavian Journal of Immunology*, *88*(3), e12694.

Westman, J., & Grinstein, S. (2021). Determinants of phagosomal pH during host-pathogen interactions. *Frontiers in cell and developmental biology*, *8*, 624958.

Wilczyński, B., Dąbrowska, A., Saczko, J., & Kulbacka, J. (2021). The Role of Chloride Channels in the Multidrug Resistance. *Membranes*, *12*(1), 38.

Williams, R. L., Hilton, D. J., Pease, S., Willson, T. A., Stewart, C. L., Gearing, D. P., Wagner, E. F., Metcalf, D., Nicola, N. A., & Gough, N. M. (1988). Myeloid leukaemia inhibitory factor maintains the developmental potential of embryonic stem cells. *nature*, *336*(6200), 684-687.

Winder, D. M., Chattopadhyay, A., Muralidhar, B., Bauer, J., English, W. R., Zhang, X., Karagavriilidou, K., Roberts, I., Pett, M. R., & Murphy, G. (2011). Overexpression of the oncostatin M receptor in cervical squamous cell carcinoma cells is associated with a pro-angiogenic phenotype and increased cell motility and invasiveness. *The Journal of pathology*, *225*(3), 448-462.

Wojciak-Stothard, B., Abdul-Salam, V. B., Lao, K. H., Tsang, H., Irwin, D. C., Lisk, C., Loomis, Z., Stenmark, K. R., Edwards, J. C., & Yuspa, S. H. (2014). Aberrant chloride intracellular channel 4 expression contributes to endothelial dysfunction in pulmonary arterial hypertension. *Circulation*, *129*(17), 1770-1780.

Wu, J., & Wang, D. (2017). CLIC1 induces drug resistance in human choriocarcinoma through positive regulation of MRP1. *Oncology Research*, *25*(6), 863.

Yamauchi, T., & Moroishi, T. (2019). Hippo pathway in mammalian adaptive immune system. *Cells*, *8*(5), 398.

Yang, L., Shi, P., Zhao, G., Xu, J., Peng, W., Zhang, J., Zhang, G., Wang, X., Dong, Z., & Chen, F. (2020). Targeting cancer stem cell pathways for cancer therapy. *Signal transduction and targeted therapy*, *5*(1), 1-35.

Yang, X., Boehm, J. S., Yang, X., Salehi-Ashtiani, K., Hao, T., Shen, Y., Lubonja, R., Thomas, S. R., Alkan, O., & Bhimdi, T. (2011). A public genome-scale lentiviral expression library of human ORFs. *Nature methods*, *8*(8), 659-661.

Yeagle, P. (2016). Membrane Receptors. *The Membranes of Cells, 3rd ed.; Academic Press: Boston, MA, USA*, 401-425.

Ying, Q.-L., Nichols, J., Chambers, I., & Smith, A. (2003). BMP induction of Id proteins suppresses differentiation and sustains embryonic stem cell self-renewal in collaboration with STAT3. *Cell*, *115*(3), 281-292.

Yu, H., Lee, H., Herrmann, A., Buettner, R., & Jove, R. (2014). Revisiting STAT3 signalling in cancer: new and unexpected biological functions. *Nature Reviews Cancer*, *14*(11), 736-746.

Zadeh, G., Bhat, K. P., & Aldape, K. (2013). EGFR and EGFRvIII in glioblastoma: partners in crime. *Cancer cell*, *24*(4), 403-404.

Zanin, S., Lidron, E., Rizzuto, R., & Pallafacchina, G. (2019). Methods to Measure Intracellular Ca 2+ Concentration Using Ca 2+-Sensitive Dyes. In *Calcium Signalling* (pp. 43-58). Springer.

Zhang, P., Xia, Q., Liu, L., Li, S., & Dong, L. (2020). Current opinion on molecular characterization for GBM classification in guiding clinical diagnosis, prognosis, and therapy. *Frontiers in molecular biosciences*, *7*, 562798.

Zhao, K., Wang, Z., Li, X., Liu, J.-l., Tian, L., & Chen, J.-q. (2019). Exosome-mediated transfer of CLIC1 contributes to the vincristine-resistance in gastric cancer. *Molecular and Cellular Biochemistry*, *462*(1), 97-105.

Zhou, B., Lu, X., Hao, Y., & Yang, P. (2019). Real-time monitoring of the regulatory volume decrease of cancer cells: A model for the evaluation of cell migration. *Analytical chemistry*, *91*(13), 8078-8084.